CAVEOLIN-1 IN RENAL DISEASE

by

Sourabh Chand

A thesis submitted to the University of Birmingham for the degree of DOCTOR of MEDICINE

Renal Research Group

School of Immunity and Infection

College of Medical and Dental Sciences

University of Birmingham

1st August 2016

ABSTRACT

Renal disease is a major global public health issue that affects 10% of the general population with premature morbidity and mortality related to cardiovascular disease and infection. Interstitial fibrosis is a common hallmark of progressive kidney dysfunction. There remains a stubborn discrepancy in identifying which patients suffer adverse events because of their disease or resulting treatment. Investigation in patient genome variation may explain this discrepancy.

Caveolin-1 is the essential structural protein for caveolae that are ubiquitously distributed in fibroblasts, endothelial and epithelial cells. They act as molecular chaperones for transcellular signalling such as degradation of the activated TGFβ-1 receptor. In this thesis, caveolin-1 single nucleotide polymorphism rs4730751 CC genotype is shown to be associated with a better outcome in renal patients for arterial stiffness, and reduced mortality from cardiovascular disease, infection, malignancy in ANCA associated vasculitis. By inducing renal models of fibrosis in caveolin-1 knockout mice, deletion of caveolin-1 leads to increased fibrosis.

In conclusion, this polymorphism could be used as a marker of disease risk either in isolation or as part of a clinical risk score to counsel patients on the likely prognosis of their condition. Manipulation of caveolin-1 expression may be a therapeutic strategy in reducing renal fibrosis.

ACKNOWLEDGEMENTS

I would like to thank my supervisors Dr Richard Borrows and Professor Lorraine Harper for their support and encouragement throughout my MD. Thank you to all the Renal Research Group and colleagues at the Centre of Translational Inflammation Research for their continued advice and guidance throughout this period of research, especially Dr Stuart Smith who trained me in the murine surgical techniques. Thank you also to Dr Amy Jayne McKnight for the opportunity to visit Belfast Regional Genetic Centre and learn DNA isolation and genotyping techniques. I would also thank my wife and children Zak and Max for all their encouragement and understanding during this time. Finally I would like to acknowledge Novartis for their kind donation of ciclosporin powder and Queen Elizabeth Hospital Birmingham Charities for their kind donation in helping fund this research.

TABLE OF CONTENTS

LIST OF FIGURES

CHAPTER 1: INTRODUCTION

CHAPTER 2: MATERIALS AND METHODS

CHAPTER 3: GENETIC VARIATION IN CARDIOVASCULAR DISEASE IN CKD

CHAPTER 4: CAV1 IN ANTINEUTROPHIL CYTOPLASMIC ANTIBODY ASSOCIATED VASCULITIS

CHAPTER 5: NEW-ONSET DIABETES AFTER TRANSPLANTATION

CHAPTER 6: RENAL EXPRESSION OF MURINE CAVEOLIN-1

CHAPTER 7: GENERAL DISCUSSION

LIST OF TABLES

CHAPTER 1: INTRODUCTION

CHAPTER 2: MATERIALS AND METHODS

CHAPTER 3: GENETIC VARIATION IN CARDIOVASCULAR DISEASE IN CKD

CHAPTER 4: CAV1 IN ANTINEUTROPHIL CYTOPLASMIC ANTIBODY ASSOCIATED VASCULITIS

CHAPTER 5: NEW-ONSET DIABETES AFTER TRANSPLANTATION

CHAPTER 6: RENAL EXPRESSION OF MURINE CAVEOLIN-1

ABBREVIATIONS

AAV: antineutrophil cytoplasmic antigen associated vasculitis

ACE I: angiotensin converting enzyme inhibitor

ACR: albumin:creatinine

aPWV: aortic pulse wave velocity

ARB: angiotensin receptor blocker

AT1: angiotensin II type 1 receptor

αSMA: alpha smooth muscle actin

CAN: chronic allograft nephropathy

CAV1: caveolin-1

CKD: chronic kidney disease

CKO: caveolin-1 knockout

CMR: cardiac magnetic resonance

CsA: ciclosporin

CSD: caveolin-1 scaffolding domain

ECM: extracellular matrix

eGFR: estimated glomerular filtration rate

ESRD: end-stage renal disease

GPA: granulomatosis polyangiitis

GWAS: genome wide associated study

MPA: microscopic polyangiitis

TGFβ-1: transforming growth factor beta 1

UUO: unilateral ureteric obstruction

WT: wild-type

CHAPTER 1:

INTRODUCTION

1.1 Introduction

1.1.1 Chronic Kidney Disease Burden

Renal disease is a major global public health issue that affects estimates of 10-16% of the general population in developed countries leading to premature morbidity and mortality (1). In 2009-2010, the economic burden of chronic kidney disease (CKD) on the English National Health Service (NHS) was an estimated £1.45 billion (equivalent to 1.3% of all NHS spending that year), with over half of the costs related to the 2% of the CKD population with end-stage renal disease (ESRD) requiring renal replacement therapy (RRT) (2). The resultant effect of the CKD burden is an excess in length of stay in hospitals, hospital associated infections as well as an excess of 7000 cerebral vascular events and 12000 myocardial infarctions compared to age/gender matched controls (2). Thus, it remains paramount to identify individuals with CKD at the earliest time-point in order to instigate therapy to prevent the progression to ESRD.

In 2004, the UK adoption of the 4 variable (age, sex, race and serum creatinine) Modification of Diet in Renal Disease equation (3) to estimate a person's glomerular filtration rate based on two readings three months apart, led to a marked increase in the number of previously undiagnosed patients with CKD especially in primary care. This equation was later updated in 2008 following standardisation of serum creatinine laboratory measurements (Figure 1-1).

Figure 1-1 Modification of Diet in Renal Disease Equation (4)

Estimated Glomerular Filtration Rate = 30849× standardized serum creatinine (micromol/l) $^{-1.154}$ × age $^{-0.203}$ × 1.212 (if black race) × 0.742 (if female); units mL/min/1.73 m^2

The 5 stage estimated glomerular filtration rate (eGFR) has further been refined to highlight those with proteinuria (Figure 1-2) and thus those who are at particular risk of progression to more advanced stages of renal disease and its complications, especially cardiovascular disease (5, 6). In a cross-sectional single point eGFR measurement study using the 2009 and 2010 Health Survey for England data, the prevalence for eGFR <60mls/min per 1.73m^2 (stages 3-5) was estimated at 5.2% (7). However, compared to 2003, the prevalence of CKD stages 3-5 is on the decline except in men aged 65-74 years old (8). Risk stratification has allowed better patient counselling and targeted therapy to reduce kidney disease progression and associated complications, with examples such as proteinuria reduction with angiotensin converting enzyme inhibitors (ACE I), angiotensin receptor blockers (ARBs), renin and aldosterone inhibitors that not only control blood pressure (5, 6, 9), but reduce the blood pressure in glomeruli by targeting the renin-aldosterone-angiotensin system and vasodilation of the glomerulus efferent arteriole thus reducing the intra-glomerular blood pressure (Figure 1-3). Further risk stratification is still required due to increasing prevalence of factors that adversely associate with CKD such as an aging population, ethnic diversity (especially South-Asians) and prevalence of diseases such as diabetes mellitus.

Figure 1-2 Heatmap of chronic kidney disease progression risk (10)

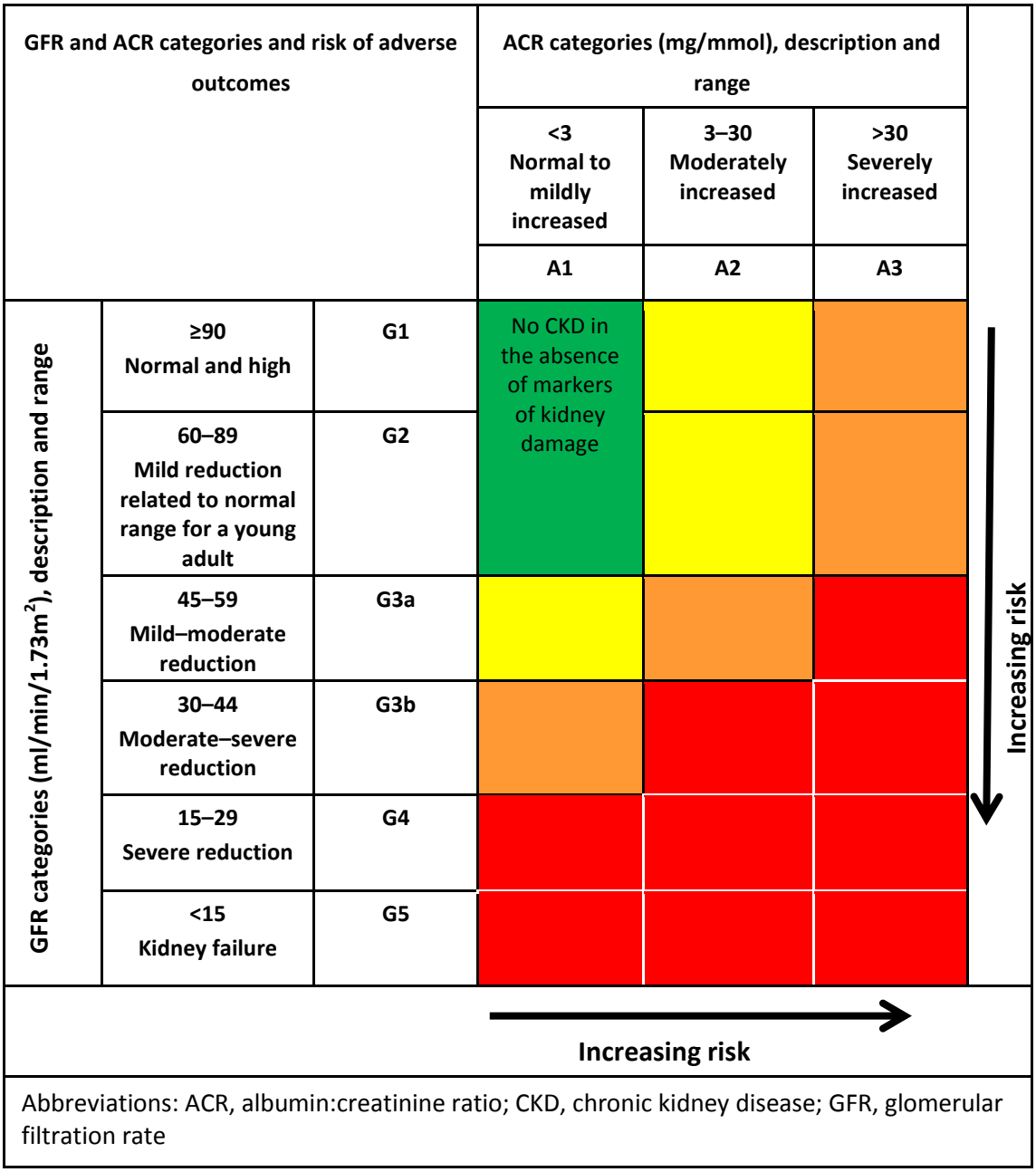

Abbreviations: ACR, albumin:creatinine ratio; CKD, chronic kidney disease; GFR, glomerular filtration rate

Figure 1-3 Schematic coronal section of a kidney (A), nephron (B) and its glomerulus (C) (11)

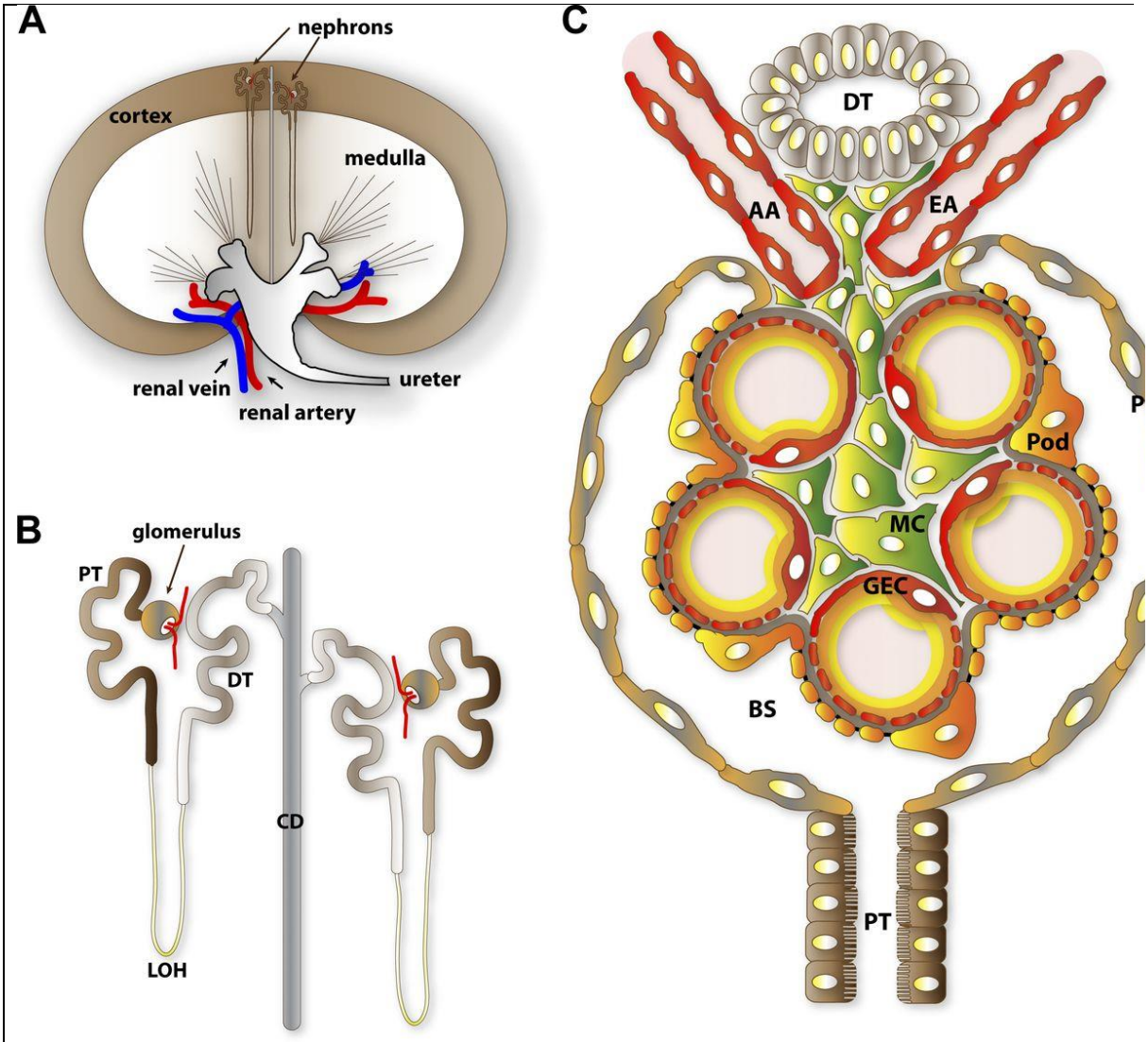

Abbreviations: AA, afferent arteriole; BS, Bowman's space; CD, collecting duct; DT, distal tubule; EA, efferent arteriole; GEC, glomerular endothelial cell; LOH, loop of Henle; MC, mesangial cell; Pod, podocyte; PT, proximal tubule

1.1.2 Adverse outcomes in renal disease

As described above, age, ethnicity, proteinuria, poorly controlled diabetes and hypertension are well described risk factors for progression of renal decline in CKD. In addition to these risk factors, renal tubulointerstitial fibrosis has been the key common pathological finding in patient's accelerated CKD irrespective of the underlying cause (12). However, patients with

CKD also have an increased morbidity and mortality due to multifactorial reasons such as accelerated cardiovascular disease, sepsis, acute kidney injury episodes, increased hospitalisations, lower socioeconomic status, frailty, depression and fracture risk (13, 14). Patients with CKD stage 3-5 also have a median three co-existing disease processes with their CKD, such as hypertension, diabetes, atrial fibrillation, heart failure or pulmonary disease in an epidemiology study of over half a million patients in Canada (14). To compound the management of patients with CKD, their underlying renal pathology and renal replacement strategies such as transplantation, mean they may suffer further complications from potential therapies used in these scenarios such as immunosuppressive regimens.

Despite the relative therapeutic success in reducing the prevalence in CKD in the UK, and understanding the associated risk factors that affect patients with CKD, there remains a stubborn discrepancy in identifying which patients would benefit the most and which suffer adverse events because of their disease or treatment. Investigation into patient genome variation may explain this discrepancy.

1.1.3 Genetic variation in kidney disease

Since the 1980s, there have been more than 3000 research papers published on the genetics of CKD (15). Initially, these had concentrated on Mendelian patterns of inheritance to understand the pathophysiology of inherited diseases such as adult polycystic kidney disease. The mutations in genes PKD1 and PKD2 have led to more informed genetic counselling regarding the progression of their disease as well as the pathways leading to this

disease (16). These techniques have been also been applied to inheritable congenital kidney resulting from single gene disorders especially in children.

Over the last decade, single gene studies have focused on biological plausible candidate gene association with kidney disease. These studies were often underpowered with inclusion of multiple ethnicities in cohort studies, with little attempt at replication and correction for multiple confounders. However, as the 1000 genome project has recently confirmed, there is a large genomic discrepancy depending on your ethnicity and ancestry (17). One method of counter-acting these issues is genome-wide linkage studies that combine the above two strategies, by examining large genomic regions in family-based collections of DNA to associate transmission of genetic variants to the development of CKD. Conditions such as CKD are likely to be more complex with many potential pathways and environmental changes leading to its development and progression. The ability to find enough numbers of related individuals with an underlying condition to track genetic change across multiple generations remains a barrier to success for this method.

The most common type of genomic variation is single nucleotide polymorphism (SNP) that must occur in over 1% of the population to be called a SNP and has the possibility of two alleles at a given site (biallelic) (18). Other types of polymorphisms include insertion/deletion or copy number variation of the number of nucleotides. This has led to genome-wide association studies (GWAS) into CKD with the advantage of examining millions of SNPs in unrelated affected individuals to controls. A GWAS typically involves using tag SNPs that are SNPs that have been 'aggregated' from haplotypes of nearby SNPs or SNPs that have been inherited together. GWAS will allow the identification of common SNPs that associate with

disease, however may miss less common SNPs that may relate to important changes in CKD and especially in a subset of this large population. In all genomic investigations, it is paramount that the correct control group is identified and that patients are phenotyped correctly. SNPs identified may infer changes to RNA thus affecting the protein function upon translation (non-synonymous) but may have small effect size to the overall condition being investigated such as CKD. To validate SNPs found by GWAS, replication studies should be performed of the single gene variant identified as well as performing functional analyses using transcripts of tissue or other samples from patients by performing an expression as a quantitative trait locus analysis (eQTL). This could either be a transcript encoded by a nearby to SNP gene (cis-QTL) or transcript away from that SNP with alteration of its abundance or function, either on the same or a different chromosome (trans-eQTL) (19). A functional context of the SNP effect can be elucidated using tissue specific transcripts such as a renal biopsy sample and possible pathways to the phenotype being studied. To further examine a functional context to the associated SNP, animal models using knockouts of gene and inducing the phenotype desired can further elucidate possible pathways and therapeutic interventions. Another high-output genomic advance is the use of next generation sequencing that allows investigation of a person's whole exome that contains the protein-coding part of the genome, 1-2% of the human genome, or whole genome sequencing (20). This technique is utilised especially when examining tissue or a subgroup of cells from tissue. The advantage of this technique is the allowance to find novel mutations with phenotype association, however also proposes the challenge of interpreting large volumes of data. The phenotypes studied in GWASs in CKD have tended to focus on estimated glomerular

filtration rate (eGFR), CKD progression, proteinuria and renal disease prevalence, rather than measures of cardiovascular disease or mortality.

Examples of success in GWAS association with renal disease, using the above strategies comes from the CKDGen study group who performed a meta-analysis of 20 GWASs. This included over 67000 patients studied of European ancestry who had biopsies of either their native or transplant kidney. The analysis was from population-based studies rather than case-control and examined the glomerular and tubulointerstitial gene expression in relation to declining eGFR. They had not only found 13 new loci related to kidney function and serum creatinine secretion but also found *vascular endothelial growth factor A* gene expression in both renal compartments with strong enrichment for the hypoxia signalling pathway (21). GWASs have also been able to confirm laboratory findings even in small populations of disease such as in membranous nephropathy. In a French cohort of just 75 cases, the *phospholipase A_2 receptor* (PLA_2R) *1* gene was found to significantly associate with membranous nephropathy (22), after previous confirmation of serological M-type PLA_2R autoantibody could be found in 70% of cases to differentiate between primary and secondary membranous nephropathy which in turn, has marked therapeutic implications (23). Subsequent investigation has revealed an odds-ratio (OR) of 2.00 with the presence of the at risk SNP genotype for *PLA_2R1* despite being located within the first intron (non-coding) part of the gene (24). GWASs have also been able to confirm that the pathogenesis of disease states such as antineutrophil cytoplasmic antibody associated vasculitis (AAV) has a genetic component and the subsets of this condition (granulomatosis with polyangiitis (GPA) and microscopic polyangiitis (MPA)) show genetic distinctions and thus are distinct autoimmune syndromes (25).

As well as inherited genetic influence on outcomes and prevalence in CKD, epigenetics is a field that is helping researchers to understand the influence that environmental factors have on the human genome and thus disease presentation and variance amongst individuals. This has been observed even in phenotypic discordant monozygotic twins (with identical DNA sequence) to explain their differences (26). There are 3 main epigenetic changes that occur, namely chromatin modification, RNA interference and DNA methylation. However, these can occur at the same time, thus unravelling their effects upon gene regulation is challenging. To add to this complexity, different cell types will express different epigenetic changes or epigenomes, thus performing epigenome-wide association studies in CKD are fraught with difficulty to understand their meaning, even if they are from the same tissue such as from kidney biopsies, due to the many cell types in this organ. Chromatin modification is thought to effect gene expression by changing DNA availability to transcriptional machinery that can result in chromatin states of transcription inactivity or activity (termed euchromatin) by histone acetylation, methylation, phosphorylation and ubiquitination. RNA interference results in impedance of translation efficiency of mRNA to protein. RNA interference can occur in short non-coding RNA (microRNAs) or long noncoding RNA and has been shown to skew the female X-chromosome in renal transplantation that is associated with a reduced allograft survival if donor female X-chromosome is skewed (27). DNA methylation occurs at sites where a methyl group is enzymatically added to the phosphate that links cytosine to guanine (CpG site). This can alter the function of the gene by more frequently silencing the gene, but also by activation via inhibiting co-factors or microRNA that repress transcription (15).

The following prose is based on 'Genetic polymorphisms and kidney transplant outcomes' with myself as first author (28).

Genetic polymorphism studies have been an area of great interest in renal transplantation recently, with the aim to improve short and long term outcomes such as acute rejection, allograft survival and patient survival respectively. The studies reflect the investigative strategies outlined above and highlight how they can be used to inform clinical practice, but also conflicting results that can be found.

1.1.3.1 T cells, innate immunity and inflammation based genetic studies in renal transplantation

One of the largest multi-centre genomic trials in renal transplantation originated from the Deterioration in Kidney Allograft Function (DeKAF) genomic study from 2010 (29). It consisted of 990 patients from North America, testing over 2700 candidate SNPs, but suffered from being multi-ethnic, consisting of kidney and simultaneous kidney-pancreas transplantation, having large centre-centre variation and end-points such as acute rejection (AR) rather than graft or patient survival. After attempted correction for this variation and ethnic diversity, 15 SNPs were identified with AR and tubulitis severity, with the two strongest associations pointing to T cell activation via protein phosphorylation and cell cycle progression (rs2227931 in *ATR*, rs2267130 in CHEK2, and rs3088142 in *DUSP13*) and inflammation (rs811925 in *PRDM1* (interferon-β) and rs2228059 in *IL15RA*).

The first GWAS in renal transplantation of medium-term allograft function was reported last year in 326 White patients. Although there was a high initial genotyping failure rate (>18%),

263 patients had a functioning graft and assessment of 5-year function by creatinine only, with 511,662 SNPs analysed. After linkage disequilibrium pattern assessment and multivariate analysis including 15 clinical variables, two SNPs rs3811321 (*TCRA* encoding for T cell receptor alpha chain conferring antigen specificity) and rs6565887 (*ZNF516* intronic for zinc finger protein (integral for DNA transcript processing) expressed mainly in the kidney, spleen and lung) were significant and explained 17.4% of 5 year-creatinine variance, with survival analysis showing AA genotype of both being significantly protective against time to transplant failure and for *ZNF516* time to patient death (30).

A meta-analysis in HLA-G-14-base pair insertion/deletion of 907 patients from 5 case-control studies showed no association with kidney allograft rejection (31), however an Italian study of 418 patients found that the homozygous deletion genotype was at risk for advancing allograft failure and subsequent loss (32). A further genomic analysis of 979 recipients enrolled in the 2010 DeKAF study was performed last year, and investigated chronic allograft dysfunction (defined as a clinical diagnosis as a ≥25% rise in serum creatinine from baseline), and assessment of severity of tubular atrophy and interstitial fibrosis on indication biopsy. However, this study had the same issues of varying centre practices e.g. immunosuppression, steroid withdrawal, dialysis post immediate transplantation, combination of kidney and simultaneous kidney pancreas recipients and ethnic diversity. None of the top 15 SNPs were significant after correction for multiple testing (false discovery rate set at 20%) for biopsy severity, though the top SNPs prior to correction were for the leptin receptor (*LEPR* – encodes for a pro-inflammatory cytokine receptor gene and leptin plays a role for regulatory T cell proliferation) and *CYP4F12* (encoding for metabolic enzyme

in the cytochrome P450 system for drug metabolism). Two further drug metabolism related SNPs in *FM03* and *FM06* were associated with chronic allograft dysfunction (33).

An interesting recent report within the last 12 months highlights the emerging importance of gene copy number variation in determining graft outcome, and represents one of the few recent single-centre studies to address graft failure as an outcome (34). Bay reported superior medium-term graft outcome when patients displayed less than four total copies of the gene encoding complement factor 4 (C4), although this held only in the subgroup receiving deceased donor kidneys (as opposed to live donation) raising the issue of gene:environment interactions (in this case the "environmental influence of ischaemia) in determining outcome.

Although such studies set the scene for further investigation, drawing robust conclusions will require further replication and validation in independent cohorts. This is clearly also the case for the multiple single-centre studies, which have directed attention to other candidate gene variants, and have investigated outcomes in populations of varied ethnicities. These studies may be of relevance in light of their biological plausibility, and may serve to guide future efforts. An interesting report described 599 Dutch de novo transplant recipients who underwent testing of the promoter region of *FOXP3* gene for the short (<16) or long (>16) number of dinucleotide (GT) repeats. The short repeat genotype was associated with improved allograft survival (HR=0.67, 95% CI 0.48-0.94, p=0.02). Of functional relevance, the short repeat has an enhanced promoter gene activity compared to the long repeat genotype (35).

Other studies reported over the last 12 months include investigation of topical Th17 pattern related genes (*IL-17*, *IL-21*, *IL-23R*) in relation to AR risk (36, 37). *TNF-α* 2/2 genotype was also a risk for AR (38), as was *UGT1A* variation, possibly mediated by its effects on bilirubin levels and concomitant anti-oxidative properties (39). *TLR9, COX-2, AIF1, and MBL2* gene variants have also shown associations with AR (40-42). Interferon gamma regulates macrophage production of human allograft inflammatory factor-1 with a recent meta-analysis of *IFNy* 874 T/A in 1650 patients revealing AA genotype to be protective amongst White deceased donor allograft recipients (43). In contrast, 2 single centre non-replicated studies that found no such association (44, 45).

Endothelial cell-leucocyte crosstalk is another pathway for potential modulation of the post-transplant immune response with a study of 269 Polish White patients showing a significant multivariate association with early and long-term (up to 5 years) allograft dysfunction as measured by serum creatinine. Gene variation in *ICAM1* (rs5498) and *VCAM1* (rs1041163) were significantly associated with graft loss, with some evidence for association with mortality (p=0.06) (46). Co-stimulatory molecular *CD28* rs3116496 TT genotype was associated for AR, but not CAN or delayed graft function (47).

The field of transplant genetics is clearly not immune to the problem of publication bias, with "positive" findings far more likely to be submitted and accepted to the literature. Recent "negative" studies include investigations showing no relationship between AR and *IL-1*, *IL-2*, *IL-6* (also no relationship with chronic allograft nephropathy [CAN]), *IL-10*, *IL-21*, *TGFβ-1* (also no effect on graft function (48)), *TNF-α*, *TLR4, CD14* (also no effect on CAN or graft survival), and *CTLA4 or PTNPN 22* (also no association with graft function, survival or

patient mortality) (36, 44, 45, 48-52). Despite negative findings for inflammatory and apoptotic genes *IL-6*, *TGFβ-1* and *Fas* individually, La Manna did find that a combination of high producing genotype IL-6 and low *Fas* production was protective for graft function (Odds Ratio [OR]: 0.79) over a 2.5 year follow-up period in 376 Italian deceased donor transplant patients (48).

These "negative" studies may be better considered "null" studies – i.e. they are underpowered to exclude a relevant clinical effect, and the last example highlights issues where secondary, multiple or post-hoc outcomes are evaluated, which in this case are clearly stated, but in other scenarios may be less transparent and lead to a type II error dominating the findings. As a result, these studies do not directly aid a clinician with which SNP requires investigation for their individual patients, but more aid in hypothesis generating which pathways may be responsible in determining patient outcome variability.

1.1.3.2 Pharmacogenetics

Most studies of transplant pharmacogenomics over the last 12 months have investigated the cytochrome P450 system with outcomes based on tacrolimus trough levels and clearance. *CYP3A5* 3*3 genotype results in far lower CYP3A enzyme activity than 1*1 genotype (53), and recent reports confirm that transplant recipients displaying the 1*1 or 1*3 genotype require higher doses of tacrolimus to reach target levels; it has also been suggested that lower drug variability ensues from administration of once-daily tacrolimus preparations (54-57). However, upon independently testing the previously developed *CYP3A5* genotype-based tacrolimus dosing DeKAF algorithm (58), it was shown to be a poorly predictive model for tacrolimus clearance when using tacrolimus doses used in routine clinical practice (59).

Shuker et al also showed in a randomised control trial, that tacrolimus dose dependent change based on *CYP3A5* genotype had no effect on clinical outcome or the number of patients reaching therapeutic tacrolimus levels early post live donor kidney transplant (60). It has also been suggested that the high intravariability of tacrolimus is a risk factor for CAN and graft loss, although *CYP3A5* genotype was not associated with intrapatient tacrolimus variability (61).

This has led to research in other drug metabolism gene variants that could be combined with the carrier status of CYP3A5 to improve identification of patients with altered tacrolimus metabolism and potential toxicity/under-dosing. Most have combined *CYP3A4* genotypes to *CYP3A5* and shown *CYP3A4* 1*1 and *CYP3A5* 3*3 genotypes require a lower tacrolimus dose to reach a desired level (62-64). *CYP3A4**22 and *CYP3A5**3 alleles might explain interindividual difference in pharmacokinetic parameters of tacrolimus (65). Variation in Multidrug-resistance-1 gene (*MDR-1*), also known as *ABCB1* (which encodes the efflux transporter p-glycoprotein involved in calcineurin-inhibitor disposition), has also been studied. Almost all studies suggest *ABCB1* C3435T SNP does not impact tacrolimus pharmacokinetics (56, 66-68). However, there may be an effect on calcineurin-inhibitor pharmacodynamics resulting in altered T cell IL-2 production (69), perhaps explaining why the C3435T genotype is associated with increased risk of AR, chronic rejection and graft loss as well as more severe periodontal disease with cyclosporine use (66, 70). Also relevant to pharmacodynamics, but this time in relation to donor genetics and donor:recipient interaction, is an instructive case report describing consistently low tacrolimus levels but severe biopsy proven tacrolimus-induced nephropathy where the donor and recipient displayed *CYP3A5* 3*3 and 1*3 genotypes respectively (71).

1.1.3.3 Post-transplant hyperglycaemia

Another area of focus in transplant outcome has been the development of impaired glucose tolerance (IGT) and new onset diabetes after transplantation (NODAT), which are associated with patient mortality and poorer allograft survival (72). A GWAS of candidate SNPs in NODAT was performed in 26 NODAT patients (and 230 controls) with subsequent *de novo* SNP genotyping in 57 NODAT patients (and 383 controls), discovered 8 SNPs associated with pancreatic β-cell apoptosis (73). This Belfast cohort was limited to White, adult recipients with NODAT defined as requirement for oral hypoglycaemics or insulin after transplantation.

Other recent studies have shown Mitochondrial DNA haplotype H is associated with increased risk of NODAT (74). Low adiponectin levels have been associated with the development of NODAT and in an adjusted model of 270 White Brazilian patients, rs1501299 TT genotype was associated with increased risk for NODAT (75). The renal-angiotensin system can modulate adiponectin levels, and a study of 372 Polish patients found an association between *ACE I/D* genotype and higher adiponectin levels in women with a lower BMI but not increased insulin resistance (76).

1.1.3.4 The importance of donor gene variation in graft failure

As discussed above, studies of donor gene variation are scarcer than those of the transplant recipient, yet may be highly informative. A study from Reeves-Daniel has shown the association between donor APOL1 variation and graft survival. This North American study suggested, in fact, that this may account for the differences in graft outcome ascribed to donor race (specifically the worse outcomes in for kidneys donated by African American

individuals), rather than race *per se* (77). A recent European case report represents a cautionary tale whereby accelerated graft failure of the recipient, and also the development of renal dysfunction and proteinuria in the donor was seen following live donation from the monozygotic twin of an African Caribbean patient. Both donor and patient displayed the at-risk APOL1 gene variant, highlighting not only the increased risk of graft failure in this setting, but also having implications for the safety of certain donors, particularly those of African origin (78).

As may be the case described for drug metabolism genes described above, the combination of donor and recipient gene variation may be relevant. A non-replicated Korean study showed an association between graft survival and the summed number of A alleles from donor and recipient in *MMP-7* and *MMP-20* (79). A report of 100 patients from Saudi Arabia described donor *IL-10* (-1082) GA genotype as a risk for transplant rejection, but not graft failure (44). A study involving 2985 genotyped donors from the Collaborative Transplant Study (CTS) has described an association between graft failure and donor *ABCB1* genotype in 2011 (80). This extends data from a study published in 2009 demonstrating increased risk for graft failure when both donor and recipient were homozygous for the C3435T variant in *ABCB1* (81).

A cohort study from Birmingham and Belfast has also described a replicated association between death censored allograft graft loss and severity of interstitial fibrosis and donor *CAV1* (caveolin-1) SNP rs4730751 (82). Interstitial fibrosis severity is a prognostic marker for progression of CKD. Caveolin-1 ubiquitous distribution and pleiotropic effects could relate to patients' adverse outcomes as their renal disease progresses.

1.2 Caveolae and Caveolin-1

1.2.1 History of Caveolae and Caveolin-1

Caveolae are sub-class of non-clathrin coated lipid rafts that were morphologically first identified in 1953 via transmission electron microscopy and appear as little cave-like invaginations of the plasma membrane of 50-100 nanometres in size (83). In 1955, Yamada first described caveolae existing in the renal mouse glomerular capillary endothelium (84). Caveolae are ubiquitously distributed though predominately found in endothelial cells, epithelial cells, striated and smooth muscle cells, fibroblasts and type 1 pneumocytes, with almost twenty percent of the total plasma membrane of adipocytes being occupied by caveolae (85, 86). There are three main isoforms of the caveolin protein, with CAV1 being essential for the formation of caveolae. In 1989, the first monoclonal antiphosphotyrosine antibody was produced against a 22-kDa protein from Rous sarcoma virus-transformed chick embryo fibroblasts in the process of oncogene related protein phosphorylation. This protein was resistant to non-ionic detergent conditions with over 90% of the protein fractionated with the cytoskeleton and punctate staining in the margins of fibroblasts and in parallel arrays along actin stress fibres (87, 88). In 1992, Rothberg et al first ascribed the protein component of the caveolae membrane coat as caveolin (89). In 1999, caveolin-2 was described as 20-kDa protein that co-localises and is dependent on CAV1 to form hetero-dimers (90) and caveolae membrane localisation to the basolateral surface of epithelial cells, whilst caveolae with CAV1 alone, are not seen on the apical surface (91). Caveolin-3 has a similar morphology to caveolin-1, and is mostly found in cardiac, smooth and skeletal myocytes (92).

1.2.2 Structure of caveolae and caveolin-1

Caveolae are largely composed of cholesterol with concentrated glycosphingolipids and sphingomyelin relative to the plasma membrane distribution, with CAV1 required for its structural stability. As shown in Figure 1-4, caveolae can form either the classical omega or little cave, enlongated (for channel formation) or a direct vesicle formation mostly at the basolateral surface. This depends on the proteins called cavins whose abundance changes the mobility of CAV1 and thus structural integrity of the caveolar structure allowing the structure and its contents to be endocytosed. If the ratio of cavin-1 to cavin-2 is higher, then the caveolae omega shape is favoured; if cavin-2 expressed levels higher than cavin-1, then the elongated shape is formed whilst cavin-3 expression directs vesicle formation (93). Depletion of cholesterol results in decreased CAV1 expression that can also lead to destabilisation of the caveolae structure to become mobile from the plasma membrane.

Figure 1-4 Electron micrograph and schematic representation of caveolae structures

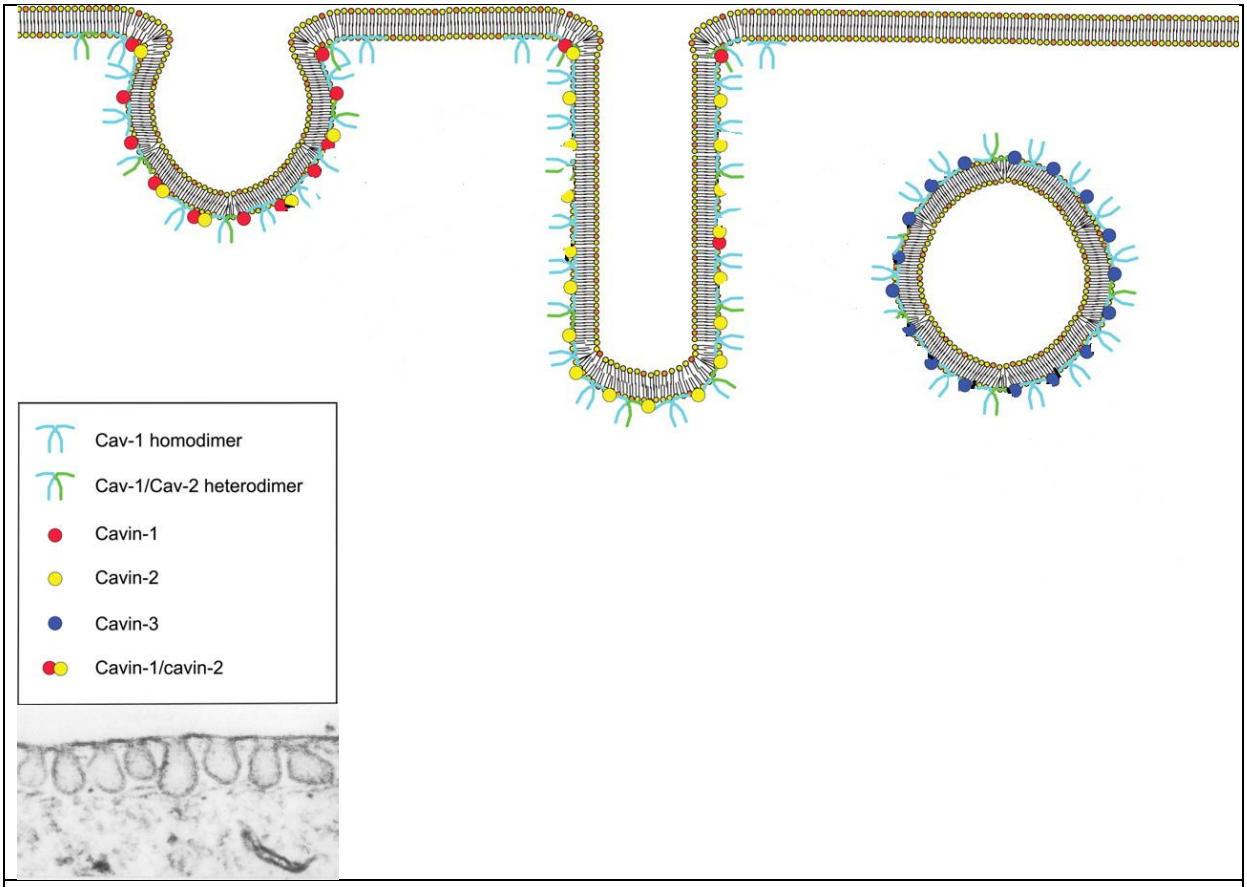

Modified from Rothberg et al (89) and Chidlow et al (93). Cav-1, caveolin-1; Cav-2, caveolin-2.

Caveolin-1 is a protein that remains intracellular, formed via the endoplasmic reticulum (ER) system and transported from the Golgi apparatus to the plasma membrane. CAV1 exit from the Golgi apparatus is accelerated by increasing cholesterol and inhibited after glycosphingolipid depletion (94). There are two isoforms of CAV1, alpha of 178 amino acid length and beta which is 31 amino acid lengths shorter, with the former isoform having a higher affinity for the plasma membrane. The N' terminal and C' termini face the cytoplasm, after tyrosine phosphorylation and palmitoylation respectively (Figure 1-5). Between the termini, there is a hairpin structure hydrophobic domain of 32 amino acids (residues 102-134) that inserts to plasma membrane and is involved in hetero-oligomerization of CAV1 with caveolin-2 (95). Residues 82-101 and 135-150 flank this region, with the latter termed

C' membrane attachment domain that contains a *cis*-Golgi targeting sequence. The N' membrane attachment domain or caveolin scaffolding domain (residue 82-101) is integral in membrane localisation and anchoring of various proteins within caveolae and regulation (both inhibition and enhancement) of their signalling activity (85). Another important site is the tyrosine-14 residue (Y14), which requires phosphorylation for caveolar endocytosis and is important in cell adhesion.

Figure 1-5 Modified colour coded primary structure to the compartments of caveolin-1 in the plasma membrane with inclusion of the Y14 site (95)

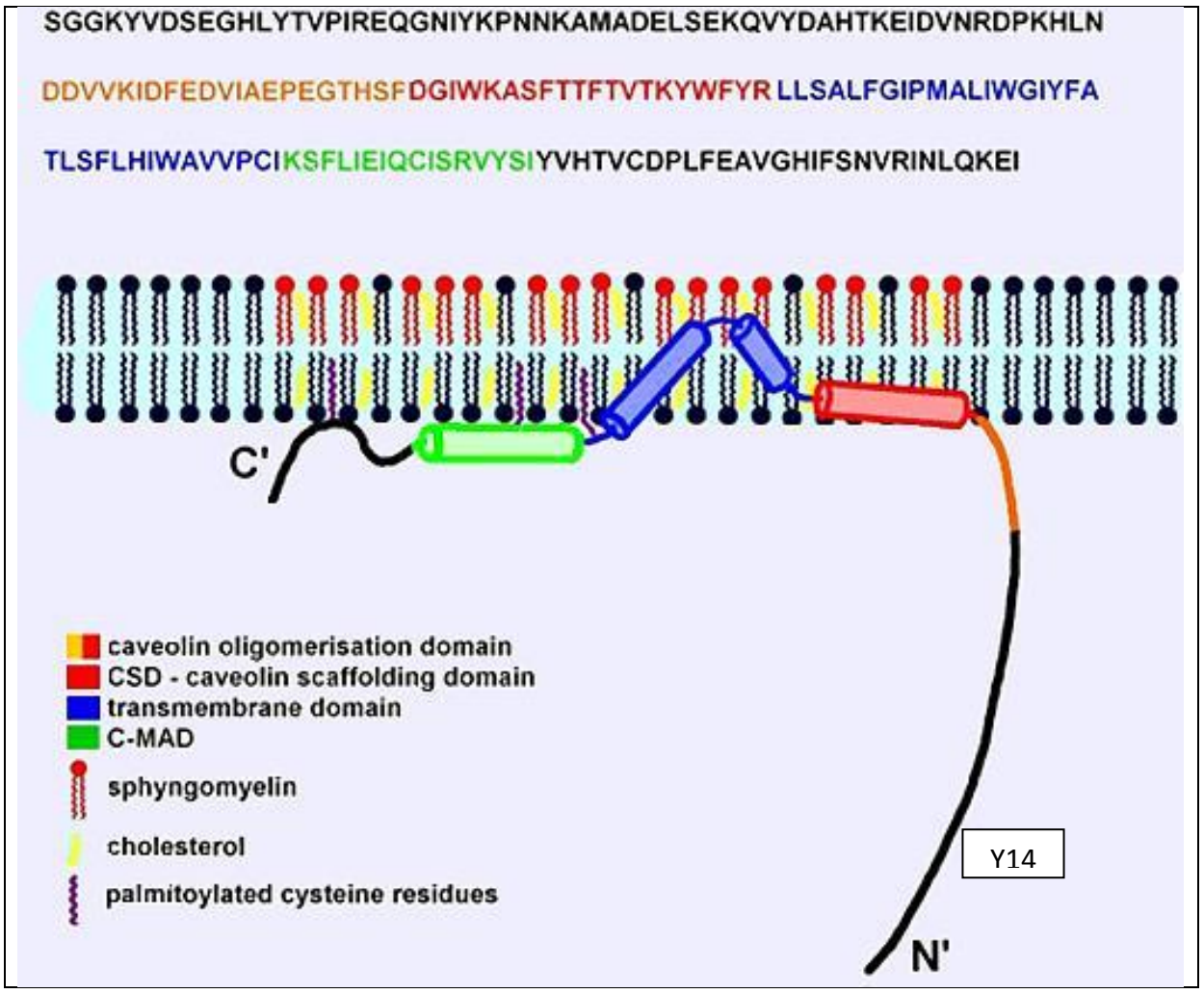

1.2.3 Caveolin-1 gene

The human caveolin-1 gene is located on the long arm of chromosome 7, at genomic locus 7q31.1 (7:116540796) as shown in Figure 1-6. It consists of 3 exons (30, 165 and 342 base pair in length respectively) and 2 introns (1.5 and 32 kilobases in length) spaced in-between. The first exons contain CpG islands that via methylation are thought to be the main part of CAV1 gene expression in cancer cell lines (96). The third exon harbours the functional oligomerisation, scaffolding, transmembrane and C' membrane attachment domains that are highly conserved across species (97).

Figure 1-6 The caveolin-1 human gene on chromosome 7 and its three exons below with size in base pairs (modified from (85))

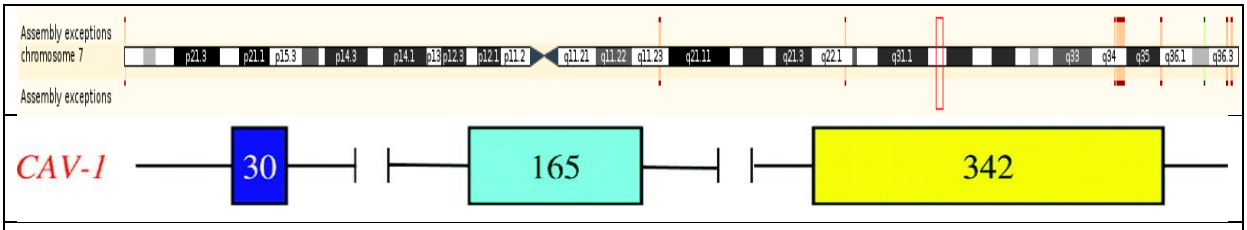

The red rectangle shows the location of the caveolin-1 gene on chromosome 7

1.2.4 Caveolin-1 signalling

There are several roles of caveolae and CAV1 which are integral to cellular function. The most common involves vesicular transport of macromolecules (such as albumin) via transcytosis from the luminal side of the capillary endothelium to the interstitial space via membrane-bound vesicles. The accumulation of gold-labelled albumin in the interstitial space is not seen in the knockout CAV1 mouse by transmission electron microscopy as compared to the wild-type mouse (98). Endocytosis is the second example of vesicular

membrane trafficking by caveolae. Caveolae share similar vesicle docking and fusion molecules (soluble N-ethylmaleimide-sensitive factor attachment protein receptors (SNARE) and dynamin) as seen in the traditional clathrin-mediated endocytosis. Pathogens such as Simian virus 40 and the cholera toxin utilise collections of caveolae for internalisation into the cell, forming with a distinct endosomal compartment with a neutral pH called a caveosome, for delivery to the ER and Golgi apparatus with recycling of CAV1 to the plasma membrane (85, 99).

CAV1 and caveolae are also integral to cellular signalling and signal transduction by compartmentalising receptors upon ligand binding, acting as a chaperone of signalling molecules and ligand bound receptors for delivery to the cell nucleus as well as concentrating such events in the confines of a specific subcellular environment (85). Receptors such as the epidermal growth factor receptor (EGFR) and transforming growth factor beta (TGFβ) receptor are internalised by caveolae upon ligand binding after phosphorylation of Y14 part of CAV1 (100). This internalisation is dependent on Src kinases and protein kinase C (101). Golgi derived CAV1 via SNARE protein syntaxin-6 is also essential for plasma membrane delivery of receptors angiotensin II type 1, insulin and the stretch activated channel short transient receptor potential channel-1 (94).

In the majority, CAV1 effects are inhibitory upon cellular signalling, acting to degrade receptors except in the case of the insulin receptors. The main outcomes of CAV1 signal association are pro-apoptotic and anti-fibrotic. The most commonly described signalling CAV1 associations are with endothelial nitric oxide synthase (eNOS) and TGFβ pathways. CAV1 via its CSD binds eNOS resulting in its inactivity and can act as a reservoir of inactivated

eNOS. The influx of calcium leads to more calmodulin recruitment and binding to the eNOS enzyme leading to its release from bound CAV1 and thus restoration of electron flow from NADPH to its reductase domain flavins and then to the heme moiety of eNOS, generating the vasodilator nitric oxide (NO) from L-arginine. The generation of NO leads to a dissociation of CAV1 scaffold, leading to termination of signal transduction. However, if the substrate L-arginine becomes limited, eNOS functions in an uncoupled mode, leading to the electron transfer to the heme moiety to react with oxygen to form reactive oxygen species (ROS) (102).

ROS releases TGFβ-1 from its latency-associated peptide and latent TGFβ-binding protein to become activated (103). Upon this ligand binding, TGFβ type 1 receptor is phosphorylated after binding with TGFβ type II receptor to form a serine/threonine kinase heterotetrameric complex (Figure 1-7). If this complex is internalised by the early-endosome antigen 1 non-lipid/clathrin raft pathway, this phosphorylates the SARA/Smad 2/3 complex downstream to induce a conformational change that results in heteromerization of Smad 4 and translocation to the nucleus to regulate transcription of pro-fibrotic target genes as well as the downregulation of CAV1 and Smad 7 (104). However, if the TGFβ receptor I/II complex is internalised by caveolae, then SMURF/Smad 7 is recruited and exerts a negative effect upon TGFβ signalling by proteasomal degradation and ubiquitination of the TGFβ receptor complex in CAV1 positive vesicles. In addition, CAV1 diminishes Smad 2 phosphorylation, disrupts its interaction with Smad 4, and prevents Smad 2 translocation to the nucleus, further reducing TGFβ signalling (104).

Other signalling events associated with caveolae endocytosis involve fibronectin degradation and integrin internalisation (105, 106). The detachment of fibroblasts triggers ganglioside GM1 internalisation via CAV1 and its Y14 phosphorylation; GM1 internalisation leads to Rac1 loss from the plasma membrane and its reduced activation (94). Thus not only is CAV1 important in compartmentalising signal transduction in caveolae by concentrating and localising signalling molecules by acting as docking points for numerous cell surface receptors after ligand binding, but also regulates cell adhesion, cell migration via β1-integrins, extracellular matrix (ECM) interactions and acts as flow sensors in endothelial cells and regulates stretch-induced cell cycle progression (94, 106). CAV1 response to chronic shear stress is to increase its levels with redistribution from the Golgi complex to the plasma membrane and formation of caveolae (107). This leads to increased mechanosensitivity with activation of signalling pathways such as eNOS and mitogen-activated protein kinase (MAPK). In *Cav1*$^{-/-}$ mice, show defects in chronic flow-dependent remodelling of blood vessels (108). Upon stretch, cell cycle progression is inhibited with CAV1 downregulation or in *Cav1*$^{-/-}$ smooth muscle cells through pathways including PI3 kinase-AKT/protein kinase B, MAPK ERK, c-Src and integrins (109).

Figure 1-7 Schematic representation of TGFβ ligand (diamond yellow) receptor complex I and II internalisation via clathrin and caveolae rafts (modified from (110))

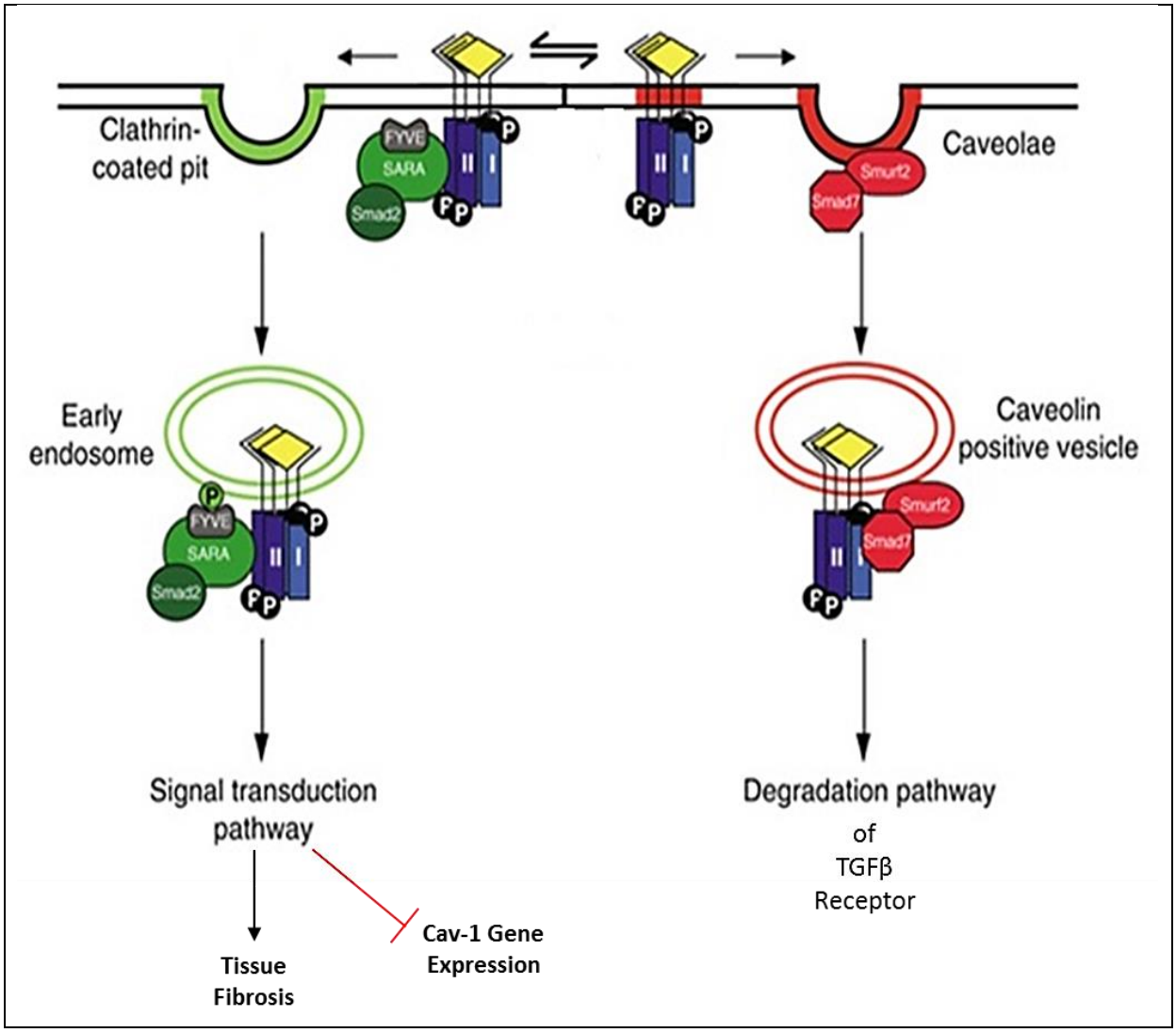

1.2.5 Caveolin-1 in renal adverse outcomes

1.2.5.1 Caveolin-1 in renal fibrosis

CAV1 has been an attractive protein to investigate in the context of organ fibrosis as suggested with its effects described in the previous section and the following section summarises renal fibrotic CAV1 research.

CAV1 interaction with TGFβ in fibrosis is a common pathway by which renal and non-renal chronic disease progresses and thus has been extensively investigated. Li et al used primary murine pulmonary endothelial cells that were capable of obtaining a myofibroblast phenotype after TGFβ-1 stimulation, inducing αSMA expression from wild-type cells. *Cav1*$^{-/-}$ cells produced very high spontaneous levels of αSMA that was corrected upon CAV1 functional restoration using its CSD peptide; thus CAV1 regulates endothelial-to-mesenchymal transition in tissue fibrosis (111). Ito et al (112) showed that adding hyaluronan with its receptor CD44 to immortalised renal proximal tubular epithelial cells (HK2) led to an increase of lipid raft internalisation of TGFβ via MAP kinase from the non-lipid pathway predominance. The authors co-cultured HK2 cells with cells transfected with a Smad responsive promoter and blocked several components (e.g. CD44 and its interaction with hyaluronan) along this pathway to confirm their finding. As the authors state, this conflicts with previous work with metastatic breast tumour cells that suggest hyaluronan promoted the non-lipid pathway, and thus the finding may be dependent on specific tissue microenvironments. Whilst Zhang et al (113) have shown stimulation with IL-6 led to more non-lipid raft pathway dominance for the TGFβ receptor in HK2 cells and a decrease in the

association of the IL-6 receptor to CAV1 upon co-immunoprecipitation. This was after the observation that IL-6 is only expressed on proximal tubular epithelial cells at times of renal disease. However despite the affinity labelling findings, it was noted that stimulation with IL-6 and TGFβ-1 did not lead to an increase in Smad 2 or 3 or 7 protein expression, but only the luciferase assay suggested more Smad activity.

As well as TGF, there have been many other signalling events associated with CAV1 in renal fibrosis and are summarised in Table 1-1 and further described below. Peng et al (114) showed a Src dependent phosphorylation of the CAV1 Y14 site occurred with RhoA activation and formation of ROS when they mechanically stretched mesangial cells via a cyclic vacuum as a model of intraglomerular hypertension leading to glomerulosclerosis. In the *Cav1* knockout mouse, there was no RhoA or ROS activation but this function was promptly restored upon restoration of Cav1 (115).

Table 1-1 Summary of cytokines, chemokines and receptors associated with caveolin-1 in renal fibrosis

Cytokine/Chemokine/Receptor	Effect of caveolin-1 interaction
Angiotensin II	In vascular smooth muscle cells, promotes angiotensin II type 1 receptor binding to caveolin-1. This promotes Rac1 into caveolae, increasing localised reactive oxygen species production and EGFR transactivation.
Angiotensin II type 1 receptor	CAV1 required for its renal expression in a basal state. This receptor is required to mediate angiotensin II induced ROS production by NAPDH oxidase. This oxidative stress is seen in spontaneously hypertensive rats. Treatment with losartan (angiotensin II type 1 receptor antagonist) to these rats results in increased CAV1 expression and co-localisation with heat shock protein 70 to the plasma membrane in proximal tubules and reduced Nox4 co-immunoprecipitation with heat shock protein 70 (116).
β1 integrins	Act as mechanosensors bound to CAV1 in human umbilical vein endothelial cells (117).
CD40	CAV1 associated with CD40 in antigen presenting cells (B lymphocytes, macrophages, dendritic cells). Upon CD40 binding to its ligand (CD40L), c jun NH2-terminal kinase, p38, MAP kinases, Src related kinases dissociate from CAV1 and are mainly pro-inflammatory. Plasminogen activator inhibitor-1 is a powerful fibrotic mediator that is released after CD40 cross-linking with tumour necrosis factor receptors which results in Lyn phosphorylation association with CAV1 (118).
CXCR4	CXCR4 dimerization induced by stromal derived factor-1 occurs in caveolae, for homing of haematopoieitic stem cells and enodthelial progenitor cells (119).
Endothelial-1	Example of regulatory activity of caveolin-1 that binds the endothelial receptor B in a basal state, but is released upon ligand binding with endothelial-1 to promote downstream signalling. However, endothelial-1 increases caveolin-1 to bind and internalise and degrade

	its receptor B, thus reducing prolonged endothelial-1 effects (120).
Endothelial nitric oxide synthase/nitric oxide release	Unbinding of endothelial nitric oxide synthase from caveolin-1 is required for its activation and release of nitric oxide. This is achieved by increased cytosolic calcium or Akt activation, leading to nitric oxide induced endothelial relaxation. Paradoxically this could lead to an impaired renal arterial autoregulation. Reduced CAV1 leads to a reduced myogenic response to stretch. Excess eNOS activity leads to increased vascular permeability to serum albumin. Also with less caveolin-1 and more eNOS activity and nitric oxide release at a basal rate, there is an impaired nitric oxide induced relaxation upon stimulation.
HO-1	Heme-oxygenase 1 is upregulated in periods of oxidative stress such as in ischaemic-reperfusion injury. CAV1 directly inhibits its anti-apoptotic actions (121).
Nephrin	In a model of angiotensin II podocyte injury, nephrin dephosphorylation resulted in podocyte apoptosis. This dephosphorylation required caveolin-1 Y14 phosphorylation with interaction with Csk (negative regulation of Src kinases) (122).
p42/44 MAP kinase	Suppressed by caveolin-1 and thus mesangial cell proliferation induced by bFGF and PDGF (123).
PDGFR	Increased PDGF results in internalisation of its receptor and increased turnover of caveolin-1 and renal cell proliferation (124).
RhoA	In primary mesangial rat cells, TGFβ-1 induced RhoA activation is prevented by caveolae disruption and downstream TGFβ-1 collagen-1 accumulation. TGFβ-1 induced RhoA activation is dependent on Y14 CAV1 phosphorylation (114).
Survivin	CAV1 acts as a tumour suppressor through survivin suppression that is dependent on β-catenin-Tcf/Lef pathway with E-cadherin. Survivin is a protein inhibitor of apoptosis and controls progression through the G2/M

	checkpoint of the cell cycle. Cyclin-1, c-myc and VEGF gene expression are also reliant on this pathway (125).
TGFβ	CAV1 suppresses TGFβ-1 signalling after it has bound to its receptor by internalising and proteasomal degradation of the receptor through recruitment of the SMURF/SMAD7 TGFβ-inhibitory complex, reduced SMAD 2 signalling and reduced TGFβ type II gene expression.
TNFα	TNF receptor 1 and CD36 are co-localised to caveolae like domains in TNFα induced apoptosis (126).
VEGF	Increases caveolae number and caveolin-1 related structures to form fenestrae in glomerular endothelial cells and thus permeability (1, 9). Causes a nearly 2.5 fold increase in VEGFR2/CAV1 association in vitro mesangial cells and this increase is seen in steptozotocin induced in vivo rat model of diabetic nephropathy via Src induced Y14 phosphorylation (127).
VEGFR2	Is negatively regulated by caveolin-1 as seen in tumour growth and permeability (128). ROS important for VEGFR2 autophosphorylation.

As another model of hypertension, Bocanegra et al (116) investigated the protective profile of losartan upon proximal tubular cells from spontaneously hypertensive rats, whose CAV1 expression was significantly reduced compared to control. Losartan (an angiotensin II type 1 receptor antagonist) was noted to reduce ROS through Nox4 downregulation and NADPH inactivation, through increased levels of CAV1 and co-localisation with Heat shock protein 70. However two questions remain: was this just a by-product of the blood pressure lowering ability of losartan and why none of these effects were seen in the control group? The editorial comment focussed on the mechanisms behind hypertension and ROS production causing reduced renal function and structural damage; this was mainly to

inappropriate activation of intrarenal angiotensin II within the proximal tubules due to its translocation of angiotensin II type 1 receptor (AT1) from the plasma membrane to CAV1 rich domains. Here, CAV1 acts as a molecular chaperone to AT1, providing a platform for redox signalling events through NADPH oxidase dependent production of ROS via Nox4 (129).

Genetically obese Zucker rats on a casein diet have also been shown to have reduced eNOS and raised CAV1 in renal structural damaged kidneys as compared to those on a soy diet, but again, CAV1 is known to fluctuate with cholesterol levels making it difficult to interpret the findings (130). From Valles et al (131), ureteric obstruction leads to an early rapid intrarenal angiotensin II rise that leads to an increase in extracellular matrix protein production and oxidative stress damage causing fibrosis. Nitric oxide can ameliorate interstitial fibrosis and in loss of eNOS leads to marked tubulointerstitial fibrosis in the inducible NOS knockout mouse. CAV1 is expressed in vascular endothelium, smooth muscle and epithelial cells of the proximal, distal and convoluted tubules and ducts. CAV1 also leads to apoptosis via inhibition of p42/44 MAP kinase signalling. Thus the authors wished to look at the role of CAV1 expression in congenital unilateral ureteropelvic junction obstruction with grade IV hydronephrosis on imaging requiring surgical intervention after vesico-ureteral reflux was excluded. The 19 children had ‘normal renal function for their age’, were on no medication and were normotensive. The scorers of interstitial volume and CAV1 staining were blinded. There were two groups with group 1 split into subset A with obstruction <1yr, subset B with obstruction >1yr, and group 2 had significant renal impairment compared to group 1 (99mTc-DPTA renal scan expression of kidney filtration rate 28.8±2% to 39.7±2.1% respectively). The results showed group 2 CAV1 was present in the proximal tubule unlike

control and group 1, as well as co-localising with the AT1 receptor. Increased CAV1 expression was confirmed on Western Blotting for protein transcription from group 2's urine. eNOS was low in group2 ($p<0.01$). Unfortunately the control was based on children with renal cell carcinoma where it is known that CAV1 has expression can be altered and may thus not act as a true control.

Further to the above human study suggesting increased CAV1 expression in the more chronic and fibrotic group in children, histological increased glomerular expression of CAV1 in Japanese patients has been identified in diseases that target the glomerulus such as diabetic nephropathy, membranous nephropathy and focal segmental glomerulosclerosis (132). It was also noted that CAV1 expression was also reduced in glomerular endothelial cells with the use of steroids. In diabetic nephropathy, murine *Cav1* knockout led to a worse glomerulosclerosis and albuminuria in the streptozotocin model of type 1 diabetic nephropathy, though there is limited tubulointerstitial fibrosis in this model (133). CAV1 increased expression was also noted in a streptozotocin rat model of diabetic nephropathy with increased VEGF receptor 2 (VEGFR2)/CAV1 association in vivo (127). In vitro, primary rat mesangial cells after stimulation with VEGF, caused more CAV1/VEGFR2, CAV1/Src expression and fibronectin upregulation via RhoA activation. Transfection of mesangial cells with an overexpression of non-phosphorylatable CAV1 Y14 prevented VEGF-induced RhoA activation and fibronectin upregulation. Another model of nodular glomerulosclerosis utilises human urinary free light chains from patients suffering from light chain deposition disease injecting to wild-type and *Cav1* knockout rats' tail veins to induce nodular glomerulosclerosis. In the *Cav1* knockout, there was increased nodular glomerulosclerosis

and increased mesangial matrix production, however there was a mix of gender used that may have influenced the results (134).

Other human studies have focussed on CAV1 in renal transplantation. Yamamoto et al (135) have previously shown that de novo caveolae formation occurs in transplant glomerulopathy in glomerular endothelial cells and now investigate CAV1 in chronic active antibody mediated rejection and thus transplant capillaropathy, where they found CAV1 to be associated with peritubular capillary endothelia that is not normally present in healthy kidney. Pontrelli et al (118) also investigated chronic allograft nephropathy secondary to immune system activation where CD40 is upregulated in acute rejection in proximal tubular epithelial cells. This led to increased Lyn phosphorylation and thus NFκB activation. Lyn phosphorylation is strictly associated with CAV1 and inhibiting Lyn blocked the profibrotic induction of PAI-1.

Park et al (119) have used an unilateral ureteric obstruction (UUO) model in FVB/N mice to investigate the surge of stem cells that occurs upon 10 days after ligation of the left ureter. In the *Cav1* knockout, the mesenchymal stem cell post obstructive surge was blunted significantly which led to no regeneration of the parenchyma and marked fibrosis as measured by Sirius red staining. Indeed some of the surge could be from the response of the resident kidney stem cells. In this model, the FVB/N wild-type mice are a different strain to the Cav1 knockout mice and the control kidney was the contralateral kidney of each mouse. These factors could affect the interpretation of their findings as different mouse strains have varying susceptibility to fibrosis and the contralateral compensation after ligation of the ureter could be different.

In summary, there appears to be negative effect of CAV1 expression leading to a worse renal phenotype especially in glomerular disease. However, this is in opposition to the non-renal literature where the CAV1 reduction in patient samples or knockout of caveolin-1 in vitro has been found to lead to a more fibrotic phenotype. This may be due to the organ and microenvironment studied such as in bleomycin induced lung fibrosis (136), idiopathic pulmonary fibrosis (137), scleroderma/systemic sclerosis (138), cardiac fibrosis (139) and keloid scars (140) which involve more TGFβ dependent processes that are reliant on the expression of CAV1 in fibroblasts.

1.2.5.2 Pleiotropic effects of caveolin-1 in adverse renal outcomes

As well as tubulointerstitial fibrosis, there are common adverse outcomes experienced by patients as their renal disease progresses as described in section 1.1.2. Due its ubiquitous nature of distribution, CAV1 has been associated with many of these outcomes.

Infection: In patients suffering from scleroderma associated lung disease, their bronchoalveolar lavage revealed activated monocytes and polymorphonuclear cells; these patients' monocytes, neutrophils and T cells had a reduced expression of CAV1 (136). In mice exposed to lipopolysaccharide challenge, the deletion of *Cav1* led to a decreased expression of CD14 and CD36 during macrophage differentiation and suppressed phagocytic ability and impaired bacterial clearance (141). *Cav1* knockout mice also had an increased mortality with induced Pseudomonas aeruginosa and Klebsiella pneumoniae sepsis (142, 143). In cystic fibrosis, effective internalisation of pathogens such as Pseudomonas aeruginosa is required for an appropriate immune response for its clearance; its

internalisation is reliant on CAV1 in type 1 pneumocytes and bladder epithelium (144). CAV1 interaction with protein kinase Cα upon activation and calcium release is essential for its translocation to caveolae in order for production of infectious enveloped human cytomegalovirus particles in fibroblasts (145). Infection with polyomavirus viraemia can cause BK nephropathy in renal transplant recipients. Moriyama et al in vitro data shows this viral entry in human proximal tubular epithelial cells requires co-localisation with CAV1 for caveolae entry into the cells (146).

Cardiovascular disease: CAV1 has been associated with an inflammatory macrophage phenotype that promotes atherosclerosis by the production of foam cells (147). Schwencke et al have found reduced CAV1 expression in VSMC of human atheroma (148). CAV1 also binds eNOS in an inactive state and with an influx of calcium, its release thus affecting vascular function (149). In the *Cav1* knockout mouse, cardiac hypertrophy occurs despite the high presence of caveolin-3, in which the latter is thought to be the predominant isoform of caveolin in the heart (150).

Malignancy: CAV1 may have a tumour suppressive role depending on the cancer type. CAV1 has been shown to promote apoptosis and in *Cav1* knockout mice, hyperactivation of the p42/44 MAP kinase cascade and cyclin D1 upregulation in breast cancer models lead to cancer progression and metastases (151). CAV1 has been considered as a prognostic marker in several cancers (152). However, in prostate cancer, CAV1 upregulation has been associated with progression of the malignancy (153), highlighting CAV1 altered function depending on the organ microenvironment studied.

Diabetes: CAV1 scaffolding domain binds to the insulin receptor and lack of CAV1 in adipocytes results in reduced phosphorylation and lack of translocation of GLUT-4 to the plasma membrane, leading to reduced glucose uptake and insulin sensitivity especially amongst patients with hypertension (154, 155). Metformin has also been shown not to reduce hyperglycaemia in *Cav1* knockout mice that are naturally hyperglycaemic compared to their wild-type counterparts (155). The *Cav1* knockout mouse adipocytes have chronically elevated hepatic gluconeogenesis and also show defects in insulin secretion and mitochondrial function (155, 156). In a lipotoxic environment, pancreatic β cells are protected against apoptosis by SREBP-1c/CAV1 signalling involved in PPARβ/δ-regulated GLP-1R expression (157).

1.3 Thesis Hypothesis

Identification of patients with relative positive or maladaptive phenotypes is necessary for the concept of personalised medicine to design treatment protocols for the individual rather than the traditional population based strategy. Thus the approach of candidate SNP association has been used in this thesis to identify patients at risk of adverse outcomes in renal disease.

HYPOTHESIS: Can the pleiotropic effects of caveolin-1 differentiate patients' phenotype in chronic kidney disease?

AIM 1: To differentiate patients' phenotype in kidney disease by *CAV1* and related candidate gene SNPs.

AIM 2: To investigate if the lack of *Cav1* leads to an increased fibrotic phenotype in experimental renal fibrosis.

1.3.1 Thesis Chapters

In renal transplantation, donor *CAV1* SNP rs4730751 has been associated with renal transplant organ survival, function and fibrosis (82, 158). In haemodialysis dependent patients, this SNP has been associated with carotid intima medial thickness (159). Thus the SNP has been used in this thesis, using a series of candidate SNP association studies to clinical phenotypes in CKD, to demonstrate if the pleiotropic effects of *CAV1* can differentiate patients with a worse phenotype. Renal tubulointerstitial fibrosis is the cornerstone of progression of CKD irrespective of the underlying cause (160); by using animal models the effects on fibrosis by the knockout of *Cav1* can be explored in this thesis. The following scenarios are used to explore the thesis hypothesis and aims:

a) Cardiovascular disease in CKD can be attributed to 2 distinct pathological processes – atherosclerosis and arteriosclerosis (161, 162). While the risk of athero-thrombotic events such as myocardial infarction is elevated, arteriosclerosis leading to vascular and myocardial damage (in particular left ventricular disease) is the predominant process resulting in a higher risk of sudden cardiac death from arrhythmias and congestive heart failure. Left ventricular disease and arterial remodelling is further exacerbated by patients undergoing haemodialysis due to recurrent fluid excess requiring removal over short haemodialysis sessions, myocardial ischaemia and myocardial stunning (159, 163, 164). The determinants of the severity of myocardial disease are poorly characterised though hypertension, oxidative stress and activation of the renal angiotensin system are all thought to be relevant.

Genetic predisposition research to the development of heart failure in CKD has been limited (165). In the general population, there has been interest in the association between the

Glu298Asp rs1799983 polymorphism within *eNOS* and heart failure (166, 167). Although this polymorphism has been associated with endothelial dysfunction and progression of CKD (168), it is not known if this polymorphism is associated with early cardiac structural changes that occur in non-dialysis CKD.

Testa et al found that there was a significant independent and interaction association between *CAV1* rs4730751 and *eNOS* rs1799983 genotype and increased carotid arterial intima thickness (vascular hypertrophy) and cross-sectional area across the common carotid artery (arterial remodelling) (159). It is not clear if these associations occur in non-dialysis CKD or just a phenomenon seen in haemodialysis patients. eNOS is bound to CAV1 requiring a calcium influx for its release from CAV1 in order to become activated.

In light of this, I investigated if these gene variants are associated with pulse wave velocity (as a cardiovascular mortality prognostic marker of arterial stiffness (169)) changes in non-dialysis CKD. These gene variants were also investigated for associated changes in systolic and diastolic left ventricular (LV) function, based on detailed cardiac magnetic resonance imaging (CMR) in non-dialysis CKD patients with no known history of heart failure.

b) Anti-neutrophil cytoplasmic antibody associated vasculitis is a multisystem disorder that affects the kidneys and lungs predominately. Despite recent therapeutic success in improving the first year survival rate over the last 2 decades, there remains up to 28% 5 year mortality rate and significant morbidity associated with the complications and treatment of the disease, such as infection, cardiovascular disease, malignancy and progression of renal disease that mirrors the pleiotropic effects of CAV1 described in section 1.2.5.2 (170).

c) Emerging paradigms of new onset diabetes after transplantation (NODAT) have focussed on understanding risk factors (e.g. post-transplant hyperglycaemia and immunosuppressive agents) involved in its pathogenesis with the aim of identifying those at risk and development of potential prevention and treatment strategies (171). Genetic risk of NODAT and identification of potential associated single nucleotide polymorphisms (SNPs) have increased our knowledge base of pathways involved in NODAT (172, 173).

d) The trigger in fibrosis is initiated by the sterile inflammation response to danger associated molecular pattern signals that are released from damaged tissue from almost any insult. This leads to two main patterns of response, namely immune activating and non-activating apoptotic pathways (174). This response of the resident stroma of the kidney via chemokines and cytokines supports the infiltration of leukocytes. The combination effect of this crosstalk appears to influence fibrotic development (175). CAV1 is reported to be found in leukocytes and stroma and is a potential link to understanding this crosstalk (136, 176).

However, as mentioned in section 1.2.5.1, the effects of CAV1 in renal fibrosis remain unclear. Hence, the aim is to investigate if *Cav1* knockout leads to more fibrosis. Two mouse fibrotic models are used to investigate tubulointerstitial fibrosis. UUO and ciclosporin-A (CsA) nephrotoxicity are two mouse models of renal fibrosis that reflect clinically significant entities in humans of obstructive uropathy, and in renal transplant patients CsA induced nephropathy. The nephropathy profile consists of tubulointerstitial fibrosis, tubular atrophy, glomerulosclerosis, loss of glomerular and peritubular capillaries, characterised by macrophage influx. The UUO model has the advantage of being a reliably reproducible and quick model with marked destruction of the renal architecture by day 14 after the ureter is

tied. It is also advantageous as the contralateral kidney undergoes hyperfiltration compensation that means the overall kidney function is not curtailed. However, the CsA model allows a less destructive patchy fibrosis to develop over a longer duration (28 days) with resulting bilateral renal disease and chronic kidney function impairment.

A search in Pubmed of 'caveolin-1 knockout mouse' (24th February 2016) reveals nearly 500 associated publications since 1998. It has mainly been utilised to highlight signalling events associated with CAV1 as discussed above as well as mirror human diseases such as scleroderma associated lung fibrosis. The *Cav1* knockout mouse (CKO) is surprisingly viable and initially fertile considering the inability to form caveolae and CAV1's ubiquitous distribution. However, the CKO does have a lower lifespan than its wild-type counterpart. In a 2 year study it was noted that the CKO lifespan was about half its wild-type, between 7-16 months of age, displaying marked pulmonary fibrosis, pulmonary hypertension and cardiac hypertrophy (177). Table 1-2 reflects some of the most important phenotypic changes seen in the CKO mouse.

Table 1-2 Phenotypes of caveolin-1 knockout mouse (Modified from (178))

Organ system and phenotype	*Proposed mechanism*
Cancer	
Increased sensitivity to carcinogens	Increased cyclin D1 and ERK 1/2 levels
Cardiac	
Cardiac hypertrophy	p42/44 MAP kinase hyperactivation
Dilated cardiomyopathy	Unknown, increased fibrosis at 12months
Central nervous system	
Reduced brain weight; multiple motor and behavioural abnormalities	Altered maintenance of cortico-striato-pallido-thalamo-pontine pathways involved in motor control
At age 3-6months develop Alzheimer's disease characteristics	Increased beta and tau deposits
Endocrine-metabolic	
Adipocyte abnormalities with impaired lipolytic activity and altered lipid droplet architecture	Altered lipid homeostasis; altered perilipin phosphorylation
Accelerated mammary gland development	Hyperactivation of prolactin signalling
Decreased glucose uptake	Insulin resistance and altered glucose transporter localization. Over 2-fold reduction in plasma leptin levels
Gastrointestinal	
Hyperproliferation of intestinal crypt cells	Upregulation of Wnt/β-catenin signalling
Reduced nitric oxide-mediated intestinal smooth muscle relaxation	Abnormalities in interstitial cells of Cajal and smooth muscle
Decreased liver regeneration post-hepatectomy	Impaired coordination of lipid metabolism and cell proliferation
Immune system	

Increased susceptibility to bacterial infection	Macrophages exhibit increased nitric oxide and inflammatory response with increased chemokines to CCL3, IL-6, IFNy TNF-α and CXCL10 3 days post Salmonella infection and reduced survival from 13 days to 7 days compared to wild-type with reduced neutrophil recruitment.
Lymphoreticular	
Reduced response to thymus-independent antigens	Unknown
Pulmonary	
Constricted alveolar spaces	Thickened alveolar wall
Pulmonary hypertension with reduced exercise tolerance after 10mins of swimming	Multiple causes
Transport	
Disruption of glycosylphosphatidyl inositol-anchored protein transport	Altered Golgi protein processing
Urogenital	
Impaired renal calcium absorption	Abnormal function of plasma membrane calcium ATPase
Enlarged seminal vesicles	Engorgement of seminal fluid
Bladder hypertrophy	Smooth muscle hyperplasia
Vascular	
Reduced aortic contractile tone	Increase in endothelial nitric oxide activity
Impaired angiogenic response	Altered VEGF protein interactions
Neointimal hyperplasia	Increased cyclin D1 and ERK 1/2 levels
Microvascular permeability	Altered clefts and tight junctions
Abnormal arterial remodelling during changes in flow	Altered mechanotransduction

CHAPTER 2:

MATERIALS AND METHODS

2.1 Material and Methods

2.1.1 Methods for Human Studies

2.1.1.1 Genotyping

2.1.1.1.1 PAXgene DNA extraction from whole blood for genotyping

In all genotyping studies in the thesis, whole blood was collected in PAXgene Blood DNA tubes (Qiagen, Manchester, UK), frozen at -20°C for 24 hours in a wire rack (to prevent tubes from cracking) and then stored at -80°C. Samples were defrosted at room temperature for 2 hours and inverted 10 times to homogenise the sample as plasma and red cells had separated, before starting the DNA extraction process. DNA extraction was undertaken using the PAXgene Blood DNA Kit (Qiagen Manchester, UK). Firstly, 8.5ml of whole blood was poured from PAXgene Blood DNA Tubes into a 50ml falcon tube and then 25ml of PAXgene cell lysis buffer was added. The solution was briefly mixed by inversion to lyse the red and white blood cells. Cell nuclei and mitochondria were pelleted by centrifugation at 2500 x *g* for 5 minutes. The excess solution was then poured into a disposable jar (containing 1% virkon solution) without disturbing the cell pellet. The cell pellet was washed by adding 5ml of PAXgene wash buffer and vortexed vigorously for 5s before discarding the supernatant. The pellet was then resuspended using 5ml of PAXGene digestion buffer/protease and vortexed for 20s. Protein contaminants were removed by incubation with 5ml of PAXgene digestion buffer/protease enzyme at 65^{o}C in a water bath for 10 minutes. To enable DNA to be precipitated from solution, 5ml isopropanol was then added and the solution inverted 20 times until visible white strands of DNA clumped together. The sample was then centrifuged for 3 min at 2500 x *g* to pellet the DNA. The supernatant was discarded and the tube

inverted on a clean piece of dry absorbent paper for 1 minute. The pellet was then washed in 5ml of 70% ethanol and vortexed for 1s before a further centrifugation step at 2500 x *g* for 3 minutes. The supernatant was then discarded and the samples was left to dry by inverting the tube on a clean piece of absorbent paper for 5 minutes, dabbed to remove any ethanol on the rim, before being left inverted for a further 5 minutes. The DNA pellet was then resuspended by adding 1ml PAXgene resuspension buffer and incubating for 1h at 65°C in a water bath. The DNA was then stored at -20^{o}C until DNA quantification.

2.1.1.1.2 PicoGreen DNA Quantification

DNA was then quantified using PicoGreen DNA quantification. Calf thymus DNA (1mg/ml) (Sigma Aldrich, St Louis, USA) was resuspended in 1ml T.E. buffer [T.E. Buffer is made from 10ml of Tris-EDTA 100x concentrate (Sigma Aldrich, St Louis, USA) added to 990ml of Baxter H_2O (Baxter, Compton, UK)] and left overnight. Using the resuspended calf thymus DNA and T.E. Buffer, a serial dilution was created, to be used as standards, with the following known concentrations produced: 800ng/ml, 400ng/ml, 200ng/ml, 100ng/ml, 50ng/ml, 25ng/ml, 12.5ng/ml and 6.25ng/ml. The DNA samples were then diluted: 2ul of neat DNA sample in 198ul T.E. Buffer. Both the serial dilutions from the calf thymus DNA and the samples were left to resuspend overnight at 4^{o}C. Standards and DNA samples were mixed with PicoGreen reagent (Invitrogen, Carlsbad, USA) in a 96 Flat-well Microplate (Alpha Laboratories, Eastleigh, UK). Duplicates of 50µl of each standard were mixed with 50µl of a PicoGreen solution A (made up from a stock of 1194µl of T.E buffer and 6µl of PicoGreen reagent). 5ul of the each diluted DNA samples in duplicate were mixed with 95ul of PicoGreen solution B

(made up of 7580µl of T.E. buffer and 20µl of PicoGreen reagent). Once the PicoGreen reagent had been applied, the plate was covered in foil and left for 10 minutes to let the picogreen integrate into the DNA. The plate was then read using the cytofluor multi-well plate reader series 4000 (Perseptive Biosystems, Framingham, USA) with excitation set at a wavelength of 485nm and emission set at a wavelength of 530nm. From this the concentration of DNA for each sample could be calculated by comparing to the known concentration of the standards (Figure 2-1).

Figure 2-1 PicoGreen standard curve using known concentrations of calf thymus

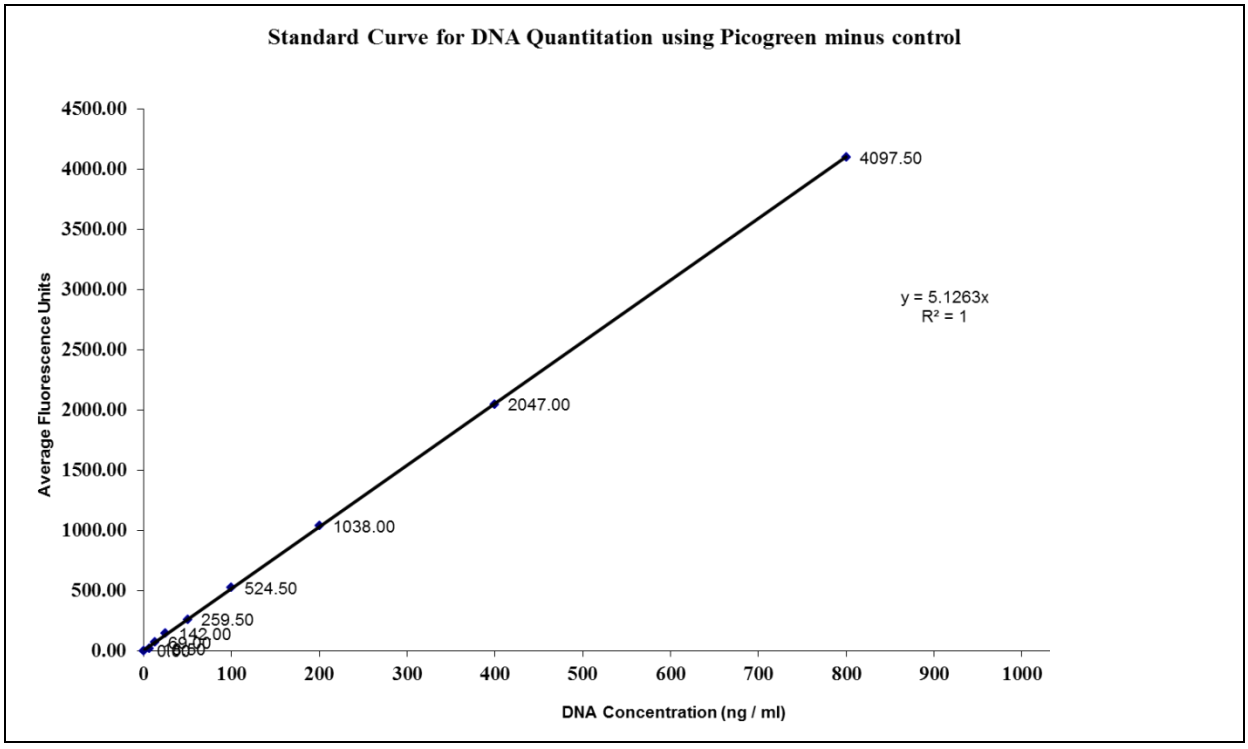

2.1.1.1.3 Genotyping of Single Nucleotide Polymorphisms using Taqman

All DNA samples were then all diluted to a working stock of 4ng/µl. To enable genotyping, 2.25µl of DNA was added to a 384-well plate along with 2.75µl of assay master mix

[consisting of 2.50µl of ABI Genotyping Master Mix (Applied Biosystems, Foster City, USA), 0.09µl of SNP Assay on Demand genotyping assay (Applied Biosystems, Foster City, USA) and 0.16µl Millq H_2O/ DNA sample]. The SNPs assayed were for *CAV1* rs4730751 and *eNOS* rs1799983. Polymerase chain reaction (PCR) amplification as performed on a M J Research PTC-225 Peltier Thermal cycler (Genetic Research Instrumentation, UK) under standard Taqman genotyping conditions with 50 PCR cycles were undertaken. Plates were read using a 7900HT Fast Real-Time PCR System (Applied Biosystems, Foster City, USA) which reads the fluorescence release from each allelic-specific Taqman probe allowing the genotype of each sample to be deduced.

2.1.1.1.4 SNP genotyping using the Sequenom MassARRAY iPLEX platform

Sequenom genotyping (Sequenom Inc., Hamburg, Germany) allows the detection of polymorphisms at multiple SNPs simultaneously (iPLEX Gold technology). Initially, PCR primers were designed to amplify all regions containing the SNPs of interest using MassARRAY Assay Designer v4.0; primers were sourced from Metabion (Martinsried, Germany). Following PCR amplification in TF-0384 PCR plates (Thermo Scientific, UK), shrimp alkaline phosphatase dephosphorylates unbound nucleotides to eliminate them from further reactions. Extension primers were designed which were specific for the DNA sequence adjacent to each SNP. These anneal to the PCR-amplified DNA in the presence of a high fidelity polymerase enzyme. Adenine, cytosine, guanine and thymine nucleotides which have been modified by the removal of the hydroxyl group at the 3' end (ddNTPs) are added to this reaction so that one modified base is added to each extension primer. The removal of the

hydroxyl group prevents subsequent base extension causing termination of the DNA sequence once these modified bases are incorporated at the SNP locus.

The determination of each individual's genotype relies upon the ability of Matrix Assisted Laser Desorption Ionization Time of Flight technology to detect the differences in mass between the incorporated bases at the SNP loci. The DNA samples are ionised by a laser and accelerate through the mass spectrometer to the detector. The allele is determined by the rapidity with which the ion is detected with heavier bases detected last (179). SNP analysis was undertaken using the MassARRAY Compact instrument with Typer version 4.0 software (Sequenom) as shown in Figure 2-2. This technology was used in Chapter NODAT studies.

Figure 2-2 Genotyping using Sequenom technology highlighting rs2265919

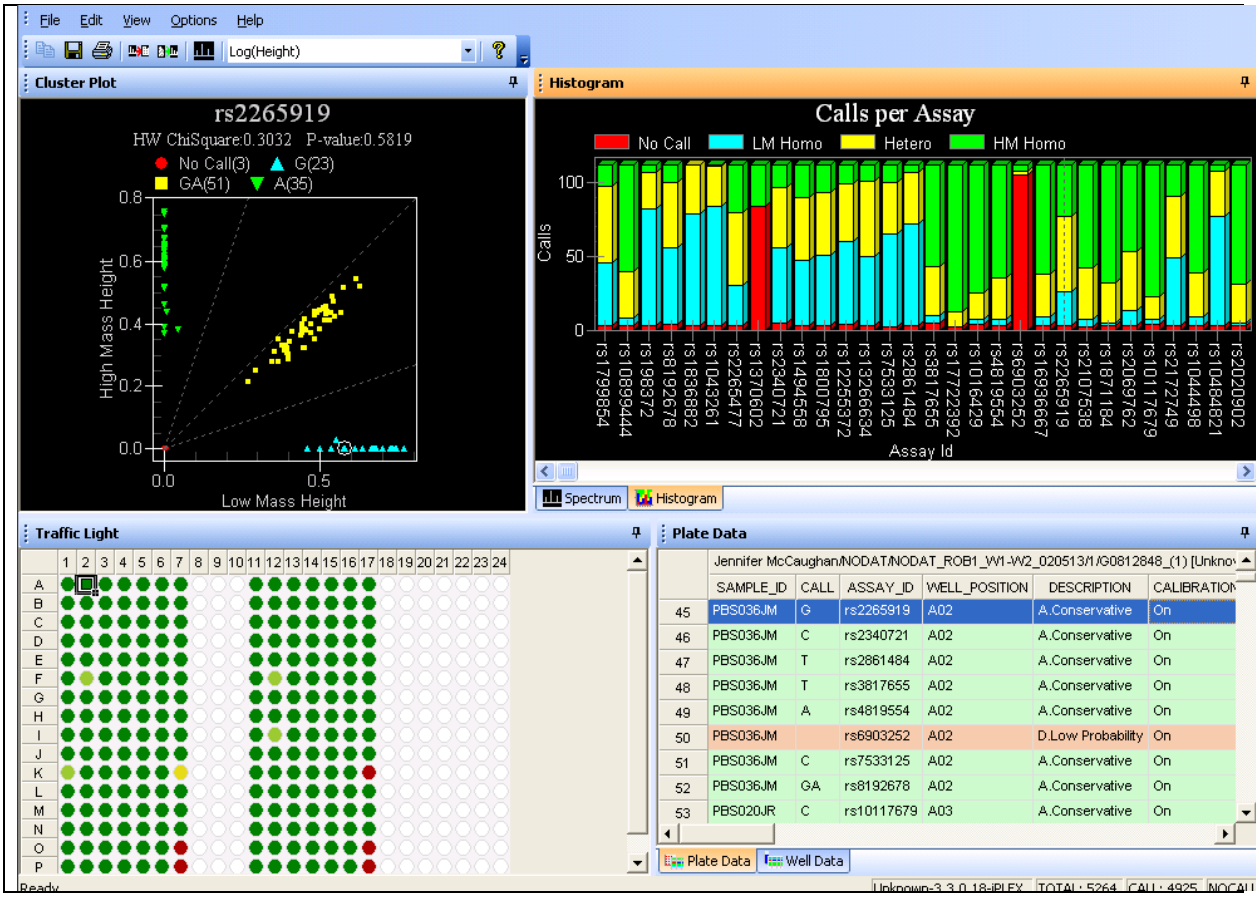

2.1.1.2 Laboratory testing

Routine laboratory testing included haematological (Beckan Coulter Haematology Analyser) and biochemical profiles and urinary albumin:creatinine measurements (Roche Hitachi 702 Analyser); performed by Queen Elizabeth Hospital Birmingham laboratory.

2.1.1.3 CAV1 in aortic pulse wave velocity

Two independent cohorts were investigated as part of this study. Baseline data including aortic pulse wave velocity (aPWV) was collected by original study investigators. Subsequent

ethical approval and genetic testing consenting was performed by me. The first included patients with early CKD enrolled into 2 randomised controlled trials as part of the larger "CRIB" studies (Chronic Renal Impairment in Birmingham). Baseline data was analysed in these patients who were participating in these two completed, single centre RCTs (CRIB-II (180) and CRIB-PHOS (181)) based at the Queen Elizabeth Hospital Birmingham, United Kingdom between 2005-2011. Both these studies were interventional in design, but baseline data was collected prior to the institution of any change in therapy. Inclusion criteria for these studies were: baseline aortic pulse wave velocity investigations, age 18-80 with eGFR 30-89ml/min/1.73m^2, total cholesterol <5.5mmol/L, resting blood pressure controlled to <140/90 for at least 6 months. Exclusion criteria were: diabetes mellitus, peripheral vascular disease, symptomatic cardiovascular disease (previous myocardial infarction, known heart failure, valvular heart disease) and atrial fibrillation.

The second ("replication") cohort consisted of patients enrolled in the "RIISC" (Renal Impairment In Secondary Care) study (182). Baseline data was collected upon entry into the "RIISC" study. This is a prospective, on-going, observational investigation of patients with later stage chronic kidney disease with inclusion criteria of at least one of a) CKD 4 and 5, or b) CKD 3 with either accelerated progression (as defined as an eGFR declined of ≥5mls/min/year or ≥10mls/min/5years) or proteinuria (as defined as a urinary albumin:creatinine ≥70mg/mmol on three occasions); exclusion criteria specific to "RIISC" included those on renal replacement therapy or immunosuppression (182). For the purposes of this genetic investigation, the exclusion criteria were extended to include those described above in the "CRIB" cohort.

To limit the confounding effect of population stratification only patients of white (self-reported) ethnicity were included in these genetic substudies. In the “CRIB” cohort, the high sensitive C-reactive protein was measured by Tina-quant CRP (Latex) ultrasensitive assay (Roche Diagnostics, United Kingdom). In the “RIISC” cohort, this was measured using the SpaPlus assay (Binding Site, United Kingdom). The studies (“CRIB” and “RIISC” and their genetic components) were approved by East Midlands Nottingham 1 Research Ethics Committee and South Birmingham Research Ethics Committee respectively and adhered to the Declaration of Helsinki. Study participants provided written informed consent.

2.1.1.3.1 Aortic Pulse Wave Velocity Measurements

In the ”CRIB” cohort, aPWV was calculated by measuring the distance (with a standard tape measure) in metres between the carotid and femoral arteries, subtracting for the distance of the carotid artery to the sternal notch. This was then divided by the transit time (time delay between the start of each waveform in seconds), sequentially recording ECG-gated carotid and femoral waveforms using an applanation tonometer in triplicate, and the SphygmoCor system (AtCor Medical, Sydney, Australia). The transit time determines the time difference between the onset of the pulse wave between the carotid and femoral artery.

In the RIISC cohort, the Vicorder system (Skidmore Medical, Bristol, UK) was used to measure aPWV by measuring simultaneous pressure waveforms by a volume displacement technique, using blood pressure cuffs placed around a patient’s neck (carotid artery) and top of their leg (femoral artery), in triplicate. The aortic path length between the carotid and femoral arteries were measured from the mid-clavicle (measured at the shoulder level to

avoid variation with patient anatomy (breast, abdomen etc)) to the mid-point of the thigh cuff.

2.1.1.3.2 Outcome measure

The primary aim was to evaluate the association between aPWV and with *CAV1* SNP rs4730751 genotype.

2.1.1.3.3 Statistical Analysis

Data are presented as median (interquartile range [IQR]) unless stated otherwise. Continuously distributed data were compared using Student's t-test, categorical data by means of χ^2 testing and non-parametric data by Mann-Whitney U. A type 1 error rate less than 5% ($p \leq 0.05$) was considered statistically significant. Genotype distributions were assessed for concordance with Hardy-Weinberg equilibrium using a χ^2 goodness-of-fit test with a type 1 error rate set at 5%. Hardy-Weinberg equilibrium is an efficient way to test that the expected frequency of a study population does not differ grossly from an expected frequency and detects potential error in genotyping or a skewed population of SNP genotype due to factors such as inbreeding (183). *CAV1* gene variation at rs4730751 and other relevant clinical and demographic characteristics were initially examined in a series of univariate analyses. Known clinical variables that influence aPWV as well as genotype were included in multivariate analysis (i.e. no selection process was used to remove these variables). Based on previous data, the analysis investigated differences between patients demonstrating and not demonstrating CC genotype at the studied locus (i.e. CC versus non-CC (82, 159)). A type 1 error rate of 5% ($p \leq 0.05$) was associated with statistical significance. SPSS software, version 21 (SPSS Inc., Chicago, Illinois) was used for analysis.

2.1.1.4 eNOS SNP in left ventricular function in CKD

The “CRIB” patient cohort with the inclusion and exclusion criteria mention above underwent cardiac magnetic resonance imaging (CMR) and tissue doppler imaging (TDI) were included in this chapter. Baseline data and imaging data was collected prior to this project. Ethical approval, patient consent and whole blood collection for genotyping was performed by me. To limit the confounding effect of population stratification only patients of white (self-reported) ethnicity were included.

The study was approved by East Midlands Nottingham 1 Research Ethics Committee and adhered to the Declaration of Helsinki. Study participants provided written informed consent.

2.1.1.4.1 Cardiovascular Magnetic Resonance Imaging

CMR was performed on a 1.5-T scanner (Sonata Symphony, Siemens, Erlangen, Germany). Serial contiguous short axis cines were piloted from the vertical long axis and horizontal long axis of the right and left ventricle (electrocardiogram gated, steady-state free precession imaging [True-Fisp]; temporal resolution 40-50ms, repetition time 3.2ms, echo time 1.6ms, flip angle 60°, slice thickness 7mm) in accordance with previously validated methodologies (184). Analysis was performed off-line (Argus Software, Siemens) by two blinded observers for the assessment of ventricular volumes (end-diastole, end-systole, stoke volume) and ejection fraction. Heart rate and baseline brachial arterial blood pressure were measured at the time of CMR.

2.1.1.4.2 Echocardiography

Transthoracic echocardiography (Vivid 7; GE Vingmed Ultrasound, Horten, Norway) was performed by an experienced echocardiographer. All parameters were measured in triplicate according to American Society of Echocardiography recommendations (185) and analysed offline (EchoPAC; GE Vingmed Ultrasound, Horten, Norway) by two blinded observers. Resting left ventricular (LV) diastolic function was assessed using standard techniques (186).

2.1.1.4.3 Arterial Stiffness and Distensibility

Pulse wave velocity, augmentation index and ascending aortic distensibility were common measures of arterial stiffness and distensibility in the two randomised control trials, they have been included here. Pulse wave analysis was performed on the radial artery using a high-fidelity micromanometer (SPC-301; Miller Instruments, Houston, TX). The peripheral arterial waveform was used to generate a central arterial waveform using a validated transfer function (SphygmoCor; AtCor Medical, Sydney, Australia). The same system was used to determine aortic pulse wave velocity by sequentially recording ECG-gated carotid and femoral waveforms as previously described. CMR data was used for the ascending aortic distensibility measurement data.

2.1.1.4.4 Outcome Measures

The primary aim was to evaluate the association between LV ejection fraction (LVEF) with *eNOS* (G894T) SNP rs1799983 genotype. Secondary outcomes included: LV end-diastolic

volume indexed to body surface area (LVEDVI), LV end-systolic volume indexed to body surface area (LVESVI) and S' lat (systolic velocity of the basal anterolateral LV wall). As there is much debate over which parameters of diastolic function should be measured as well as their variability in assessment (187), six diastolic parameters were assessed in a cluster analysis (see section 2.1.1.4.5) to separate the cohort into two risk categories of diastolic dysfunction; these were then assessed by eNOS genotype. The "diastolic" parameters included: e' lat (early diastolic velocity of the basal anterolateral LV wall on tissue doppler), E/e' lat (maximum velocity of the E-wave of mitral valve inflow by the maximal anterolateral LV wall velocity of e'), mitral valve E/A (ratio of early to late mitral inflow velocities), LVMI (left ventricular mass index), mitral valve propagation velocity (MV VP) and LAVI (left atrial volume index).

2.1.1.4.5 Statistical Analysis

Baseline demographics and cardiac investigations were compared across the genotype groups, using Kruskal-Wallis (continuous data) and Fisher's Exact tests (categorical data) as appropriate. The relationship between these was then investigated using regression analysis. Initially, univariate linear regression models were produced, with variables being log-transformed where there was evidence of a non-linearity. Multivariate regression models were used (including all factors simultaneously) in order to adjust for potentially confounding and clinically relevant factors. Genotype distributions were assessed for concordance with Hardy-Weinberg equilibrium using a $\chi 2$ goodness-of-fit test with a type 1 error rate set at 5%.

A cluster analysis was then performed, to divide patients into groups based on the values of a range of diastolic parameters. The Two-Step cluster analysis in IBM SPSS 19 was used, with the number of clusters determined automatically (in this study, two main clusters). Demographic factors were then compared between the resulting clusters, using t -tests or Fisher's Exact test, as applicable. All analyses were performed using IBM SPSS 19 (IBM Corp. Armonk, NY), with $p \leq 0.05$ deemed to be indicative of statistical significance.

2.1.1.5 CAV1 in antineutrophil cytoplasmic antibody associated vasculitis

Two independent cohorts were investigated as part of this study that had banked genomic DNA genotyped by Taqman assay for *CAV1* SNP rs4730751. To limit the confounding effect of population stratification only patients of white (self-reported) ethnicity were included. Patients were diagnosed as antineutrophil cytoplasmic antibody (ANCA) associated vasculitis (AAV) according to the European Medicines Agency algorithm (clinical diagnosis of either granulomatosis with polyangiitis (GPA) or microscopic polyangiitis (MPA), supported by either a positive ANCA assay or a diagnostic biopsy, and the absence of an alternative explanation (25), after I reviewed patients' data in the UK. In the United Kingdom, patients with AAV presenting to the nephrology service at Queen Elizabeth Hospital Birmingham between 1979 and 2009, in who genomic DNA had also been isolated as part of the clinical research program at the centre, were included. The replication Northern European cohort included patients from the Vasculitis Centre Lübeck/Bad Bramstedt, Germany and the Maastricht University Medical Centre+, the Netherlands who presented with GPA or MPA between 1982 and 2009 to the rheumatology services of the respective centres.

ANCA testing was performed by indirect immunofluorescence (United Kingdom) and ELISA methods (Germany and the Netherlands) depending on how the data was collected historically.

The study was performed in accordance with the principles expressed in the Declaration of Helsinki. Respective separate National Ethics Committee approval was sought from: South Birmingham Regional Ethics Committee 0723 by me, Ethics Committee of the University of Lübeck AZ-06-087 and the Maastricht Local Ethics Committee 05-158. Study participants provided written informed consent and the data were analysed anonymously.

2.1.1.5.1 Outcome measures

The primary outcome measure was a composite of time to all-cause mortality or time to renal replacement therapy (RRT – either dialysis or kidney transplantation beyond 3 months from initial presentation). Secondary outcomes included time to: all-cause mortality, RRT, death from infection, death from a vascular cause (ischaemic heart disease, heart failure, abdominal aortic aneurysm or cerebral vascular accident), and time to cancer development from AAV diagnosis. Cancer onset dates were not available from the replication cohort, only if cancer developed post diagnosis. Non-melanoma skin cancers were excluded. Data was retrieved from prospectively maintained institutional database, updated by me and corroborated by my requesting and reviewing death certificate records. The independent effect of *CAV1* genotype was adjusted for: age at diagnosis, gender, type of ANCA, and serum creatinine level at presentation.

2.1.1.5.2 Statistical Analysis

Data are shown as median (1st and 3rd quartiles) unless otherwise indicated. Group comparisons were assessed using Mann-Whitney U and χ^2 testing as appropriate. Cumulative events were analysed with Kaplan-Meier estimates, with the log-rank test used for intergroup comparison. Time-to-event analyses were performed using a Cox proportional hazards model. Categorical outcome data was analysed by logistic regression. Genotype distributions were assessed for concordance with Hardy-Weinberg equilibrium using a χ^2 goodness-of-fit test with a type 1 error rate set at 5%. *CAV1* gene variation at rs4730751 and other relevant clinical and demographic characteristics were initially examined in a series of univariate analyses. Known variables that influence AAV outcomes as well as genotype were included in multivariate analysis (i.e. no selection process was used to remove these variables). In addition, an interaction term "*CAV1* genotype x diagnosis" was analysed to examine a differential effect of genotype depending on clinical diagnosis. A type 1 error rate of 5% ($p \leq 0.05$) was associated with statistical significance. SPSS software, version 18 (SPSS Inc., Chicago, Illinois) was used for analysis.

2.1.1.6 New onset diabetes after transplantation – can genetics identify pathways to its development?

From 2009 to 2012, live and deceased donor renal transplant recipients were prospectively followed-up over a 12 month period in a single-centre adult tertiary centre at Queen Elizabeth Hospital Birmingham, United Kingdom. To exclude pre-existing diabetes, patients underwent glucose testing (after a minimum of eight hours fasting) immediately prior to

transplantation and excluded if ≥6.1mmol/l or HbA1c ≥6.5% (48mmol/mol). In addition, live donor recipients underwent oral glucose tolerance testing (OGTT) with a standard 75g glucose load within a week prior to transplantation. Following transplantation, OGTTs were then performed at 7 days, and then 3 months and 12 months in all patients except those who developed clinically manifest hyperglycaemia requiring treatment. NODAT was diagnosed if a] fasting glucose ≥7mmol/l or 2-hour OGTT was ≥11.1mmol/l from day 7 onwards and persisted at the 3 month time-point, b] HbA1c ≥6.5% (48mmol/mol) from 3 months onwards, or c] requirement for institution of therapy for NODAT in which case OGTT was not undertaken (fasting clinic glucose was ≥7mmol/l in all such patients). Exclusion criteria of pre-transplant diabetes and the requirement for exclusion of non-white patients to avoid population stratification were essential in a genetic investigation such as this.

All patients received an identical immunosuppression regimen consisting of anti- CD25 monoclonal antibody induction followed by maintenance tacrolimus (target per-dose trough levels 5-8ng/ml by liquid chromatography with tandem mass spectrometry), mycophenolate mofetil (2g daily dose) and prednisolone (20mg/day initially weaning to 5mg/day by 3 months, and then continued). Literature review to identify candidate gene variants was undertaken as described previously (73) with the inclusion of *CAV1* SNP rs4730751. Genotyping were performed using Sequenom iPLEX technology. The study received approval from the local research ethics committee (NRES West Midlands Black Country 08/H1204/103) prior to commencement, and was conducted in accordance with the Declarations of Helsinki and Istanbul with patient written consent.

2.1.1.6.1 Outcome measure

SNP genotype association with development of NODAT was the primary outcome.

2.1.1.6.2 Statistical Analysis

Data are shown as median (1st and 3rd quartiles) if not normally distributed or mean (±standard deviation) if normally distributed. Baseline demographics were assessed using Mann-Whitney U (non-parametric data) or Student's t test if normally distributed for continuous data, and Fisher's exact testing for categorical data as appropriate using SPSS software, version 20 (SPSS Inc., Chicago, Illinois) for analysis. Genotype distributions were assessed for concordance with Hardy-Weinberg equilibrium using a $\chi 2$ goodness-of-fit test with a type 1 error rate set at 5% analysed using PLINK (188). Genotype to phenotype associations and event analyses were conducted using logistic regression with the development of NODAT at any time during the first 12 months post-transplantation as the end measure of interest (time to event analysis was not undertaken due to only 2 post-transplant time-points). Univariate genotype:phenotype relationships and then the relationship in a multivariate model fully adjusted for age, sex, baseline body mass index (BMI) and change in BMI over 12 months from transplantation (no selection process) were calculated using PLINK.

2.1.2 Materials and Methods for Murine Studies

The following was performed by me. Mice were commercially bought with their genetic alterations.

2.1.2.1 Mice

The *Cav1*$^{-/-}$ (CKO) mouse (JAX, the Jackson Laboratory, United States) was created by Michael Lisanti by replacement of a 2.2 kb region of the caveolin-1 gene including exons 1 and 2 and part of the promoter region, with a neo resistance cassette via homologous recombination, named *Cav1*^{tm1Mls}. This mouse was originally crossed on C57BL/6J (C57 Black6 substrain J) mice for five generations, but was later noted this backcross had a diminished reproductive performance. Therefore, it was backcrossed on to the 129S6/SvEv background for one generation to improve reproductivity. The mice bought from JAX via Charles River (UK), are primarily a mix of 129 and C57BL/6 with a minor contribution from the originating mutant embryonic stem cell linage of the Swiss Jim Lambert (SJL). The control caveolin-1 wild-type strain for CKO mouse experiments was therefore based on the same strain as the CKO, due to known differing propensities to develop renal fibrosis between mouse strains. These were also brought from JAX via Charles River. Both wild-type and CKO were inbred at purchase, with a colony established at the Biomedical Sciences Unit. For all experiments, males were used only at age 6-8 weeks. Mice were maintained in 12 hour light/12 hour dark cycles with free access to food and water.

2.1.2.2 Genotyping of mice

Genomic DNA was isolated from newborn mice ear clippings. DNA was then extracted using the DNAeasy Tissue Kit (Qiagen) using the manufacturer's instructions with DNA concentration and DNA wavelengths analysed using Nanodrop 2000 (ThermoScientific, Figure 2-3). Mice were then genotyped for caveolin-1 wild-type (WT) or knockout (KO) using primers (AltaBioscience, Table 2-1) and protocols as stated on the JAX website. The mix used for polymerase chain reactions (PCR) is shown in Table 2-2. The programme used for PCR is shown in Table 2-3. Samples were run on a 1.5% agarose gel (0.75g agarose, 50ml x1 TBE buffer) with 5µl of GelRed (Biotium) x10000 stock, ran at 85 volts and visualised using the ChemiDoc (Biorad). Caveolin-1 wild-type band is noted at 690bp, knockout band at 410bp and heterozygote double band at 410bp and 690bp (Figure 2-4).

Table 2-1 Primers used for mouse genotyping for caveolin-1

Primer	Sequence 5' --> 3'	Primer Type
oIMR1972	GTG TAT GAC GCG CAC ACC AAG	Wild type
oIMR1973	CTA GTG AGA CGT GCT ACT TCC	Mutant
oIMR1974	CTT GAG TTC TGT TAG CCC AG	Common

Table 2-2 Polymerase chain reaction mix

	Volume (µl)
ddH_20	3.2
oIMR1972 20µM	0.6
oIMR1973 20µM	0.6
oIMR1974 20µM	0.6
DNA	1
REDtaq ReadyMix (Sigma R2523)	6
Total volume	12

Table 2-3 Techne TC Plus thermocycler programme for polymerase chain reaction

Step #	Temp °C	Time	Note
1	105	'Prelid'	
2	94	3 mins	Stage 1, x1 cycle
3	94	30 seconds	Stage 2
4	65	1 min	Stage 2
5	72	1 min	Stage 2
			Repeat stage 2 (steps 3-5) for 35 cycles
6	72	2 min	Stage 3, x1 cycle
7	10		hold

Figure 2-3 Example of DNA concentrations and wavelengths using Nanodrop 2000 (ThermoScientific)

#	Sample ID	User name	Date and Time	Nucleic Acid Conc.	Unit	A260	A280	260/280	260/230	Sample Type	Factor
1	L33 M1 1st	Lab	01/03/2013 16:45:45	28.8	ng/µl	0.575	0.301	1.91	1.89	DNA	50.00
3	L33 F1 1st	Lab	01/03/2013 16:48:31	18.9	ng/µl	0.378	0.196	1.93	1.75	DNA	50.00
5	L37 M1 1st	Lab	01/03/2013 16:50:22	23.3	ng/µl	0.466	0.245	1.90	1.56	DNA	50.00

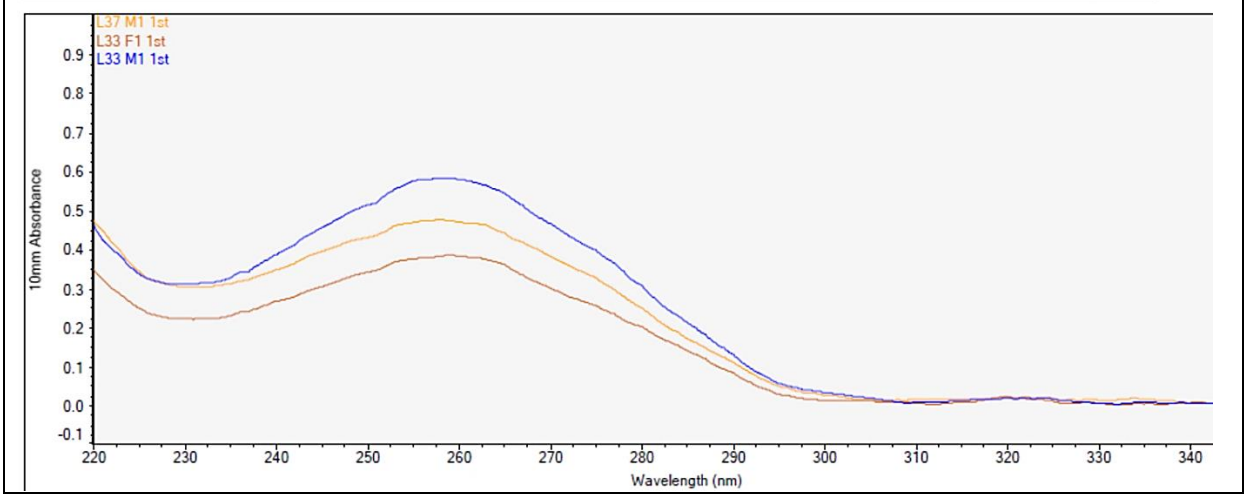

Figure 2-4 Genotyping fragment sizes shown far right, with caveolin-1 wild-type 690bp, knockout 410bp, and ladder fragment sizes shown far left. Negative control in the far right non-ladder lane

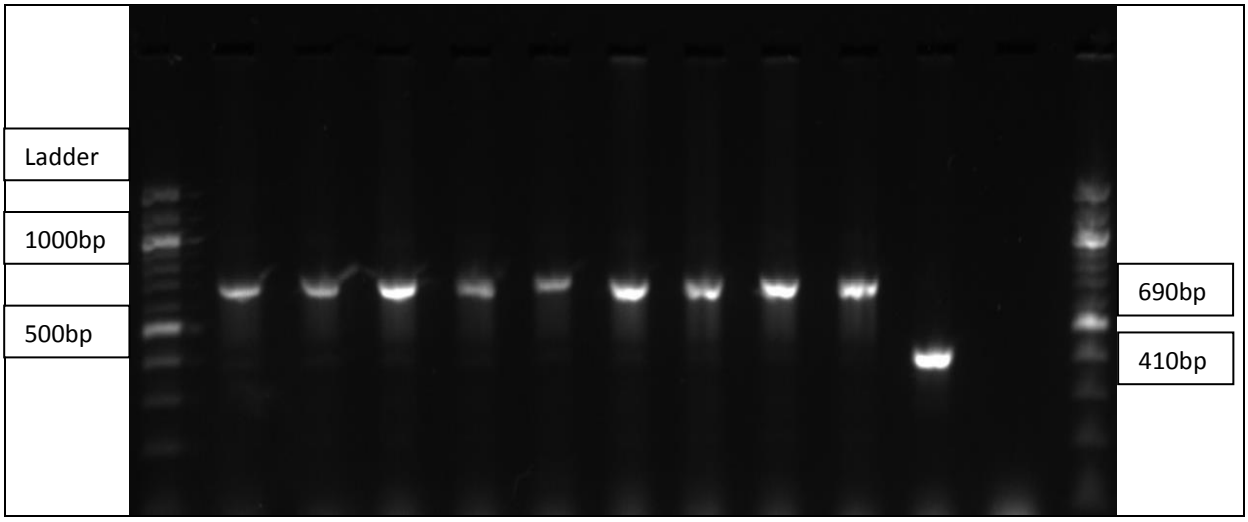

2.1.2.3 Small animal models of renal fibrosis

Two small murine models of renal fibrosis previously described in the literature, were performed at University of Birmingham. A successful application was made to the United Kingdom Home Office for a personal licence for murine experiments to be carried out at the Biomedical Sciences Unit at the University of Birmingham (PIL 30/9343, replaced by electronic PIL IB5C52417, project licence 40/3352).

2.1.2.3.1 Ciclosporin-A nephrotoxicity pilot model (189)

A pilot model was performed as this model of patchy interstitial renal fibrosis (as seen in human prolonged use in renal transplants) had not been performed in Birmingham before. C57/BL6 male mice from Charles River, aged 6-8 weeks, weight 20-24g were given a low <0.025% salt diet (Special Diet Services, UK) for a week prior to either daily ciclosporin-A (CsA) or control vehicle subcutaneous injections for 28 days. At the end of the model, mice were placed in metabolic cages for 24 hours for urinary collection, prior to cardiac puncture for whole blood under general anaesthesia. After cervical dislocation to induce death, their kidneys were harvested.

CsA powder was kindly donated by Novartis. As per their protocol for animal subcutaneous injections, a CsA (Sandimmun) microemulsion is required by stirring 50mg of CsA powder in a mixture of Cremophor EL (Sigma C5135) – a polyethoxylated castor oil – made to a volume of 1ml with 94% ethanol. This microemulsion was too thick to draw up into a 1ml syringe which was required for subcutaneous (s/c) injection, thus was further diluted adding 2/3rds 94% ethanol to 1/3rd Cremophor EL. In total 200mg CsA powder dissolved overnight in

8.9mls Cremophor EL and 17.7mls 94% ethanol (final concentration 7.5mg/ml) with 30mg/Kg being injected daily and 4mls/Kg daily of vehicle in control mice after aliquoting 30mls of vehicle (9.75mls Cremophor EL and 20.25mls 94% ethanol). The microemulsion was protected from light.

2.1.2.3.2 Unilateral ureteric model of obstruction

Kidneys were harvested at day 3 and day 14 after unilateral ureteric obstruction (UUO). Using inhalational anaesthesia (4% Isofluorane, 3L/min oxygen), mice underwent a midline laparotomy at day 0 with a heating mat underneath after receiving 0.05mg/Kg Temgesic (opiate based analgesia) subcutaneously. Their bowel was lifted and covered with sterile saline soaked gauze to prevent dehydration. The left ureter was identified and ligated using two 5.0 non-absorbable sutures. After bowel replacement using cotton buds, the midline peritoneal membrane incision was closed using absorbable 5.0 sutures, and the abdomen with clips (Figure 2-5). The mouse was then placed in a warming box to recover for 24 hours. Sham-operated mice underwent the same procedure, except the left ureter was mobilised instead of ligated.

Before kidneys were harvested after cervical dislocation, mice were placed for a 24 hour urine collection in metabolic cages (for protein estimation). The following day via cardiac puncture under inhalational anaesthesia, blood sampling was performed for urea and creatinine.

Figure 2-5 Representative images of unilateral ureteric obstruction model. A) abdomen shaved and cleaned with chlorhexidine. B) Midline laparotomy and retractors. C) Bowel displaced on to saline soaked gauze. D) Left ureter identified. E) Ureter ligated. F) Clips applied to close abdomen

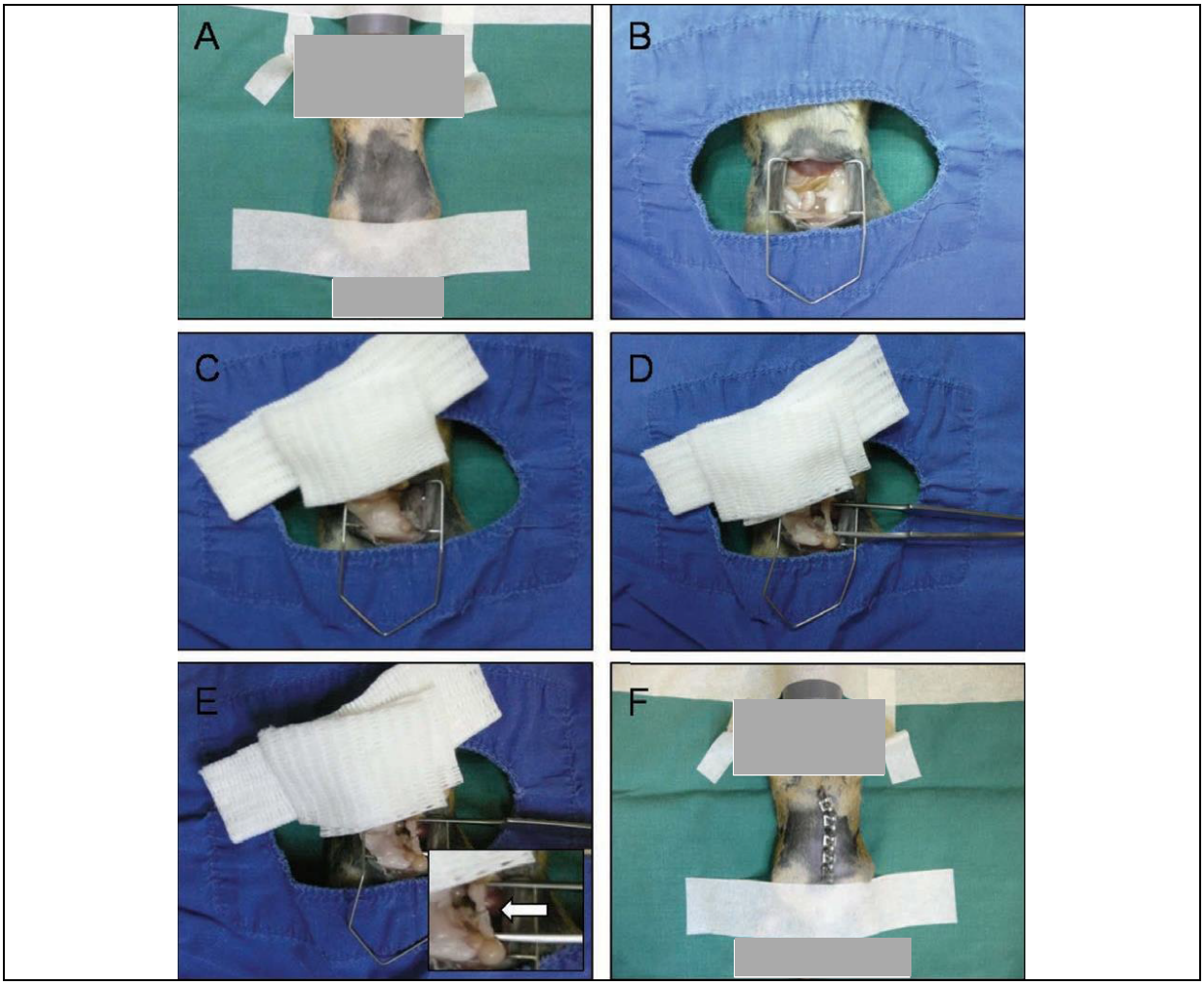

2.1.2.4 Kidney harvesting and sectioning

Mice were weighed pre models of fibrosis and prior to blood sampling and cervical dislocation, weighed again. Kidneys were then removed and the kidney capsule removed. The kidneys were weighed using the same scales, then cut in half to reveal the coronal section of the kidney (Figure 1-3) with a scalpel and blotted to remove any remaining blood. There are wide variations in collagen content depending on the area of kidney investigated, thus areas of pre injury high collagen concentrations (renal capsule and renal pelvis) were

removed (190). Also, the same pole was used for analysis in all subsequent experiments via quarters of kidney sectioned as shown in Figure 2-6 (cutting the coronal section in half again).

Figure 2-6 Sectioning of kidneys. The left upper quarter was used for polymerase chain reactions (PCR), lower left quarter for Western blotting (WB), upper right quarter for confocal microscopy and the lower right quarter for histology. The 'hashed' area representing the renal pelvis, was removed before sectioning into quarters

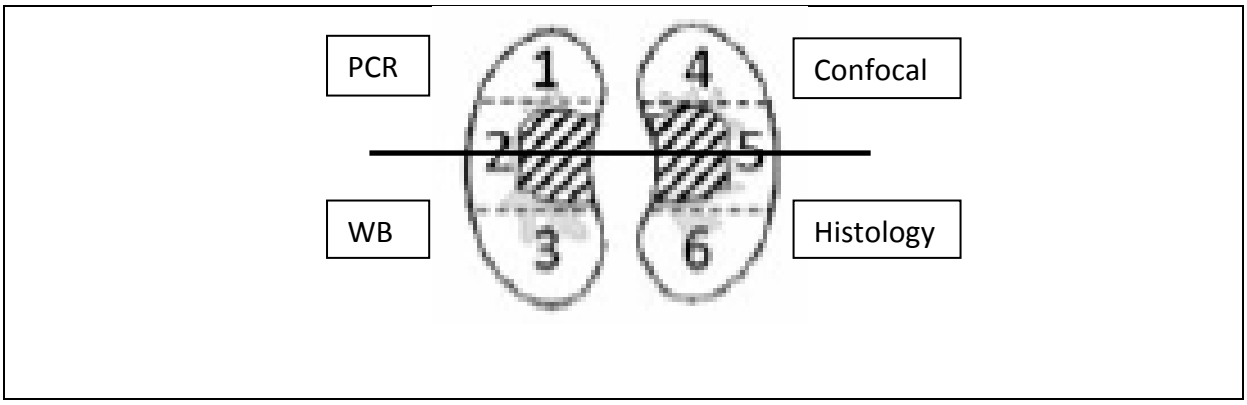

2.1.2.5 Blood sampling

A 1ml syringe was used to collect whole blood after cardiac puncture under inhalational anaesthesia prior to cervical dislocation. The blood was mixed with 75µl of EDTA 0.02% solution (Sigma), in a sterile 1.5ml eppendorf and kept on ice for 1 hour prior to being frozen at -20°C and sent to MRC Harwell (Oxford) for analysis.

2.1.2.6 Real time quantitative polymerase chain reaction

The left upper quarters of sectioned kidney were weighed prior to be being snap frozen in a cryovial in liquid nitrogen and kept frozen at -80°C until analysis. The whole quarter was homogenised using the gentleMac dissociator and M tubes (Miltenyi Biotec) and an

equivalent volume to a maximum of 30mg of tissue homogenised (to avoid overloading the spin columns) in RLT lysis buffer was used to extract RNA using the RNEasy Mini Kit (Qiagen) using the manufacturer's instructions. RNA was analysed for concentration and A260/A280 quality using the Nanodrop 2000 (ThermoScientific). RNA was then diluted with RNAse free water so that 1µg was used in each reverse transcription reaction to cDNA using the Taqman Reverse Transcription (Applied Biosystems). The mix and programme used for RNA to cDNA is shown in Table 2-4 and Table 2-5 respectively.

Table 2-4 Reverse Transcription Mix

	Volume (µl)
X10 reverse transcription buffer	5
Magnesium Chloride 25mM	11
dNTPs mix 10mM	10
Random hexamers	2.5
RNAse inhibitor (20u/µl)	1
Multiscribe ReverseTranscriptase (50u/µl)	1.25
RNA	15
Total volume	45.75

Table 2-5 Reverse transcription thermocycler programme

Step #	Temp °C	Time	Note
1	105	'Prelid'	
2	94	5 mins	Initial denaturisation
3	25	10 mins	Stage 1
4	37	1 hour	Stage 2
5	48	30 mins	Stage 3
6	95	5 mins	Stage 4
7	10		hold

cDNA concentration and wavelength quality was again analysed using the Nanodrop 2000 (ThermoScientific). Quantitative PCR was performed on 384 well plates, single plex, using the following Taqman Gene Expression assays TGFβ-1 (Mm01178820_M1 FAM-MGB), collagen 1α1 (Mm00801666_M1 FAM-MGB), collagen 3α1 (Mm01254476_M1 FAM-MGB), caveolin-1 (Mm00483057_M1 FAM-MGB) and GAPDH (Mm99999915_g1 VIC-MGB) was used as a housekeeping gene. Assays were run using the Lightcycler 480 II (Roche) using the mix and programme shown in Table 2-6 and Table 2-7. The cycle number (C_t) for the target gene was subtracted from the C_t for the control gene (ΔC_t). This was then normalised to a calibration of the control sample mean of the ΔC_t. Sham operated mice was used as control. The relative quantity was calculated as $2^{-\Delta\Delta Ct}$ (delta-delta method). This relative quantity is known as the mRNA fold induction relative to control. Fold increase ratios were then expressed to demonstrate fold changes between groups.

Table 2-6 Quantitative polymerase chain reaction mix

	Volume (µl)
Taqman Gene Assay x20	1
Mastermix x2	10
DNAse free water	7
cDNA (20ng/µl)	2
Total volume	20

Table 2-7 Lightcycler programme

Step	Temp °C	Time	Note
Pre-incubation	95	10 mins	x1 cycle
Amplification a)	95	15 seconds	a) b) c) for 45 cycles
b)	60	1 min	
c)	72	1 second	
Cooling	40	30 seconds	x1 cycle
Melting Curve	20	10 minutes	x1 cycle
Hold	10		

2.1.2.7 Western Blotting for Caveolin-1

2.1.2.7.1 Tissue lysate preparation

Tissue lysates were prepared using the gentleMACs M tubes for homogenisation from the left lower quarters of sectioned kidneys. The tissue had been placed in cryovials and snap frozen in liquid nitrogen before being stored at -80°C. Each frozen tissue sample was placed in 890µl sterile phosphate buffered saline (PBS), 100µl of 10x RIPA lysis buffer (Sigma-

Aldrich) and 10µl of protease cocktail inhibitor (Calbiochem) prior to homogenisation. The lysate protein concentration was then assayed using Pierce BCA protein assay (ThermoScientific). The equivalent volume of 300µg protein concentration was then placed in a new eppendorf. An equal volume of cold 20% trichloroacetic acid (TCA) was added, left on ice for 30 minutes and then centrifuged for 5 minutes at 4°C at 15000rpm with the resultant supernatant discarded. 500µl of cold acetone was added to the pellet, vortexed quickly and left on ice for 5 minutes before centrifuging for 5 mins at 4°C at 15000rpm with the resultant supernatant discarded; this process was repeated. The eppendorf was placed in a heat block at 100 with the lid open, to drive off the remaining acetone. 60µl of x2 sodium dodecyl sulphate (SDS) sample buffer (4% SDS (Geneflow, UK); 0.1M dithiothreitol (Sigma-Aldrich); 20% glycol (BDH Limited, UK); 0.0625M Tris-HCL (pH 6.8); 0.004% bromophenol blue (Sigma-Aldrich)) was added and boiled for 5 minutes at 100°C.

2.1.2.7.2 SDS-polyacrylamide gel electrophoresis and Western blotting

Eppendorfs were spun for a few seconds so any debris was confined to the bottom. 20µl of equal protein concentration of lysates were then loaded onto a 12% SDS-polyacrylamide gel (see Table 2-8) and run for 1.5 hours at 100 volts with pre-stained markers (BioRad). Proteins were then wet transferred on to methanol-activated 0.2µm polyvinylidene difluoride membranes (Biorad). Following blotting, membranes were washed quickly with Tris buffered saline (TBS) containing 0.1% tween-20 (Sigma-Aldrich) (TBS-T), then incubated with 5% bovine serum albumin (BSA)/TBS-T at room temperature for a minimum of an hour. Overnight at 4°C, blots were probed with anti-mouse caveolin-1 antibody (Santa-Cruz Biotechnology), 1:500 dilution in 5% BSA/TBS-T on an orbital shaker. The antibody was then poured off and frozen for further use, and the membrane was washed 4 times with TBS-T

over an hour. The blot was then probed with an anti-rabbit HRP secondary antibody (Dako), 1:5000 dilution in 5% BSA/TBS-T for 1 hour at room temperature. After 4 washes with TBS-T over 1 hour, proteins were visualised with enhanced chemiluminescence prime (Amersham Pharmacia Biotech) and proteins imaged using the Chemidoc (Biorad). After 4 washes with TBS-T the blot was probed with anti-mouse β-actin antibody (Sigma-Aldrich), 1:5000 dilution in 5% BSA/TBS-T for 1 hour at room temperature as a control; the same process of washes and secondary anti-rabbit HRP antibody incubation, enhanced chemiluminescene prime visualisation and imaging was performed to confirm equal protein loading.

Table 2-8 SDS Gel recipes

	12% Resolving Gels		**5% Stacking Gels**
Protogel *(Geneflow EC-890)*	4mL		1.3mL
dH_2O	3.5mL		6.1mL
Tris HCl 1.5M pH 8.8	2.5 mL	0.5M pH 6.8	2.5mL
20% SDS (*Geneflow EC-874)*	50µL		50µL
10% APS	100µL		100µL
Temed (*Geneflow EC-503)*	10µL		10µL
Abbreviations: APS, ammonium persulfate; SDS, sodium dodecyl sulphate			

2.1.2.8 Confocal microscopy

The right upper quarter kidney (Figure 2-6) was placed in 4% paraformaldehyde (PFA) for 2 hours, and then kept in 18% sucrose overnight at 4°C. The tissue was then embedded in a cryomold (Tissue-Tek) containing optimum cutting temperature compound (OCT) and froze using the vapour of liquid nitrogen. 6µm sections were prepared using a cryostat and fixed by immersion in cold acetone for 20 minutes at 4°C, and allowed to air dry for 30 minutes. The slides were frozen at -80°C and allowed to equilibrate to room temperature prior to PBS washing for 5 minutes with gentle agitation. Primary and secondary fluorescent antibody

concentrations are shown in Table 2-9 and Table 2-10 respectively. Primary and secondary antibodies were diluted in PBS containing 1% BSA, 2% foetal calf serum. Primary antibodies were incubated overnight at 4°C, and then the antibody was tapped off and washed in PBS three 5 minute intervals with gentle agitation. The secondary antibody was added next for 1 hour at room temperature before PBS x3 5minute washes. Nuclei staining was performed with DAPI (4',6-diamidino-2-Phenylindole, dihydrochloride from Invitrogen). The slide was then fixed in 1% PFA for 5 minutes at room temperature, washed x2 for 5 minutes in PBS, before a drop of VectaShield mounting medium (Vector Laboratories) was applied and a coverslip was mounted and clear nail vanish applied on the outer edges of the coverslip. The slide was then stored in the dark at -20°C until visualisation using the Zeiss confocal LSM 510 microscope and processed using the LSM Image Examiner software (Zeiss, Germany). Images are presented with respect to the objective used of the microscope (x10, x40 or x63).

Table 2-9 Primary anti-mouse antibodies for confocal microscopy (IF: immunofluorescence) and Western blotting (WB)

Specificity	Isotype	Clone	Supplier	Working dilution
Caveolin-1 (N20)	polyclonal rabbit	polyclonal	Santa-Cruz	WB 1:500 IF 1:100
αSMA	mouse IgG_{2a}	1A4	Sigma	1:100
CD31	rat IgG_{2a} kappa	390	ebioscience	1:1000
Synaptopodin	mouse IgG_1	G1D4	Progen	neat
E-cadherin	rat IgG_1	DECMA-1	ebioscience	1:100
CD45	rat IgG_{2b}	30-F11	ebioscience	1:100
F4/80	rat IgG_{2a} kappa	BM8	ebioscience	1:100
CD3	rat IgG_{2b} kappa	17A2	ebioscience	1:100
β-actin	rabbit IgG	13E5	Cell signaling	WB 1:1000

Table 2-10 Secondary antibodies for confocal microscopy and Western blotting

Specificity	Conjugate	Host	Supplier	Working dilution
Anti-rabbit IgG	Alexa 488	goat	Invitrogen	1:1000
Anti-mouse IgG_{2a}	Alexa 568	goat	Invitrogen	1:2000
Anti-mouse IgG_1	Alexa 680	goat	Invitrogen	1:200
Anti-rat IgG	Cy5	goat	Invitrogen	1:2000
Anti-rabbit IgG	Cy5	goat	Invitrogen	1:1000
Anti-rabbit IgG	HRP	goat	Dako	WB 1:5000

2.1.2.9 Histology staining

Sections were obtained as described above in '2.1.2.8 Confocal microscopy' but from the right lower kidney quadrant. The Queen Elizabeth Hospital Birmingham pathology department kindly stained the frozen sections using haematoxylin and eosin and for collagen using Gomori trichrome staining. I then imaged the sections digitally using the Nikon Eclipse E400 microscope and NIS Elements Version 3.0 (Nikon). The kidney images were then analysed for percentage Gomori staining for collagen (as a surrogate for fibrosis scoring) in a blinded fashion by myself and a renal histopathologist, via a 5x3 grid-grid method.

2.1.2.10 Statistical Analysis

Results are presented as mean ± standard error of the mean (SEM). Statistical mean difference was assessed by a two-tail Student's t test if normally distributed, otherwise Mann-Whitney U testing was used. One-way ANOVA was used to compare the difference between three groups and post-hoc analysis with Dunnett's multiple comparison test. Analysis and graphical data were prepared by either GraphPad Prism 5 software or SPSS software, version 21 (SPSS Inc., Chicago, Illinois).

CHAPTER 3:

GENETIC VARIATION IN

CARDIOVASCULAR DISEASE

IN CKD

3.1 Genetic variation in cardiovascular disease in CKD

3.1.1 *CAV1* in aortic pulse wave velocity

This section is based on my first author publication (191).

3.1.1.1 Introduction

Cardiovascular disease (CVD) is the leading cause of mortality in patients with CKD and is driven by two main pathological processes, atherosclerosis and arteriosclerosis. Traditional "atheromatous inducing" risk factors such as smoking and obesity do not fully account for this excess CVD risk (161). This is despite the increased presence of traditional cardiovascular risk factors such as diabetes mellitus, hypertension, and dyslipidaemia in CKD populations. Non-traditional risk factors include advancing renal dysfunction, proteinuria, homocysteinaemia and uraemic toxins (192). However, arteriosclerosis is a prominent component of the non-traditional risk for increased CVD mortality that arises from multiple factors. For example, there are alterations in the renin-angiotensin-aldosterone system in CKD, resulting in higher angiotensin II and thus, endothelial dysfunction from its stimulation of vascular smooth muscle cells that increase inflammation by these cells generation of intracellular superoxides, inflammatory cytokines and increased production collagen and matrix metalloproteinases (193, 194). Arteriosclerosis results in arterial stiffness due to medial arterial layer hypertrophy and fibrosis (195). This is exacerbated by altered calcium and phosphate handling (known as CKD-mineral bone disease), leading to increased vascular calcification and therefore, arterial stiffness. The normal aorta is elastic and acts as a reservoir to buffer the oscillatory changes in blood pressure during a cardiac cycle, by expanding in systole and recoiling in diastole. This process allows adequate coronary

perfusion that predominately occurs during diastole, as well as offering a dampened aortic pressure waveform and thus steady pressure flow to organs such as the kidney. However, with increased arterial stiffness, there is loss of this buffering resulting in greater fluctuations of systolic pressures, pulse pressures and greater shear stress. This leads to renal microvasculature damage and myocardial hypertrophy, fibrosis and reduced coronary perfusion due to reduced diastolic pressures.

Aortic pulse wave velocity (aPWV) is the gold standard method for measuring arterial stiffness and has been consistently associated with all-cause and cardiovascular mortality in multiple conditions including CKD (169, 196). The purpose of this chapter was to assess the association of *CAV1* rs4730751 SNP with arterial stiffness as measured by aPWV in an early CKD stage non-dialysis cohort (CRIB) and corroborate this relationship in an advanced CKD stage non-dialysis cohort (RIISC).

3.1.1.2 Results

Baseline data for the cohorts are shown in Table 3-1. In the Chronic Renal Impairment in Birmingham ("CRIB") cohort, 235 patients were screened, with 24 patients excluded due to non-white ethnicity. 152 patients had consented for DNA to be collected and 144 of 152 (>95%) tested patients were successfully genotyped. The median age was 57 years [IQR: 47-65], estimated glomerular filtration rate (eGFR) 51 mls/min/1.73m2 [IQR: 41-58] and aPWV 8.4 m/s ([IQR: 7.3-9.9]. Patient genotypes were 74 CC (51.4%), 64 AC (44.4%) and 6 AA (4.2%), which was within Hardy-Weinberg equilibrium ($p>0.05$). Patients with CC genotype demonstrated lower aPWV (8.1 m/s; IQR: 7.0-9.4) than patients with non-CC genotype

(aPWV 8.6 m/s; IQR: 7.5-10.8) (p=0.003). Patients with non-CC genotype were significantly older (p=0.02). In multivariate regression analysis, adjusted for age, gender, eGFR and mean arterial pressure (Table 3-2), CC was associated with a lower aPWV (coefficient -0.621 [-1.218 to -0.24]; p=0.042; adjusted R squared 0.325).

In the Renal Impairment in Secondary Care (RIISC) cohort, 639 patients were screened of which 202 met inclusion and exclusion criteria. 153 patients had consented for DNA to be collected and 147 of 153 tested patients were successfully genotyped (>96%). The median age was 58 years [IQR: 47-69], with eGFR 28 mls/min/1.73m2 [IQR: 21-37] and aPWV 8.8 m/s [IQR: 8.0-10.3]. Patient genotypes were 92 CC (63%), 49 AC (33%) and 6 AA (4%), which was within Hardy-Weinberg equilibrium (p>0.05). As seen in the CRIB cohort, patients with CC genotype in the RIISC cohort demonstrated lower aPWV (8.7 m/s; IQR: 7.9-9.8) compared with 9.4 m/s (IQR: 8.0-10.8) (p=0.021) in patients with a non-CC genotype. In multivariate regression analysis, adjusted for age, gender, eGFR and mean arterial pressure (Table 3-2), CC was also associated with a lower aPWV (coefficient -0.984 [-1.523 to -0.445]; p<0.001; adjusted R squared 0.433).

Table 3-1 Baseline demographic and measurement data for the CRIB and RIISC cohorts by genotype

p* (p value comparing CC and non CC genotype in CRIB); p** (p value comparing CC and non-CC genotype in RIISC); p*** (p value comparing across all patients in CRIB versus RIISC cohorts). p value by Student's t-test for continuous variables and χ^2 for categorical variables unless stated. [1]variables p value tested by Mann-Whitney U.

	CRIB			RIISC			
Characteristic	**CC genotype**	**Non-CC genotype**	**p* value**	**CC genotype**	**Non-CC genotype**	**p** value**	**P*** value**
Number of patients (%)	74 (51)	70 (49)		92 (63)	55 (37)		0.05
Age (years)	54 (45-63)	61 (49-67)	**0.02**	58 (49-69)	57 (39-70)	0.368	0.5
Male (%)	41 (55)	38 (54)	0.9	49 (53)	36 (66)	0.147	0.6
Current Smoker (%)	9 (12)	11 (16)	0.5	19 (21)	8 (15)	0.355	0.3
Previous Smoker (%)	28 (38)	26 (37)	0.9	35 (38)	24 (44)	0.503	0.6
Diagnoses							
Glomerular diseases (%)	44 (59)	28 (40)	**0.02**	25 (27)	14 (25)	0.819	**<0.001**
Systemic Diseases (%)	11 (12)	13 (19)	0.6	11 (12)	8 (15)	0.651	0.2
Tubulointerstitial diseases (%)	5 (7)	7 (10)	0.5	13 (14)	8 (15)	0.945	0.1
Familial nephropathies (%)	10 (14)	8 (11)	0.7	17 (18)	5 (9)	0.123	0.5
Miscellaneous (%)	6 (8)	14 (20)	**0.04**	26 (28)	20 (36)	0.305	**<0.001**
Medication frequency							
Angiotensin conversion enzyme inhibitors (%)	52 (70)	39 (56)	0.07	35 (38)	14 (26)	0.117	**<0.001**
Angiotensin II receptor blockers (%)	17 (23)	22 (31)	0.3	27 (29)	19 (35)	0.511	0.4
β blockers (%)	10 (14)	16 (23)	0.1	28 (30)	12 (22)	0.256	0.06
Calcium channel blockers (%)	16 (22)	19 (27)	0.4	42 (46)	21 (38)	0.376	**0.001**
Alpha blockers (%)	9 (12)	7 (10)	0.7	15 (16)	14 (26)	0.177	**0.04**
Diuretics (%)	24 (32)	19 (27)	0.5	28 (30)	19 (35)	0.605	0.7
Statins (%)	31 (44)	32 (43)	0.9	45 (49)	24 (44)	0.535	0.6
Active vitamin D (%)	6 (8)	6 (9)	0.9	26 (28)	17 (31)	0.733	**<0.001**

Measurement Data							
Body surface area (m^2)	1.9 (1.8-2.1)	1.9 (1.8-2.0)	0.5	1.9 (1.7-2.1)	2.0 (1.8-2.1)	0.424	0.8
Body mass index (Kg/m^2)	27.9 (24.1-29.9)	27.6 (24.6-32.0)	0.6	27.9 (24.1-32.7)	28.2 (24.1-31.6)	0.687	0.4
Mean arterial pressure (mmHg)	92 (85-98)	93 (85-102)	0.4	104 (97-114)	102 (97-112)	0.487	**<0.001**
Systolic blood pressure (mmHg)	124 (115-135)	129 (119-143)	0.2	124 (114-136)	122 (113-137)	0.994	0.4
Diastolic Blood Pressure (mmHg)	73 (68-80)	73 (66-82)	0.9	79 (71-86)	78 (74-84)	0.485	**<0.001**
Haemoglobin (g/dl)	13.3 (12.5-14.3)	13.6 (12.5-14.3)	0.7	12.8 (11.5-14.0)	13.3 (12.2-14.0)	0.077	**0.04**
Estimated glomerular filtration rate ($mls/min/1.73m^2$)	53 (40-59)	50 (42-57)	0.9	27 (20-37)	28 (21-38)	0.153	**<0.001**
Albumin:creatinine (mg/mmol)[1]	5.1 (1-50)	12 (1-37)	0.7	28 (7-111)	18 (7-111)	0.702	**<0.001**
High sensitive C-reactive protein (mg/l)[1]	1.4 (0.7-4.8)	2.1 (0.7-6.4)	0.4	2.3 (0.8-4.9)	2.1 (1.4-4.4)	0.431	0.3
Fasting glucose (mmol/l)	4.9 (4.4-5.2)	4.9 (4.4-5.3)	0.995	4.9 (4.6-5.4)	4.9 (4.4-5.2)	0.678	0.3
Total cholesterol (mmol/l)	4.8 (4.4-5.5)	4.6 (4.0-5.1)	**0.024**	4.9 (4.0-6.0)	4.8 (4.2-5.6)	0.604	0.07
HDL cholesterol (mmol/l)	1.47 (1.15-1.96)	1.33 (1.10-1.80)	0.244	1.31 (1.10-1.54)	1.35 (1.10-1.50)	0.470	**0.01**
Triglycerides (mmol/l)[1]	0.97 (0.68-1.75)	1.18 (0.85-1.87)	0.180	1.65 (1.01-2.55)	1.40 (1.10-2.19)	0.559	**0.001**
Serum phosphate (mmol/l)	1.1 (0.9-1.2)	1.1 (1.0-1.2)	0.744	1.2 (1.0-1.3)	1.1 (0.9-1.2)	0.122	0.4
Aortic pulse wave velocity (m/s)	8.1 (7.0-9.4)	8.6 (7.5-10.8)	**0.003**	8.7 (7.9-9.8)	9.4 (8.0-10.8)	**0.021**	0.07

p* (p value comparing CC and non CC genotype in CRIB); p** (p value comparing CC and non-CC genotype in RIISC); p*** (p value comparing across all patients in CRIB versus RIISC cohorts). p value by Student's t-test for continuous variables and χ^2 for categorical variables unless stated. [1]variables p value tested by Mann-Whitney U.

Table 3-2 Multivariate analysis of aortic pulse wave velocity adjusted for age, gender, estimated glomerular filtration rate (eGFR) and mean arterial pressure (MAP) in the Chronic Renal Impairment in Birmingham and Renal Impairment in Secondary Care cohorts

Variable	Coefficient (95% Confidence Interval)	p value
Chronic Renal Impairment in Birmingham		
Age	0.094 (0.068, 0.119)	<0.001
Gender (Female)	0.452 (-0.161, 1.065)	0.1
eGFR (mls/min/1.73m^2)	-0.014 (-0.036, 0.008)	0.2
MAP (mmHg)	-0.005 (-0.030, 0.021)	0.7
Genotype (CC)	-0.621 (-1.218, -0.024)	0.04
Renal Impairment In Secondary Care		
Age	0.087 (0.067, 0.106)	<0.001
Gender (Female)	0.116 (-0.423, 0.654)	0.7
eGFR (mls/min/1.73m^2)	0.015 (-0.004, 0.034)	0.1
MAP (mmHg)	0.040 (0.019, 0.061)	<0.001
Genotype (CC)	-0.984 (-1.523, -0.445)	<0.001

3.1.1.3 Discussion

Independent of other key risk factors, I found that *CAV1* rs4730751 CC genotype is associated with lower arterial stiffness in patients with early and late stage non-dialysis CKD. Whilst CKD is major risk factor for CVD, the pathological basis for this relationship is uncertain, with inclusion of non-traditional risk factors as mentioned earlier that could include a genetic influence as shown in this study. Importantly, as CKD becomes more

advanced the dominant vascular lesion is arteriosclerosis and associated vascular stiffness, rather than atheromatous disease as seen in the general population (161).

The robustness of this finding is strengthened by the investigation of two independent cohorts, with similar effect sizes seen in each cohort, and also the investigation of patients of white ethnicity to limit population stratification. The exclusion of patients of non-white ethnicity, and also those with previous myocardial infarction, peripheral vascular disease and diabetes mellitus (due to these exclusion criteria in the CRIB trials from which the first cohort were derived) may limit generalisability of the results. However, the differences in the severity of CKD between the 2 studied cohorts, and the use of different methods of aPWV measurement between cohorts, serve to increase potential generalizability of the results. aPWV was measured using the SphygmoCor system in CRIB and the Vicorder system in RIISC. Whilst the former has been used as a reference standard when comparing other aPWV measurement methodologies, the latter has the advantage of requiring less training to use and is less intrusive (197). The Vicorder system has been shown to underestimate aPWV at higher values measured by the SphygmoCor system mainly due to measured transit times, however when directly compared, the systems are considered highly correlated (slope=0.64, $r=0.85$, $p<0.001$) in their aPWV recordings (197). This underestimation occurred with aPWV measures over 10m/s, yet the average aPWV for CRIB RCTs was 8.4 m/s and RIISC 8.8 m/s respectively, thus was unlikely to have had a significant bearing on the study findings. Despite the differing systems used, the investigated *CAV1* polymorphism remained significantly associated with aPWV in multivariate analysis in both cohorts, with the potential of aPWV underestimation by the Vicorder system in RIISC with the cohort having more advanced CKD.

This study would be strengthened by longitudinal data on the CVD outcomes in the cohorts. It should also be noted no formal assessment of ischaemia was made with non-invasive (stress echocardiogram) or invasive investigations (coronary angiography) so its influence cannot be excluded. Data related to erythropoietin and intravenous iron use was not fully collected for both cohorts (no use of erythropoietin in "CRIB") and thus I am unable to exclude if these therapies may have confounded the results.

The finding of this association in a cohort of patient with early to moderate CKD which is replicated in a cohort with advanced CKD suggests that the pathological processes associated with *CAV1* occur irrespective of the degree of renal impairment. CAV1 is ubiquitously distributed in cells pertinent to this current study. In vascular endothelium CAV1 interacts with eNOS such that reduced CAV1 increases eNOS activity which may have a deleterious effect on endothelial health and arterial stiffness, due to "uncoupling" of eNOS which leads to the generation of superoxide anion radicals (198) in oxidative stress characteristic of CKD (199). Similarly, caveolin-1 deficient aortic smooth muscle cells have been shown to be pro-arteriosclerotic with increased neointimal hyperplasia, cell proliferation and migration (200). These observations may underlie the findings of the current study. Conversely, lower levels of CAV1 in macrophages are associated with an anti-inflammatory phenotype, reduced foam cell formation and therefore protection from atheroma (147). Interestingly, these contrasting functions of CAV1 in endothelium ("anti-arteriosclerotic") and macrophages ("pro-atheromatous") may consolidate the findings of the current study whereby CC genotype associates with a reduced aPWV ("anti-arteriosclerotic") and the findings of Testa et al (159) who showed an association between CC genotype and increased carotid arterial intima media thickness (a measure of atheroma

rather than arteriosclerosis (201)). Patients included in the Testa et al non-replicated study were dialysis dependent (87 patients on haemodialysis, 47 on chronic ambulatory peritoneal dialysis) and had not excluded patients with diabetes or symptomatic heart disease which may account for their co-dominant model being associated with an adverse outcome. Further potential limitations of the study could be the lack of control for types of access used in the haemodialysis patients, or adequate control for electrolyte and fluid removal requirements that may have affected the left ventricular function of these patients and resultant arterial manifestations (202). Indeed, it has been suggested due to the complexity of patients in end stage renal disease, that controlling for potential confounders is difficult and thus may have affected the genotype:phenotype relationship found (203). For example, uraemic toxins such as high asymmetric dimethylarginine levels have been associated with, and shown to predict the progression of increased carotid arterial intima media thickness in dialysis dependent patients (204).

In summary, *CAV1* rs4730751 CC genotype is associated with lower aPWV in patients with non-dialysis CKD. This gene variant may represent a non-traditional risk factor for CVD associated with CKD.

3.1.2 eNOS SNP in left ventricular function in early CKD

This section is based on my first author publication (205).

3.1.2.1 Introduction

eNOS SNP rs1799983 for NOS3 is also known as Glu298Asp and G894T polymorphisms and has been associated with heart failure in the non-CKD population. This polymorphism is the

nucleotide guanine substitution of thiamine at position 894 of exon 7 on chromosome 7, resulting in glutamate or aspartate respectively at position of 298 on the protein. Thus, there is different cleavage of the eNOS enzyme depending on genotype and thus basal endothelial nitric oxide (NO) levels (206, 207). The mutant Asp variant has been shown to have a lower NO production in vitro, pre and post shear stress, with lower (approximately 40%) NOS3/CAV1 association at basal levels and impaired NOS3/CAV1 dissociation after acute shear stress, in immunoprecipitation experiments (208). The same authors later used human umbilical endothelial cells to show that the Glu/Asp and the Asp/Asp variant also had significantly less NOS3/CAV1 association compared to Glu/Glu using immunoprecipitation (209).

In the general population, there has been interest in the association between the Glu298Asp polymorphism within endothelial nitric oxide synthase (eNOS) and heart failure (166, 167). Although this polymorphism has been associated with endothelial dysfunction and progression of CKD through NO effects (168), it is not known if this polymorphism is associated with early, sub-clinical cardiac structural changes that occur in non-dialysis CKD as manifested by left ventricular dysfunction. In light of this, I investigated if this gene variant is associated with changes in systolic and diastolic function, based on detailed cardiac magnetic resonance imaging (CMR) in non-dialysis CKD patients with no known history of heart failure.

3.1.2.2 Results

Genomic DNA was successfully genotyped in 132 (>94%) patients. The eNOS SNP rs1799983 patient genotype frequency was GG in 47% (62/132), TG in 39% (51/132), and TT (Asp/Asp) in 14% (19/132). This distribution was within Hardy-Weinberg equilibrium bounds ($p>0.05$). Patient demographics are presented in Table 3-3 for the cohort as a whole and stratified by genotype (GG, TG and TT).There were no significant demographic differences across the three genotypes. Median age was 57 years, eGFR was 50.5 mls/min/1.73m2, with 85% of patients prescribed an angiotensin converting enzyme inhibitor or angiotensin II receptor blocker. The most common renal disease group was glomerular disease, with 16% of the cohort patients been diagnosed with IgA nephropathy on renal histology.

Table 3-3 Baseline demographics (p value across the three genotype groups)

Characteristic	GG genotype	TG genotype	TT genotype	All	p value
Number of patients (%)	62 (47)	51 (39)	19 (14)	132	
Age (years)	57 (46-63)	59 (47-66)	58 (42-69)	57 (46-65)	0.690
Estimated glomerular filtration rate (mls/min/1.73m^2)	50 (40-61)	51 (38-56)	45 (32-59)	51 (38-59)	0.686
Male (%)	30 (48)	28 (55)	15 (79)	73 (55)	0.063
High sensitive C-reactive protein (mg/l)	1.59 (0.57-5.00)	1.75 (0.91-5.97)	2.79 (0.67-9.87)	1.87 (0.72-5.62)	0.550
Total cholesterol (mmol/l)	4.7 (4.4-5.4)	4.5 (4.0-5.0)	4.8 (3.6-5.9)	4.6 (4.0-5.2)	0.374
Mean arterial pressure (mmHg)	92 (85-101)	90 (85-100)	91 (85-99)	91 (85-100)	0.898
Systolic blood pressure (mmHg)	129 (117-139)	127 (114-135)	124 (111-139)	127 (115-139)	0.539
Diastolic Blood Pressure (mmHg)	72 (66-81)	73 (67-81)	73 (66-79)	73 (66-80)	0.938
Body surface area (m^2)	1.87 (1.77-2.02)	1.90 (1.73-2.03)	1.97 (1.92-2.13)	1.92 (1.79-2.03)	0.061
Body mass index (Kg/m^2)	27.5 (24.1-31.4)	27.5 (24.2-31.1)	29.2 (25.7-32.2)	27.7 (24.2-31.4)	0.350
Brain natriuretic peptide (ng/L)	86.6 (34.9-176.2)	84.3 (30.9-205.7)	70.0 (37.1-160.9)	84.4 (33.8-193.0)	0.989
Current Smoker (%)	8 (13)	5 (10)	2 (11)	15 (11)	0.930
Previous Smoker (%)	24 (39)	13 (25)	8 (42)	45 (34)	0.250
Diagnoses					
Glomerular diseases (%)	25 (40)	18 (35)	11 (58)	54 (40)	0.230
Systemic Diseases (%)	10 (16)	11 (22)	1 (5)	22 (17)	0.296
Tubulointerstitial diseases (%)	7 (11)	9 (18)	0	16 (12)	0.124
Familial nephropathies (%)	9 (15)	7 (14)	1 (5)	17 (13)	0.681
Miscellaneous (%)	11 (18)	6 (12)	6 (32)	23 (17)	0.147
Medication frequency					
Angiotensin conversion enzyme inhibitors (%)	35 (56)	29 (57)	14 (74)	78 (60)	0.401
Angiotensin II receptor blockers (%)	20 (32)	15 (29)	4 (21)	39 (30)	0.681
B blockers (%)	13 (21)	10 (20)	3 (16)	26 (20)	0.956
Calcium channel blockers (%)	13 (21)	16 (31)	5 (26)	34 (26)	0.449
Alpha blockers (%)	7 (11)	6 (12)	2 (11)	15 (11)	0.999
Diuretics (%)	14 (23)	18 (35)	5 (26)	37 (28)	0.311
Statins (%)	28 (45)	20 (39)	9 (47)	57 (43)	0.765

Univariate analysis revealed a significant difference across genotypes for LVEF and LVESVI (p=0.006 and p=0.024 respectively, Table 3-4).

Table 3-4 Cardiac investigations relationship to genotype (p value across the three genotype groups)

Cardiac Investigations	GG genotype	TG genotype	TT genotype	All	p value
Cardiac Magnetic Resonance Imaging					
Left ventricular ejection fraction (%)	71 (65-76)	76 (71-80)	73 (66-78)	74 (68-77)	**0.006**
Left ventricular end-diastolic volume index (mls/m^2)	61 (52-70)	57 (51-66)	59 (51-64)	59 (52-66)	0.344
Left ventricular end-systolic volume index (mls/m^2)	17 (13-23)	14 (12-17)	16 (12-20)	16 (12-21)	**0.024**
Left Ventricular Mass Index (g/m^2)	54.0 (45.0-67.0)	54.6 (45.0-67.1)	56.0 (47.0-61.9)	54.1 (45.3-65.7)	0.996
Ascending Aortic Distensibility (x10^{-3} $mmHg^{-1}$)	2.53 (1.24-4.19)	2.15 (1.18-3.31)	2.11 (1.08-3.41)	2.35 (1.24-3.68)	0.692
CMR Cardiac Output (l/min)	5.12 (4.37-6.17)	5.19 (4.64-5.94)	6.38 (4.37-7.57)	5.26 (4.57-6.30)	0.177
CMR Heart Rate (beats/min)	66 (60-77)	64 (58-77)	78 (62-87)	66 (60-78)	0.074
Tissue Doppler Echocardiography					
S' lat, cm/s	8 (7-10)	9 (7-10)	9 (7-11)	8 (7-10)	0.688
e' lat, cm/s	9 (7-12)	9 (8-12)	9 (8-11)	9 (8-12)	0.790
E/e' lat	7.17 (5.73-8.96)	6.95 (6.08-8.40)	6.73 (6.13-7.80)	7.00 (6.00-8.56)	0.786
Mitral valve inflow E/A ratio	1.02 (0.87-1.23)	0.95 (0.81-1.20)	0.93 (0.70-1.12)	0.97 (0.81-1.20)	0.273
Mitral valve propagation velocity	50.3 (41.9-66.7)	50.5 (43.6-65.1)	45 (37.7-65.8)	50.0 (41.0-66.4)	0.701
Left Atrial Volume Index (mls/m^2)	26.3 (21.8-32.9)	24.5 (20.6-32.3)	27.3 (22.5-30.5)	26.2 (21.6-32.3)	0.760
Pulse wave velocity (m/s)	8.3 (7.3-9.5)	8.3 (7.2-10.0)	9.5 (6.6-10.7)	8.3 (7.2-10.0)	0.808
Augmentation Index (%)	29.0 (22.8-35.1)	27.3 (20.0-35.3)	27.2 (13.3-33.8)	28.3 (20.7-35.0)	0.691

Key: CMR (cardiac magnetic resonance); S' lat (systolic velocity of the basal anterolateral LV wall); e' lat (early diastolic velocity of the basal anterolateral LV wall on tissue doppler); E/e' lat (maximum velocity of the E-wave of mitral valve inflow by the maximal anterolateral LV wall velocity of e')

Post hoc Mann-Whitney U testing demonstrated significant differences between GG genotype and combined TG and TT genotypes (p=0.005, Figure 3-1).

Figure 3-1 Left ventricular ejection fraction by genotypes (Mann-Whitney U, p=0.005 for GG vs non-GG), and Kruskal-Wallis test between genotypes, p=0.006)

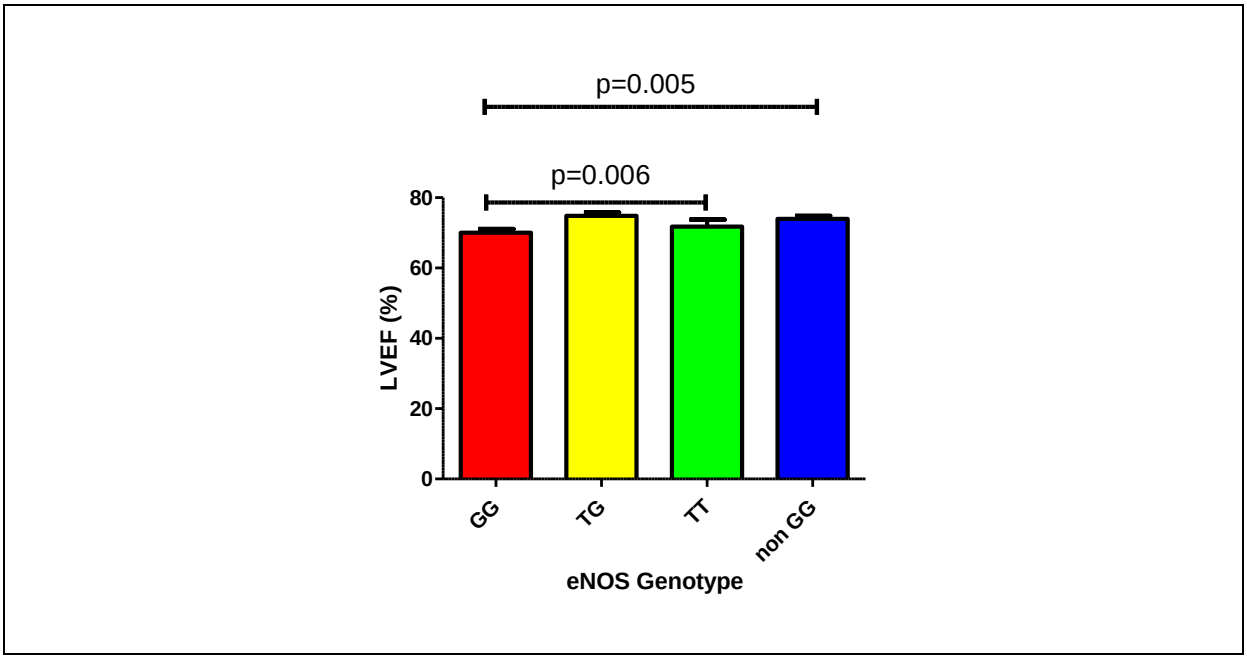

Because of this, and to align with existing literature (209), further analysis compared the GG group with the non-GG (TG+TT) group, i.e. a "dominant" model. Linear regression analysis revealed an absolute 4% lower LVEF (p=0.005) and a 21% relative increased LV end-systolic volume index (p=0.011) in GG versus non-GG (TG+TT) genotyped patients as shown in Table 3-5.

In multivariate analysis, (adjusting for age, gender, estimated glomerular filtration rate (eGFR), CMR heart rate (HR), total cholesterol, high sensitive C-reactive protein (hsCRP), body mass index (BMI – if variables were indexed accounting for body surface area, BMI was excluded in the analysis) and brachial mean arterial pressure (BMAP)) the GG genotype and

male sex were associated with significantly lower LVEF (p=0.004 and p=0.017 respectively; Table 3-5). Male gender, GG genotype, eGFR, and heart rate were independently associated with a higher end systolic and diastolic volume index. A trend for GG genotype association with lower S' lat was seen, but this failed to reach statistical significance (p=0.106).

Table 3-5 Univariate and multivariate analysis of systolic function as compared to GG vs non-GG

Factor	Univariate		Multivariate	
	Coefficient (95% CI)	*Sig.*	*Coefficient (95% CI)*	*Sig.*
		LVEF		
Age	0.07 (-0.04, 0.18)	0.228	0.07 (-0.05, 0.19)	0.274
eGFR	0.00 (-0.09, 0.08)	0.915	0.03 (-0.06, 0.11)	0.541
BMAP	-0.09 (-0.21, 0.03)	0.158	-0.06 (-0.19, 0.06)	0.318
CMR HR	0.02 (-0.09, 0.12)	0.737	0.00 (-0.12, 0.12)	0.987
Total Cholesterol	-0.68 (-2.14, 0.77)	0.354	-0.70 (-2.32, 0.92)	0.394
Log_2 hsCRP[‡]	0.03 (-0.75, 0.81)	0.936	-0.22 (-1.02, 0.58)	0.586
BMI	0.18 (-0.11, 0.47)	0.218	0.13 (-0.18, 0.45)	0.392
Gender (Female)	3.10 (0.30, 5.90)	**0.030**	3.62 (0.66, 6.58)	**0.017**
GG (Yes)	-3.95 (-6.70, -1.21)	**0.005**	-4.24 (-7.12, -1.35)	**0.004**
		LVEDVI		
Age	-0.01 (-0.20, 0.17)	0.878	0.03 (-0.16, 0.21)	0.782
eGFR	0.16 (0.03, 0.30)	**0.015**	0.14 (0.01, 0.27)	**0.033**
BMAP	-0.14 (-0.34, 0.06)	0.169	-0.18 (-0.38, 0.01)	0.066
CMR HR	-0.20 (-0.37, -0.04)	**0.018**	-0.23 (-0.41, -0.04)	**0.017**
Total Cholesterol	-0.83 (-3.15, 1.49)	0.478	0.65 (-1.84, 3.15)	0.606
Log_2 hsCRP[‡]	-1.09 (-2.32, 0.15)	0.084	-1.20 (-2.40, 0.00)	0.050
Gender (Female)	-4.68 (-9.17, -0.18)	**0.041**	-5.02 (-9.56, -0.48)	**0.031**
GG (Yes)	4.04 (-0.45, 8.53)	**0.078**	4.46 (0.02, 8.90)	**0.049**
		LVESVI[#]		
Age	-0.40% (-1.00%, 0.20%)	0.195	-0.3% (-0.9%, 0.3%)	0.271
eGFR	0.50% (0.10%, 0.90%)	**0.021**	0.4% (0.0%, 0.8%)	0.076
BMAP	-0.20% (-0.80%, 0.50%)	0.614	-0.3% (-0.9%, 0.3%)	0.336
CMR HR	-0.53% (-1.07%, 0.02%)	0.059	-0.6% (-1.2%, 0.0%)	0.057
Total Cholesterol	0.3% (-7.0%, 8.2%)	0.936	3.5% (-4.7%, 12.3%)	0.413
Log_2 hsCRP[‡]	-1.9% (-5.8%, 2.2%)	0.357	-1.4% (-5.3%, 2.6%)	0.474
Gender (Female)	-16.6% (-28.0%, -3.5%)	**0.015**	-19.4% (-30.6%, -6.4%)	**0.005**
GG (Yes)	21.0% (4.6%, 40.0%)	**0.011**	21.9% (5.3%, 41.1%)	**0.009**
		S' Lat		
Age	-0.03 (-0.07, 0.00)	**0.040**	-0.04 (-0.08, 0.00)	**0.040**
eGFR	0.00 (-0.03, 0.02)	0.759	-0.01 (-0.03, 0.02)	0.606
BMAP	0.02 (-0.02, 0.06)	0.294	0.02 (-0.02, 0.06)	0.248
CMR HR	-0.01 (-0.04, 0.02)	0.576	-0.02 (-0.06, 0.02)	0.347
Total Cholesterol	0.13 (-0.28, 0.55)	0.529	0.15 (-0.36, 0.65)	0.571
Log_2 hsCRP[‡]	0.00 (-0.22, 0.22)	0.988	0.00 (-0.24, 0.25)	0.992
BMI	0.03 (-0.06, 0.11)	0.543	0.05 (-0.04, 0.15)	0.278
Gender (Female)	0.30 (-0.51, 1.11)	0.465	0.39 (-0.53, 1.30)	0.405
GG (Yes)	-0.45 (-1.26, 0.36)	0.270	-0.73 (-1.62, 0.16)	0.106

p-Values from linear regression analysis

#Outcome was log_2-transformed prior to analysis to normalise the distribution. Quoted coefficients represent

the percentage increase in the outcome for an increase in one of the factors (or for the stated category relative to the reference).
‡hsCRP was log_2-transformed, hence the quoted coefficients relate to an increase of one unit in the log (i.e. a two-fold increase)
Key: eGFR (estimated glomerular filtration rate; BMAP (brachial mean arterial pressure); CMR HR (cardiac magnetic resonance heart rate); hsCRP (high sensitive C-reactive protein; BMI (body mass index)

A cluster analysis was performed with the assistance of Queen Elizabeth Hospital Birmingham statistician James Hodson, based on diastolic parameters in order to group patients based on their risk of diastolic function (Table 3-6). The most important factor in defining the clusters was found to be e' lat, with mitral valve E/A (MV E/A) and E/e' lat being moderate contributors, and the remaining parameters being minimally discriminative. The first cluster had lower levels of e' lat, MV E/A and MV VP and higher levels of E/e' lat and LAVI, hence represented those patients at most risk of diastolic dysfunction.

Table 3-6 Relative importance of diastolic parameters and their respective values for cluster separation

Factor	Relative Importance	Cluster 1	Cluster 2
Early diastolic velocity of the anterolateral left ventricular wall (e' lat)	1.00	7.8 (7.4 - 8.3)	12.7 (11.9 - 13.5)
Mitral valve inflow E/A ratio	0.73	0.87 (0.82 - 0.92)	1.27 (1.18 - 1.37)
Peak E velocity to early diastolic velocity of the anterolateral left ventricular wall (E/e' lat)	0.62	8.1 (7.6 - 8.6)	5.7 (5.4 - 6.1)
Mitral valve velocity propagation	0.37	46.5 (43.3 - 49.9)	67.6 (58.8 - 77.7)
Left Atrial Volume Index	0.12	27.0 (25.4 - 28.6)	23.8 (22.4 - 25.4)
Left Ventricular Mass Index	0.00	54.5 (51.1 - 58.1)	54.1 (50.3 - 58.2)

Data reported as: "Mean (95% CI)".
Key: e' lat (early diastolic velocity of the basal anterolateral LV wall on tissue doppler); mitral valve E/A (ratio of early to late mitral inflow velocities); E/e' lat (maximum velocity of the E-wave of mitral valve inflow by the maximal anterolateral LV wall velocity of e')

Comparisons between the clusters found that increased age ($p<0.001$) and reduced eGFR ($p=0.014$) were significantly associated with the risk of diastolic dysfunction clusters on univariate analysis (Table 3-7).

Table 3-7 Univariate analysis of diastolic parameters clusters

Factor	Cluster 1	Cluster 2	p-Value
Age	60.9 (1.1)	43.8 (1.7)	**<0.001**
Estimated Glomerular Filtration Rate	47.3 (1.8)	54.5 (2.3)	**0.014**
Brachial Mean Arterial Pressure	92.2 (1.4)	91.4 (1.9)	0.700
Gender (Male)	37 (56.1%)	19 (48.7%)	0.545
Genotype (GG)	28 (42.4%)	22 (56.4%)	0.225

Continuous factors are reported as: "Mean (SE)", with p-values from independent sample t-tests.
Dichotomous factors are reported as: "N (%)", with p-values from Fisher's Exact Test.

3.1.2.3 Discussion

In this cohort of white patients with non-dialysis dependent CKD, and without heart failure, GG genotype for *eNOS* SNP rs1799983 was associated with a significant lower LVEF, greater LVESVI and greater LVEDVI than those found in non-GG genotypes. The burden of myocardial disease in CKD suggests the investigation of stratification by genetic risk in this setting to be a worthwhile endeavour, and this study represents the first such attempt with this eNOS polymorphism.

Previous data from the general population suggest this gene variant represents an attractive candidate SNP, and support the findings of the current study. For instance Velloso et al studied a multi-ethnic Brazilian population and demonstrated increased frequency of GG genotype in patients with systolic heart failure compared with healthy controls (167). Another Brazilian study showed GG genotype was associated with a near 5% reduction in LVEF compared with TT genotype patients, findings very similar to those of the current study (210). Also noteworthy is the higher all-cause mortality associated with the GG genotype in hypertensive patients (211). An important aspect of the current study is the inclusion of white patients only, in an attempt to reduce confounding by population stratification. Indeed this is highlighted by the study of Velloso et al which did indeed show differences in genotype frequency at this locus between White and Afro-Brazilian individuals (167). It should be acknowledged, however, that further validation of these findings in diverse populations are required to confirm the robustness of my (and other's) findings.

The functional change associated with this gene variant also supports the clinical data as described earlier. The GG genotype of the studied SNP is associated with increased eNOS

activity and nitric oxide levels (212, 213) and experimental overexpression of eNOS (which is present within ventricular myocytes) results in reduced ventricular function (212, 214). This is particularly the case in conditions of oxidative stress such as CKD (199), since “uncoupling” of eNOS may lead to generation of superoxide anion radicals that further exacerbate cardiac dysfunction (198).

The influence of genotype on cardiac function and outcome may be context-specific. Of note, McNamara et al suggested a beneficial effect of GG genotype outcome in patients with established, clinically evident heart failure (166). Whilst at first sight this data conflicts with the current study, and with that of other reports (167, 168), it should be noted that 84% of patients displayed an ejection fraction ≤35% (97.2% of participants were in NYHA stage II or greater, with >50% in stages III or IV). Furthermore there were differences in age and aetiology (ischaemic versus non-ischaemic) between genotype groups which may have influenced the results as well as variation in the technique used in measuring ejection fraction. Thus, it is certainly possible that this *eNOS* SNP influences outcome differentially depending on the stage of heart failure studied. Although the present study’s exclusion criteria (diabetes mellitus, peripheral vascular disease, myocardial infarction, known heart failure, valvular heart disease, atrial fibrillation, dialysis-dependence and uncontrolled hypertension) limits the generalizability of its findings, the exclusion criteria does allow removal of these potential external factors that affect both eNOS activity and left ventricular function, allowing a more ‘pure’ analysis of *eNOS* polymorphism association with LVEF in early CKD.

This study benefits from a uniform technique of detailed CMR assessment of cardiac volumes and systolic function, and very careful clinical phenotyping. Although no association with “diastolic dysfunction” parameters derived from echocardiography and genotype was evident, the size of the cohort means that such an effect cannot be excluded, and further study in larger cohorts is required.

In summary, eNOS Glu298Asp polymorphism in non-dialysis CKD patients is associated with relevant sub-clinical cardiac remodelling as detected by CMR.

CHAPTER 4:

CAV1 IN ANTINEUTROPHIL CYTOPLASMIC ANTIBODY ASSOCIATED VASCULITIS

4.1 *CAV1* in antineutrophil cytoplasmic antibody associated vasculitis

This section is based on my first author publication (215).

4.1.1 Introduction

The vasculitidies represent an inflammatory group of disorders affecting small to large sized blood vessels. They can be secondary due to underlying connective tissues disorders, infection, malignancy and medication), and be localised or systemic. Anti-neutrophil cytoplasmic antibody (ANCA) associated vasculitis represent a group of primary autoimmune disorders that are systemic, mainly involving small to medium sized vessels and have a peak age affecting 60 to 70 year olds (216). ANCAs are directed against proteinase 3 (PR3) and myeloperoxidase (MPO) which are present in the primary granules of neutrophils and monocytes. The three main ANCA associated vasculitidies (AAV) are granulomatous polyangiitis (GPA), microscopic polyangiitis (MPA) and eosinophilic granulomatous polyangiitis (EGPA). There is now gathering evidence that these diseases are genetically distinct, with EGPA being often ANCA negative, much less common and thus treated in a different manner (25, 216, 217). The global incidence of GPA and MPA is increasing with an estimated 5-10 million people per year diagnosed (218).

If left untreated AAV resulted in devastating multi-organ failure affecting organs such as the kidneys, lungs and skin resulting in high mortality of 90% at 2 years post diagnosis, prior to advent of potentially highly toxic treatment with cyclophosphamide and high-dose corticosteroids (219, 220). Despite success in improving patient life expectancy, there remains high mortality at 5 years (up to 28%) and significant morbidity associated with complications of the disease and its treatment such as infection, cardiovascular disease,

malignancy and chronic kidney disease. These types of clinical outcomes have been associated with the pleiotropic effects of CAV1, thus the purpose of this study was to investigate whether the *CAV1* gene variant rs4731751 was associated with these clinical outcomes in AAV. The primary outcome measure was chosen as a combined end-point of time to all-cause mortality and time to renal replacement therapy (RRT), as this encompassed the increased risk of death from the co-morbidities associated with AAV and the progression of kidney disease (and interstitial fibrosis). Following preliminary results in an AAV cohort from Birmingham, UK, a combined Northern European replication AAV cohort from Germany and the Netherlands was studied to validate the findings.

4.1.2 Results

4.1.2.1 Birmingham Cohort

In the Birmingham cohort, genomic DNA was successfully genotyped in 187 (>93%) patients. The CAV1 SNP was within Hardy-Weinberg equilibrium bounds ($p>0.05$). Demographics of this cohort are shown in Table 4-1. The genotype of the patients at the studied locus was AA in 12.3% (23/187), AC in 38.5% (72/187), and CC in 49.2% (92/187). During a median follow-up of 110 months (interquartile range, 67-166 months), 58 patients died and 37 patients required RRT. There were 78 (41.7%) primary composite outcome events.

Table 4-1 Demographics for Birmingham and Northern European cohorts are shown

Characteristic	Birmingham	Northern Europe	p value
Number of patients	187	589	
Age, years	67 (56-77)	63 (52-71)	<0.001
Age at diagnosis, years	58 (46-68)	54 (42-63)	0.003
Male (%)	104 (56)	302 (51)	0.314
Genotype			
AA (%)	23 (12)	30 (5)	0.001
AC (%)	72 (39)	231 (39)	0.93
CC (%)	92 (49)	328 (56)	0.130
Granulomatosis with polyangiitis (%)	110 (59)	531(90)	<0.001
Microscopic polyangiitis (%)	77 (41)	58 (10)	<0.001
Age at diagnosis, years	58 (46-68)	54 (42-63)	0.003
Creatinine at presentation, µmol/L	182 (100-385)	90 (90-150)	<0.001
Cytoplasmic (c) ANCA (%)	109 (58)	Not measured	
Perinuclear (p) ANCA (%)	71 (38)	Not measured	
Proteinase 3 (PR3) (%)	Not measured	438 (74)	
Myeloperoxidase (MPO) (%)	Not measured	97 (17)	
Negative (%)	7 (4)	54 (9)	

Kaplan-Meier estimate of the primary combined outcome of time to all-cause mortality/RRT revealed significant differences between genotypes at rs4730751 (Figure 4-1; p=0.022), with inferior outcomes in patients with non-CC genotype.

Figure 4-1 Kaplan-Meier analysis of time to all-cause mortality and renal replacement therapy in the Birmingham cohort by genotype of *CAV1* SNP rs4730751. The number of patients at risk at separate time points is shown by year of follow-up. Graphic data shown to the last surviving 10% patients. p=0.022

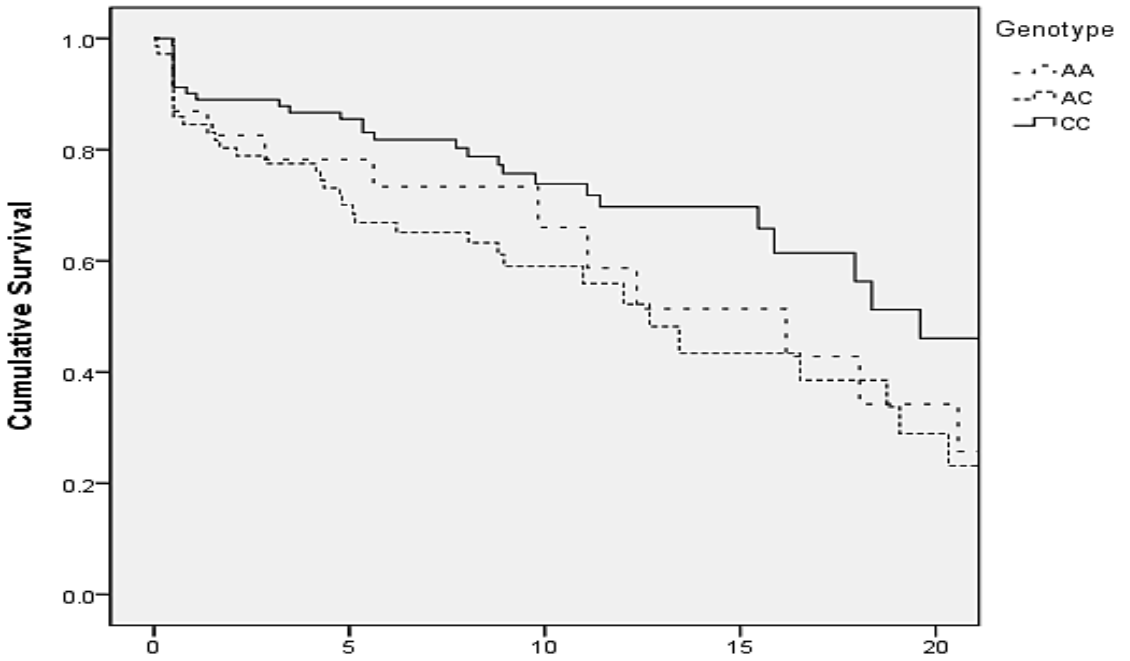

Year:	0	1	5	10	15	20
AA	23	20	16	9	6	4
AC	72	60	45	23	9	5
CC	92	82	70	40	18	9

Overall primary outcomes rates were 60.9% (14/23) for patients with genotype AA, 48.6% (35/72) for AC, and 31.5% (29/92) for CC genotypes. The Cox model examined patient genotype as non-CC (i.e. AA and AC combined) genotype versus CC genotype. A univariate association was found between genotype and time to all-cause mortality/RRT (non-CC vs. CC hazard ratio [HR]: 1.90; 95% confidence interval [CI], 1.19-3.02; p=0.007). This effect persisted in the multivariate analysis, where a similar HR was observed (non-CC vs. CC HR, 1.86; 95% CI, 1.14-3.08; p=0.013), adjusted for age at diagnosis, gender, type of ANCA and serum creatinine level at presentation.

4.1.2.1.1 Secondary Analyses

After adjusting for age at diagnosis, gender, creatinine at presentation and type of ANCA, non-CC genotyped patients were at significantly increased risk for time to all-cause mortality, time to death from infection, time to death from a cardiovascular cause and time to cancer development from AAV diagnosis. There was some evidence for an increased risk of RRT for non-CC genotype, but this did not meet criteria for statistical significance (Table 4-2).

Table 4-2 Multivariate regression analysis of genotypes non-CC vs. CC for CAV1 SNP rs4730751. Times to event endpoint for both cohorts were adjusted for age at diagnosis, gender, creatinine at presentation and type of ANCA

Variable	HR	95% Confidence Interval	p value
Birmingham Cohort			
Time to All-cause mortality	1.83	1.02-3.27	0.042
Time to Death from Vascular cause	3.13	1.07-9.10	0.037
Time to Death from Infection	3.71	1.28-10.77	0.016
Time to Cancer Development from AAV diagnosis	5.55	1.59-19.31	0.007
Time to Renal Replacement Therapy	1.79	0.86-3.73	0.119
Northern European Cohort			
Time to All-cause mortality	0.90	0.44-1.84	0.764
Time to Death from Vascular cause	1.33	0.27-6.67	0.729
Time to Death from Infection	1.24	0.28-2.00	0.196
Cancer	0.77*	0.28-2.17	0.625
Time to Renal Replacement Therapy	1.37	0.63-2.96	0.427

*Exact date of cancer onset during follow-up period not available, thus logistic regression analysis used, expressed as Odds Ratio

4.1.2.2 Northern European Cohort

In the Northern European cohort, genomic DNA was successfully genotyped in 589 (>98%) patients. CAV1 SNP rs4730751 was within Hardy-Weinberg equilibrium bounds ($p>0.05$). As shown in Table 4-1, there was a significantly lower AA genotype and higher CC genotype prevalence in Northern Europe as compared to the Birmingham cohort: AA genotype in 5.1% (30/589); AC genotype in 39.2% (231/589), and CC genotype in 55.7% (328/589). The Northern European cohort had over 90% of patients diagnosed with GPA as compared to fewer than 60% Birmingham. The Northern European cohort also had significantly lower creatinine values (suggesting a better kidney function) at presentation. During a median follow-up of 89 months (interquartile range, 48-132 months), there were 33 deaths and 32 patients who required RRT. In all, there were 61 (10.4%) primary outcome events as compared to the 41.7% event rate in Birmingham described above.

No association was seen between genotype and Kaplan-Meier estimates of time to primary outcome measure (Figure 4-2; p=0.427).

Figure 4-2 Kaplan-Meier analysis of time to all-cause mortality and renal replacement therapy in the Northern European cohort by genotype of *CAV1* SNP rs4730751. The number of patients at risk at separate time points is shown by year of follow-up. Graphic data shown to the last surviving 10% patients. p=0.427

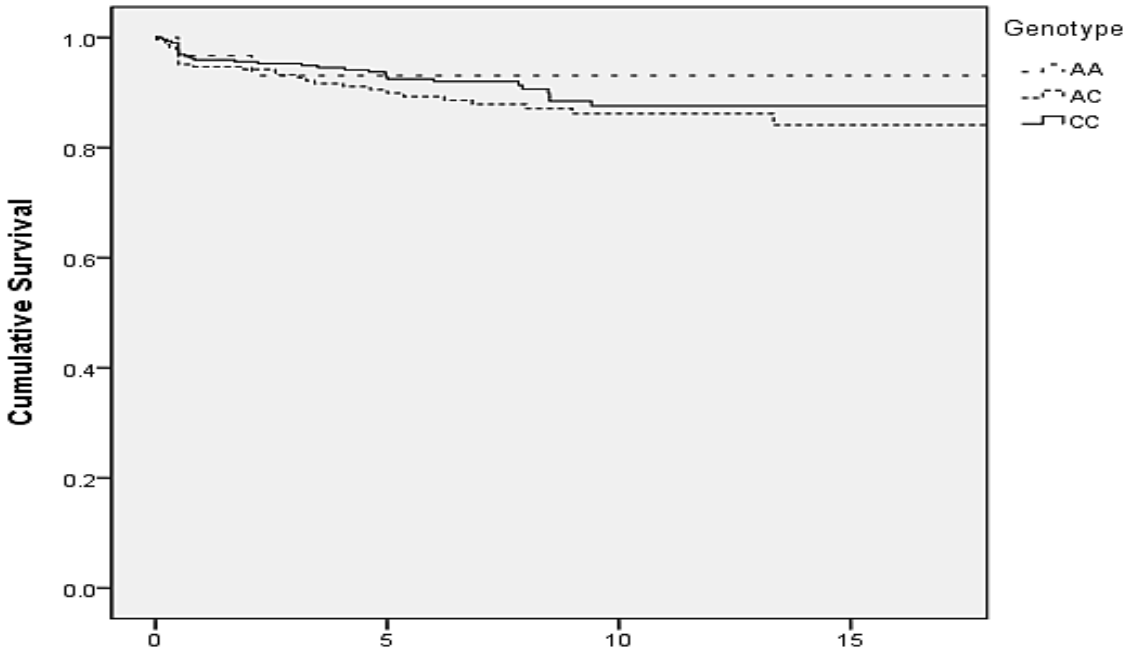

Year:	0	1	5	10	15	20
AA	30	29	20	8	2	4
AC	231	205	146	79	31	10
CC	328	300	219	82	38	14

Overall primary outcome rates were 10.9% (2/30) for patients with AA genotype, 12.6% (29/231) for AC genotype, and 9.1% (30/328) for CC genotype. The Cox model showed no evidence of association between genotype and the primary outcome measure (non-CC genotype vs. CC genotype HR: 1.29; 95% CI, 0.78-2.13; p=0.319). As shown in Table 4-2, no evidence for an association between genotype and any of the secondary outcome measures was evident in the replication cohort.

4.1.2.3 Interaction between CAV1 genotype and Clinical Diagnosis

Due to current evidence of GPA and MPA being considered separate genetic disease entities, the influence of genotype for each diagnosis was next examined. The primary methodology for this was to examine a statistical interaction between *CAV1* genotype and diagnosis. In addition a subgroup analysis for each secondary outcome was performed. This was performed with the assistance of Queen Elizabeth Hospital Birmingham statistician James Hodson.

For all outcomes, the CC genotype was associated with lower risk. A significant interaction (last column of Table 4-3) between *CAV1* genotype and diagnosis was observed only for the 'Renal Replacement Therapy' outcome, whereby the influence of genotype was greater in patients with GPA. Although at first sight the results of the subgroup analyses seem to suggest a difference between diagnostic groups (second to last column of Table 4-3), this is likely a result of numbers in the study. The results of the interaction analyses (a more robust way of examining this issue) do not point to a differential effect of genotype between diagnoses.

Table 4-3 Cox regression analyses assessing the association of genotype upon the outcomes when the cohort is divided into diagnoses and then an assessment of the significance of interaction to address if the *CAV1* SNP genotype effect varied between diagnoses

Time to Event	Diagnosis	Hazard Ratio (95% CI)	CC vs. non-CC p-value	Interaction p-value
All-cause mortality or Renal Replacement Therapy	GPA MPA	0.56 (0.36, 0.86) 0.67 (0.39, 1.15)	0.009 0.15	0.66
All-cause mortality	GPA MPA	0.74 (0.43, 1.29) 0.47 (0.25, 0.90)	0.29 0.02	0.25
Death from vascular cause	GPA MPA	0.33 (0.11, 1.04) 0.33 (0.10, 1.06)	0.06 0.06	0.95
Death from infection	GPA MPA	0.63 (0.24, 1.66) 0.40 (0.15, 1.09)	0.35 0.07	0.49
Cancer (*)	GPA MPA	0.18 (0.04, 0.82) 0.11 (0.01, 0.87)	0.03 0.04	0.62
Renal Replacement Therapy	GPA MPA	0.39 (0.20, 0.76) 1.16 (0.54, 2.51)	0.006 0.70	0.04

(*) Analysis performed on Birmingham data only, as time to cancer data was unavailable for the Northern European cohort.

4.1.3 Discussion

This is the first study to evaluate the role of *CAV1* gene variation in determining clinical outcome in patients with AAV. In the Birmingham cohort, gene variation at the *CAV1* SNP rs4730751 was associated with the chosen combined primary end-point of time to all-cause mortality or RRT. In addition, secondary analyses showed an association between this SNP and all-cause mortality, death from infection, death from cardiovascular disease, and the development of cancer from AAV diagnosis. These findings are plausible from previous studies in caveolin-1 biology, specifically with its role in vascular disease, sepsis, cancer and fibrosis.

The association between genotype and clinical outcome was not replicated in the Northern European cohort. There may be a number of reasons underlying this. The Northern European cohort appeared to have a lower expected event rate for an AAV cohort. Flossmann et al studied 535 patients with GPA or MPA as part of the European Vasculitis Study Group. Over a median follow-up of 5.2 years, there was a 25% mortality rate, with 32.3% of deaths from infection, 21.1% of deaths from cardiovascular cause, and a 9.3% cancer incidence (170). Outcomes in the Birmingham cohort were similar, as over a median follow-up of 9.2 years the respective rates were 31.0%, 11.8%, 10.2% and 11.8%. In contrast, in the Northern European cohort over a median follow-up of 7.4 years, the respective rates were only 5.6%, 1.2%, 1.0% and 2.9%. The Northern European cohort was younger than that of Birmingham, and in particular had better kidney function at presentation. This likely reflects the "rheumatological" nature of the Northern European cohort versus the "nephrological" nature of the Birmingham cohort. Certainly kidney function at presentation is an important determinant of outcome in AAV, and this may explain the discrepancy between the cohorts, and the lack of association in the replication study. In addition, a difference in proportions of patients with GPA versus MPA was seen between the cohorts. Interestingly, we found some evidence that the influence of genotype differed between diagnoses for the time to requirement of renal replacement therapy, with a more marked effect in patients with a clinical diagnosis of GPA. This preliminary observation is relevant in light of emerging evidence that MPA and GPA are genetically distinct condition (25). As well as a HLA association, this study found PR3 genetic variation to be associated with GPA. Other examples of an antigen-specific autoimmunity include PLA_2R in membranous nephropathy with associated genetic variation of PLA2R associated with membranous nephropathy

variant. However caution is required in the case of α1-antitrypsin genetic variation in AAV. This protease inhibitor is known to be a major inhibitor of proteinase 3 activity (221). However, despite altered activity of the protease inhibitor with patients with the Z allele of the gene *SERPINA1*, the Z allele carriage was not associated with disease severity, survival or replapse (222). Thus the SNP rs7151526 of this gene is likely to be in linkage disequlibrium with a nearby gene that is more likely to be the causal variant (25).

It should be acknowledged that the study design did not take in to account the varying immunosuppression protocols of the differing institutions, nor the severity of the disease activity. In addition, there is the possibility of ascertainment bias with regard to patient outcomes in this observational study. Finally, the issue of cryptic population stratification always exists in studies such as this, although the inclusion of only white patients goes some way to limit the confounding effect of this.

In summary, this is the first study to describe the association between *CAV1* variation and the outcomes of patients with ANCA associated vasculitis and renal involvement. This study suggests a relationship between the *CAV1* SNP rs4730751 and complications of AAV and its treatment, although the effect may be context-specific.

CHAPTER 5:

NEW-ONSET DIABETES AFTER TRANSPLANTATION

5.1 New-onset diabetes after transplantation – can genetics identify pathways to its development?

This section is based on my first author publication (223)

5.1.1 Introduction

Despite excellent first year outcomes in kidney transplantation, there remain significant long-term complications of premature graft loss, morbidity and mortality related to infection and cardiovascular disease. New-onset diabetes after transplantation (NODAT) is the major form of post-transplant hyperglycaemia that is associated with such complications. Thus research has focussed on measures to prevent post-transplant hyperglycaemia development, identification of those at risk in a timely manner and investigating molecular pathways to its development. Investigation of single nucleotide polymorphism (SNP) variants offers such a strategy. A number of previous studies have investigated specific candidate gene variants, usually on the basis of prior evidence of association with type 2 diabetes in non-transplanted individuals. Whilst some such SNPs have shown an association with NODAT, little attempt has been made to replicate findings in independent cohorts. During the last few years the nomenclature has interchanged with NODAT and post-transplant hyperglycaemia, with the latter now preferred. However, NODAT has been used for the purpose of the following chapter as pre-transplant diabetic status has been excluded for the study population below.

More recently, the first genome-wide association study (GWAS) in the field has been reported from Ireland (73). In the GWAS study, NODAT was defined as the use of oral hypoglycaemics or insulin over a 12 year follow-up period, with the median time of NODAT onset of 100 months. However this approach potentially misses a number of cases of NODAT, hence recent research highlights the growing momentum to use biochemical testing when identifying post-transplant hyperglycaemia (224, 225). It is also worth noting that 25% of patients in this GWAS study were treated with a calcineurin inhibitor-free maintenance regimen. Calcineurin inhibitors are widely used and are a known risk for NODAT development (226).

The purpose of this study was to validate the findings of the GWAS and other candidate NODAT SNPs investigated in the Belfast study (73), but in a prospective study of patients undergoing a protocolised, contemporary immunosuppression regimen, and using detailed serial biochemical testing to identify the development of NODAT. The insulin receptor has a CAV1 binding motif to the CAV1 scaffolding domain, with CAV1 peptides stimulating insulin receptor kinase activity especially seen in adipocytes (97). The CKO mouse, although not overtly diabetic itself, does show features consistent with insulin resistance, with the mouse developing postprandial hyperglycaemia after 9 months of a high-fat diet (150). Thus *CAV1* rs4730751 was included with the potential SNPs associated with NODAT.

5.1.2 Results

Demographics of the cohort are shown in Table 5-1. The cohort was aged 45 years (±15), human leucocyte antigen (HLA) mismatched 2.41 (±1.43), body mass index increase of 1.0 (±2.2) with 68% undergoing live kidney transplantation. Eighteen patients (26.5%) were diagnosed with NODAT, of whom 11 patients (61.1%) were diagnosed on the basis of the result of OGTT testing alone. Patients developing NODAT were older and displayed greater changes in BMI over the first year post-transplantation ($p<0.05$ for both). There were no significant differences between patients developing and not developing NODAT for HLA mismatch, rejection episodes, overall steroid dose used per day, tacrolimus levels or presence of adult polycystic kidney disease ($p>0.05$ for all). No patients had a prevalent or incident hepatitis C virus infection (this infection has been associated with NODAT). This is likely a reflection of the sample size and population investigated, as these are known risk factors for post-transplant hyperglycaemia.

Table 5-1 Demographics of renal transplant study cohort

Characteristic	NODAT	Non-NODAT	All	p value
Number of patients (%)	18 (26)	50 (74)	68	
Age (years)	54 (±12)	41 (±15)	45 (±15)	0.002
Female (%)	8 (44)	20 (40)	28 (41)	0.785
Body Mass Index (Kg/m^2)	27.5 (±4.9)	26.3 (±4.8)	26.6 (±4.8)	0.375
Body Mass Index Change (Kg/m^2)	-0.5 (±2.5)	1.5 (±1.9)	1.0 (±2.2)	0.002
Polycystic Kidney Disease (%)	3 (17)	7 (14)	10 (15)	0.717
Transplant type, live (%)	13 (72.2)	33 (66)	46 (67.6)	0.775
Human Leucocyte Antigen mismatch	2.82 (±1.59)	2.45 (±1.36)	2.56 (±1.43)	0.371
Total Rejection Episodes	0.39 (±0.61)	0.25 (±0.64)	0.29 (±0.63)	0.179
1^{st} Month Rejection Episodes	0.11 (±0.32)	0.13 (±0.33)	0.12 (±0.33)	1.000
Prednisolone dose (mg/day)	9.0 (6.3-9.7)	6.3 (6.3-9.3)	6.3 (6.3-9.7)	0.120
FK Level (micrograms/l)	8.8 (±1.5)	8.1 (±1.3)	8.3 (±1.4)	0.107

Out of the remaining 50 candidate SNPs that were identified by literature review (73), 45 were successfully genotyped (rs1800961 [*HNFA*], rs2069763 [*IL-2*], rs2265917 [*SHPRH*], rs6903252 [intergenic] and rs7903146 [*TCF7L2*] were unavailable as they were not amenable to the Sequenom iPLEX genotype bundle designs). The genotype success rate for the 46 SNPs (including rs4730751 [*CAV1*]) was >99%. Seven SNPs (rs10117679 [*GRIN3A*], rs1016429 [*GRIN3A*], rs12255372 [*TCF7L2*], rs17657199 [*NDST1*], rs2070874 [*IL-4*], rs2240747 [*ZNRF4*], rs4730751 [*CAV1*]) demonstrated deviation from Hardy-Weinberg equilibrium ($p<0.05$).

In the adjusted logistic regression model, five SNPs were significantly associated with NODAT: rs16936667 [*PRDM14*: OR 10.57; 95% CI 1.8-63.0; p=0.01], rs1801282 [*PPARG*: OR 8.5; 95% CI 1.4-52.7; p=0.02], rs8192678 [*PPARGC1A*: OR 0.26; 95% CI 0.08-0.91; p=0.03], rs2144908 [*HNF4A*: OR 7.0; 95% CI 1.1-45.0; p=0.04] and rs2340721 [*ATF6*: OR 0.21; 95% CI 0.04-1.0; p=0.05] (Table 5-2).

Table 5-2 Univariate (p value) and multivariate analysis (p value adj) of the candidate single nucleotide polymorphisms for the development of new-onset diabetes after transplantation

SNP	Gene	Location	Minor Allele	MAF	p value	p value adj	Odds ratio (95% CI)
rs16936667	*PRDM14*	8:70975726	G	0.16	0.03	**0.01**	10.6 (1.8-63.0)
rs1801282	*PPARG*	3:12393125	G	0.1	0.12	**0.02**	8.5 (1.4-52.7)
rs8192678	*PPARGC1A*	4:23815662	A	0.34	0.17	**0.03**	0.26 (0.08-0.91)
rs2144908	*HNF4A*	20:42985717	A	0.18	0.05	**0.04**	7.0 (1.1-45.0)
rs2340721	*ATF6*	1:161849385	A	0.3	0.006	**0.05**	0.21 (0.04-1.0)
rs198372	*NPPA*	1:11909514	A	0.12	0.14	0.08	0.11 (0.01-1.3)
rs5219	*KCNJ11*	11:17409572	T	0.34	0.08	0.12	2.7 (0.77-9.8)
rs10899444	*SHANK2*	11:70606500	G	0.15	0.77	0.15	0.32 (0.07-1.5)
rs1025689	*IL-17RB*	3:53883722	G	0.44	0.14	0.15	0.45 (0.15-1.34)
rs1124053	*IL-17E*	14:22914819	T	0.23	0.05	0.16	2.7 (0.68-10.3)
rs2265477	*SHPRH*	6:146212338	C	0.46	0.54	0.17	0.45 (0.14-1.4)
rs6793265	*ITPR1*	3:4735533	T	0.13	0.22	0.23	2.2 (0.60-8.4)
rs7145618	*PPP2R5C*	14:102329098	C	0.07	0.64	0.25	3.1 (0.44-21.5)
rs1783606	*SHANK2*	11:70576651	A	0.14	0.99	0.26	0.42 (0.09-1.9)
rs2265919	*SHPRH*	6:146221753	G	0.44	0.74	0.29	0.54 (0.18-1.7)
rs3212574	*ITGA2*	5:52366779	A	0.23	0.94	0.30	2.1 (0.50-9.2)

rs2107538	*CCL5*	17:34207780	T	0.18	0.07	0.34	2.1 (0.46-9.5)
rs2240747	*ZNRF4*	19:5456930	C	0.21	0.86	0.37	2.0 (0.45-8.7)
rs7533125	*DNAJC16*	1:15883744	C	0.23	0.43	0.40	0.61 (0.19-1.9)
rs17657199	*NDST1*	5:149950246	T	0.03	0.37	0.41	2.5 (0.28-23.3)
rs3817655	*CCL5*	17:34199641	A	0.18	0.12	0.48	1.8 (0.37-8.5)
rs4819554	*IL-17RA*	22:17565035	G	0.12	0.62	0.49	1.7 (0.38-7.9)
rs341497	*DIAPH3*	13:60429001	C	0.06	0.45	0.49	2.0 (0.28-14.1)
rs2020902	*CASP9*	1:15834360	C	0.16	0.26	0.52	0.65 (0.17-2.4)
rs1800795	*IL-6*	7:22766645	C	0.43	0.90	0.53	0.72 (0.26-2.0)
rs1836882	*NOX4*	11:89232161	C	0.16	0.53	0.53	1.6 (0.36-7.2)
rs1044498	*ENPP1*	6:132172368	C	0.14	0.21	0.55	0.58 (0.10-3.5)
rs4394754	*INPP5A*	10:134343062	T	0.26	0.05	0.56	0.67 (0.17-2.6)
rs11580170	*AGMAT*	1:15909744	T	0.28	0.40	0.58	0.72 (0.23-2.3)
rs2280789	*CCL5*	17:34207003	C	0.13	0.14	0.59	1.7 (0.26-10.7)
rs4730751	*CAV1*	7:116540796	A	0.26	0.16	0.60	0.70 (0.18-2.6)
rs1799854	*ABCC8*	11:17448704	T	0.4	0.51	0.60	0.75 (0.25-2.2)
rs1016429	*GRIN3A*	9:104402364	C	0.1	0.41	0.64	1.6 (0.24-10.0)
rs2069762	*IL-2*	4:123377980	G	0.25	0.21	0.66	1.3 (0.39-4.4)
rs1494558	*IL-7R*	5:35861068	A	0.35	0.79	0.70	1.2 (0.46-3.2)

rs2172749	*IL-7R*	5:35855264	C	0.35	0.79	0.70	1.2 (0.46-3.2)
rs1043261	*IL-17RB*	3:53899276	T	0.11	0.23	0.71	0.73 (0.14-3.8)
rs2861484	*CELA2B*	1:15812665	T	0.22	0.18	0.72	0.82 (0.28-2.4)
rs10484821	*ATP5F1P6*	6:139868910	C	0.19	0.34	0.74	0.80 (0.21-3.1)
rs2070874	*IL-4*	5:132009710	T	0.17	0.60	0.78	0.82 (0.21-3.3)
rs10117679	*GRIN3A*	9:104378479	T	0.06	0.44	0.81	1.4 (0.1-18.3)
rs1169288	*HNF1A*	12:121416650	G	0.36	0.96	0.82	1.1 (0.35-3.8)
rs13266634	*SLC30A8*	8:118184783	T	0.38	0.53	0.84	0.89 (0.30-2.7)
rs12255372	*TCF7L2*	10:114808902	T	0.28	0.94	0.91	1.1 (0.41-2.7)
rs1871184	*ITGA1*	5:52234323	T	0.13	0.14	0.92	1.1 (0.16-7.4)
rs17722392	*KIDINS220*	2:8940154	C	0.05	0.44	0.93	1.1 (0.09-13.8)

Key:

SNP: single nucleotide polymorphism, MAF: minor allele frequency, p value adj: p value adjusted for age, sex, body mass index at baseline and change after 12 months, CI: confidence interval.

SNPs in red: 8 'glucotoxic' SNPs from (73)

5.1.3 Discussion

This study identifies SNP variants in common genes which are associated with the development of NODAT following kidney transplantation, thereby generating hypotheses to aid our understanding of mechanisms involved (discussed below) and the potential for risk-stratifying patients pre-transplantation.

Some of the features of the study are relevant and worth noting in the context of its findings. Firstly, all patients underwent screening for diabetes prior to transplantation, and so the episodes of diabetes following transplantation were truly “new onset” rather than pre-transplant diabetes which was picked up post-transplantation. Indeed for the live donor recipients in the study, OGTTs were also undertaken to exclude pre-transplant diabetes. For the diagnosis of diabetes following transplantation, OGTTs were undertaken at serial time-points in a carefully phenotyped prospective cohort, and so this study in particular, is sensitive to the development of NODAT. Interestingly, the majority of patients were only diagnosed as a result of the OGTTs conducted specifically and additionally as part of this research study, and would have been missed (or the diagnosis delayed) in routine clinical practice. The original GWAS (73) reported 9.6% NODAT incidence over 12 years follow-up (57 patients with a median time of onset over 8 years), using a clinician-based diagnostic of NODAT, whilst in Birmingham after one year post-transplantation, over 25% (18 patients) developed NODAT in keeping with previous European cohorts. This may reflect two differing ‘types’ of NODAT; Belfast appears to have a prolonged time to NODAT that could represent a ‘wearing’ out of the pancreatic β cell, where the Birmingham cohort represents an ‘inflammatory’ response to hyperglycaemia. This may explain why none of the top 8 SNPs

(Table 5-2, in red) identified in the Belfast GWAS, were significantly associated in this chapter.

Secondly, although the inclusion of only white patients (self-reported) does limit generalisation to other ethnicities, it does nevertheless make the study's findings more robust by limiting (albeit not fully excluding) the confounding effect of population stratification. Finally, the identified SNPs have been previously recognised as risk factors for diabetes and also for NODAT, and the current study therefore replicates these findings. As such, the p values have not been corrected for multiple comparisons. At 5% risk of false positives in the 46 SNPs would result in approximately 2 false positives assuming that the SNPs were independent of each other, yet, in view of the potential inter-relationship (discussed below) of the SNPs, the actual number of false positives is likely to be lower.

The potential detrimental effects of hyperglycaemia on pancreatic human β cells resulting in reduced proliferation and increased apoptosis after 2 days and loss of secretory function after 4 days, have been shown in vitro which is reflected in the time to the potentially 'inflammatory' NODAT onset in this study (227, 228). The five reported SNPs associated with NODAT in this study mirror the above mechanisms, and fall into three main interrelated categories, namely β cell apoptosis with reduction in cell mass, insulin sensitivity/release and mitochondrial dysfunction (Figure 5-1). The mammalian target of rapamycin (mTOR) is a member of the phospho-inositide 3-kinase (PI3K)-related kinase family and has a central role in the regulation of these SNPs.

Figure 5-1 Schematic of how the significant candidate genes may lead to new-onset diabetes after transplantation development, with mTOR being the central regulator to this

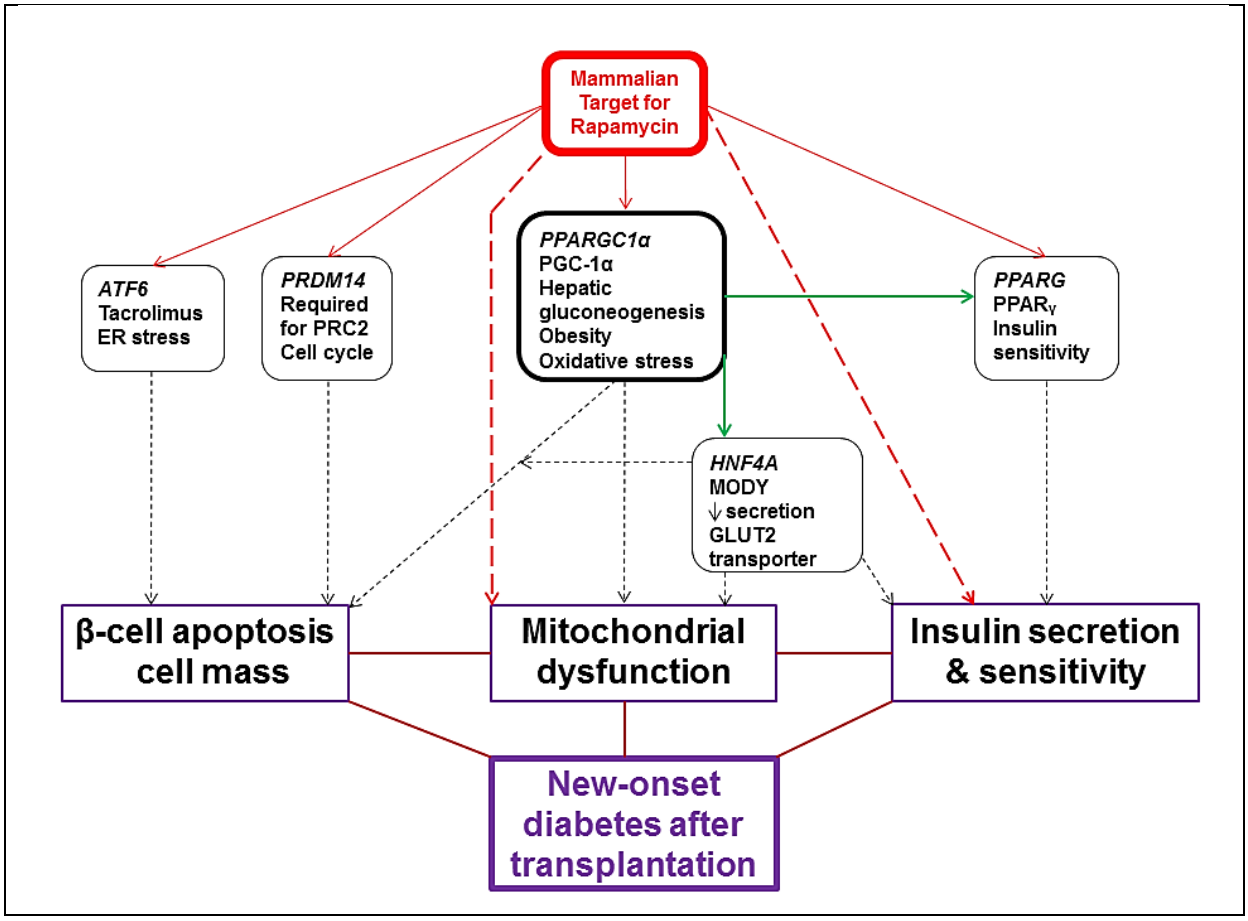

mTOR regulates peroxisome proliferator-activated receptor gamma co-activator 1 alpha (PGC1α - *PPARGC1α* rs8192678) and peroxisome proliferator-activated receptor gamma (PPARy – *PPARG* rs1801282) signalling to promote cell growth, proliferation, metabolism and survival; both these SNPs have been associated with type II diabetes previously (229, 230). mTOR enhances the activity of these transcription factors PPARy and PGC1α by the regulation of lipid synthesis, thus acts as a key sensor for mitochondrial and B cell nutrient status via leucine and its regulation of AMP-activated protein kinase inhibiting secretion of insulin, controlling mitochondrial oxidative metabolism and biogenesis through transcription PGC1α physical interaction with yin-yang 1 (231, 232). mTOR regulates the transcription

regulator, PR domain zinc protein 14 (*PRDM14* rs16936667) which interacts directly with the chromatin regulator polycomb repressive complex 2 to exert its effects via trimethylation of histone H3 lysine27 and enhancer of zeste homolog 2 to regulate β cell proliferation, cell mass and apoptosis (233-235). This SNP was associated with NODAT in the recent GWAS (73).

Activated transcription factor 6 (*ATF6* rs2340721) is present in pancreatic β cells, adipocytes and hepatocytes. It becomes activated during periods of tacrolimus induced endoplasmic reticulum stress in transplantation, to improve cell survival via mTOR in combating the unfolded protein response that leads to apoptosis, lipogenesis and gluconeogenesis (236, 237). Although not previously associated with NODAT, this SNP has been associated with an increased BMI in a renal transplant cohort 15, pre-diabetes in a Chinese cohort (238) and has been found in tight linkage disequilibrium (in Caucasians) with rs2070150 which is associated with type II diabetes in Pima Indians (239). Mutations in the gene hepatocyte nuclear factor 4 (*HNF4* rs2144908) have been associated with NODAT (240) and reduced insulin secretion to glucose stimulation due to progressive β-cell dysfunction, with defects in the GLUT2 transporter and mitochondrial dysfunction in the pathogenesis of maturity onset of diabetes in the young (241-243). mTOR has an indirect effect on HNF4α by its regulation of PPARGC1α which co-activates with HNF4α thus regulating downstream gluconeogenic targets (244, 245).

In vivo studies have shown chronic inhibition of mTOR by rapamycin leads to insulin resistance and lipid dysregulation associated with defective insulin, insulin growth factor signalling and β-cell toxicity (231, 246, 247). However, there remains controversy over the

use of sirolimus and the development of NODAT with some studies suggesting its use is an independent risk factor for NODAT (248) whilst in others, sirolimus has been used to improve the metabolic parameters in a small number of NODAT patients as a substitute for calcineurin inhibitors (249). Recent studies have also highlighted the dyslipidaemia, need for more anti-lipid medication (250) and the requirement for higher steroid dose in a sub-analysis of the SYMPHONY trial with the use of sirolimus (251) and thus questions if conversion to sirolimus will improve the cardiovascular survival outcomes in patients with or at risk of NODAT. A recent meta-analysis of 21 randomised control trials has shown an increased risk of death with sirolimus conversion in kidney transplantation despite a significant decrease in malignancy (252).

For the number of SNPs tested in this study compared to the 18 cases of NODAT and 50 non-NODAT control patients, the power is 60% to identify OR of 2, with 20% minor allele frequency, thus the 5 identified SNPs in this study requires further validation in another cohort as the optimal way of confirming these findings (253). *CAV1* rs4730751 was not associated with NODAT. This may have been due to the higher frequency of the minor allele at over 25% which meant the SNP demonstrated deviation from Hardy-Weinberg equilibrium and thus the interpretation is unreliable.

In summary, this study represents a replication study of candidate SNPs in regard to the risk of developing NODAT following kidney transplantation. It is hypothesis generating into the prevailing mechanisms of this important complication of transplantation, and may even serve to stratify the risk for individual patients. Though previous attempts to use genetic variation in improving the risk for future type 2 diabetes development in addition to clinical

risk factors have only led to a net risk reclassification of 4% in the Framingham Offspring study risk (age, sex, parental history of type 2 diabetes, body mass index, high density lipoprotein cholesterol, triglycerides, fasting glucose) (254) and 5% to the Cambridge risk score (age, sex, drug treatment, family history of type 2 diabetes, body mass index, smoking status) (255). This chapter also highlights the importance of careful biochemical phenotyping with OGTTs to diagnose NODAT in reducing time to diagnosis and missed cases and how this can potentially change the genotype:phenotype associations found.

CHAPTER 6:

RENAL EXPRESSION OF MURINE CAVEOLIN-1

6.1 Renal expression of murine caveolin-1

6.1.1 Non-immune and stromal kidney cell staining

By using confocal microscopy, it is possible to visualise where the expression of caveolin-1 resides in the kidney. From the initial staining of wild-type frozen kidney tissue, Cav1 appears to be expressed in the in the glomerulus, lining of tubules as well as the vasculature (Figure 6-1).

Figure 6-1 Confocal microscopy showing caveolin-1 staining (green) in a x40 image of a wild-type mouse kidney frozen section. Nuclei appear as grey with DAPI staining

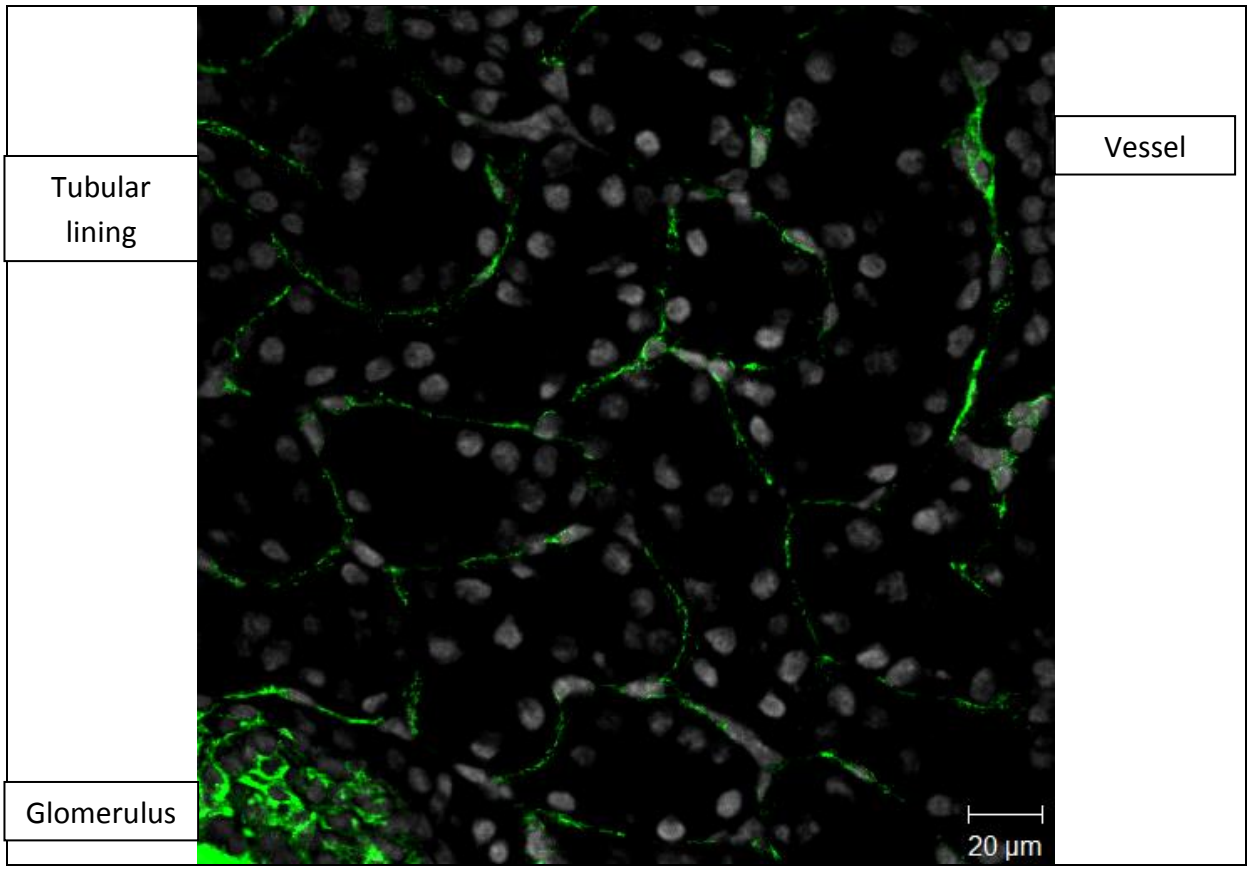

By staining with another antibody, it is possible to visualise how Cav1 expression resides near endothelial cells (CD31), vasculature (αSMA), tubular epithelial cells (E-cadherin) and podocytes (synaptopodin). For all confocal images, Cav1 staining is coloured green, other antibody staining red, nuclei staining grey and merged co-localisation yellow.

As shown in Figure 6-2, caveolin-1 co-localises with CD31, especially in the glomerular endothelial cell and capillary loops. Cav1 is also aligned with the renal vasculature smooth muscle cells as represented by αSMA staining (Figure 6-3). αSMA is also a marker of myofibroblasts that were not present in the non-injured kidney.

Figure 6-2 CD31 (red) and caveolin-1 (green) confocal images. Caveolin-1 co-localisation with CD31 especially in glomerular capillary loops and endothelium

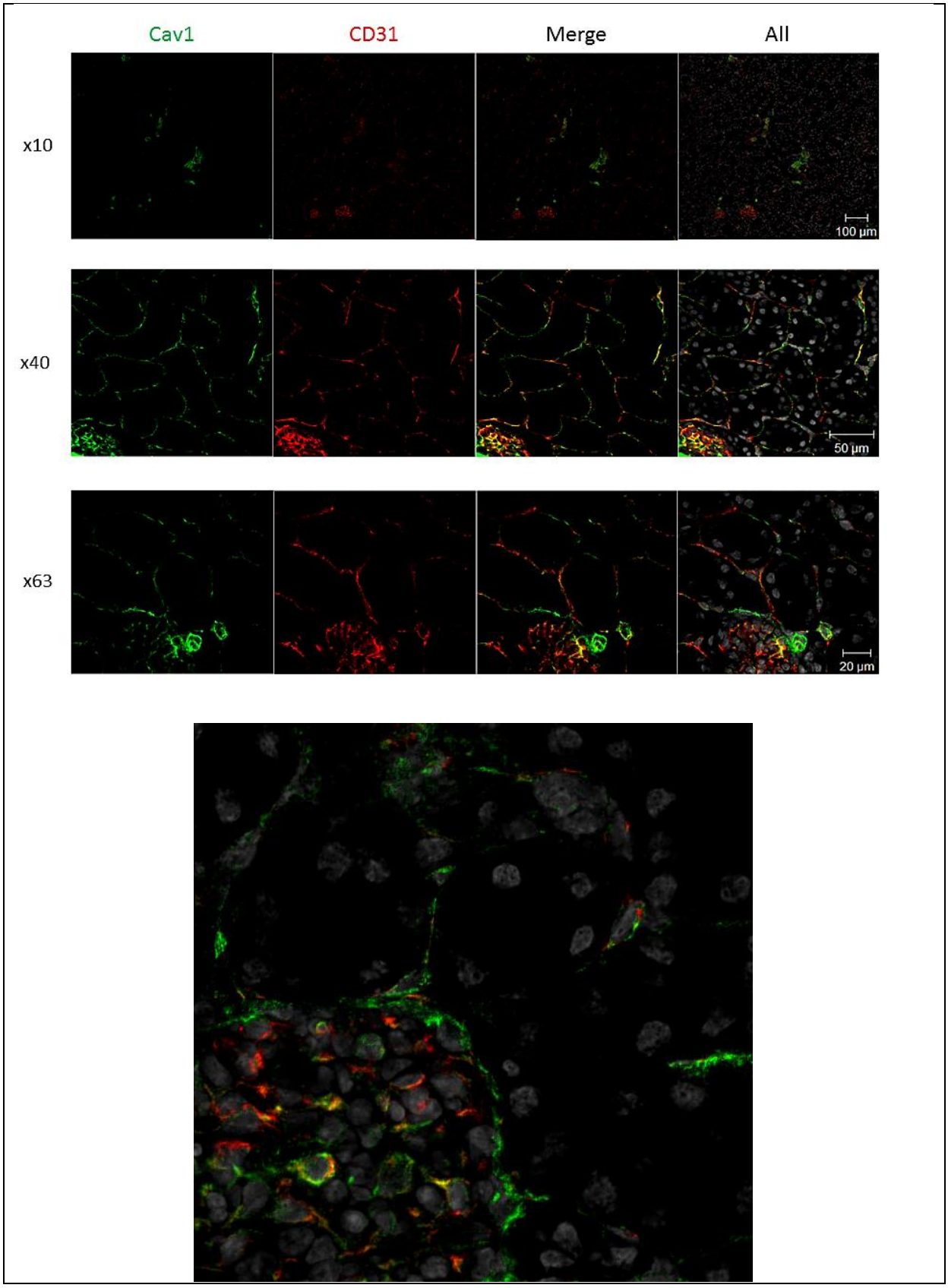

Figure 6-3 αSMA (red) and caveolin-1 (green) confocal images highlighting the renal vasculature

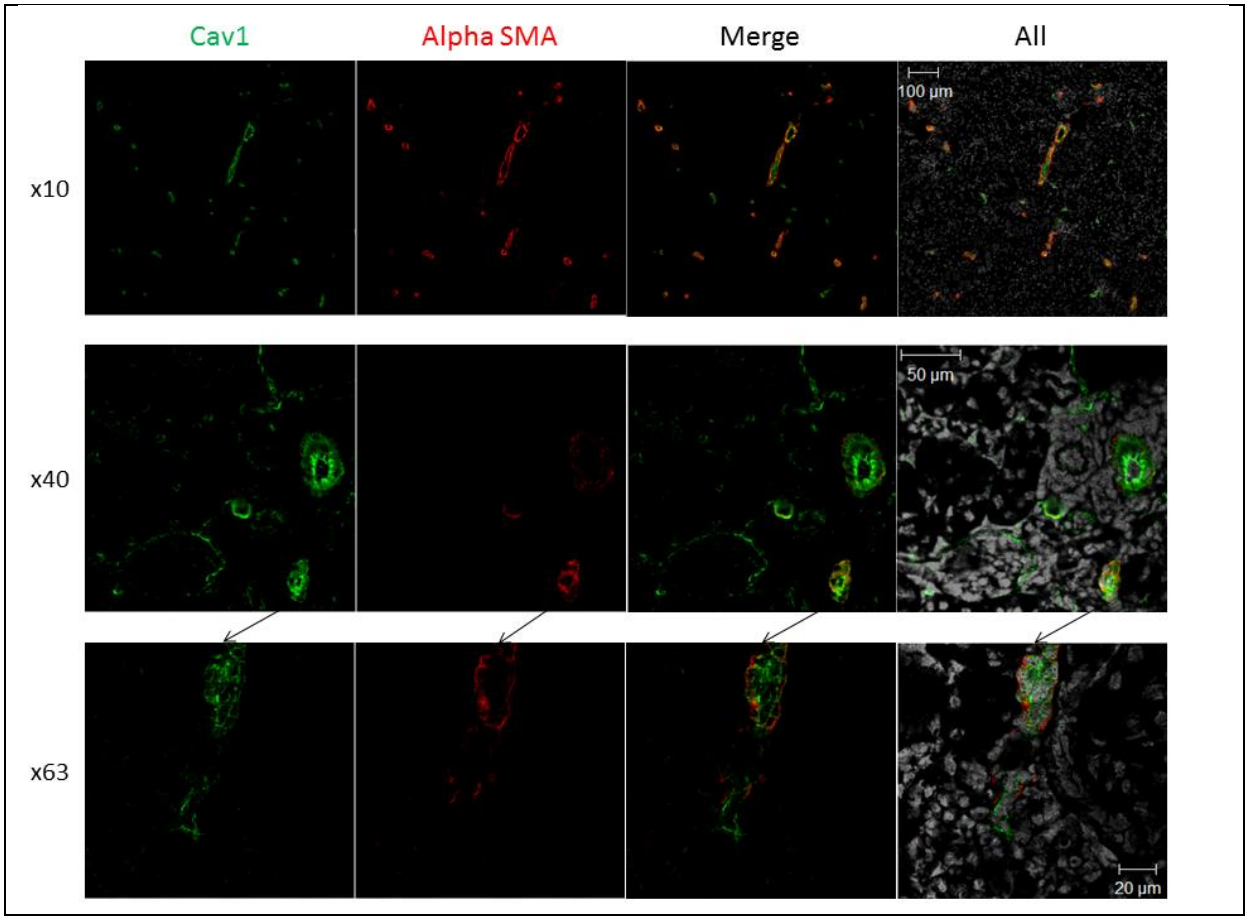

In Figure 6-4, Cav1 staining reveals a basolateral tubular distribution and does not co-localise with tubular epithelial cell marker E-cadherin in the mouse kidney that has not been injured. E-cadherin stains more abundantly in distal tubules, collecting ducts and medullary segments, but less so in proximal tubules (256, 257). It is an important molecule in tubular epithelial health by maintaining cell polarity (258).

Figure 6-4 E-cadherin (red) and caveolin-1 (green) confocal images

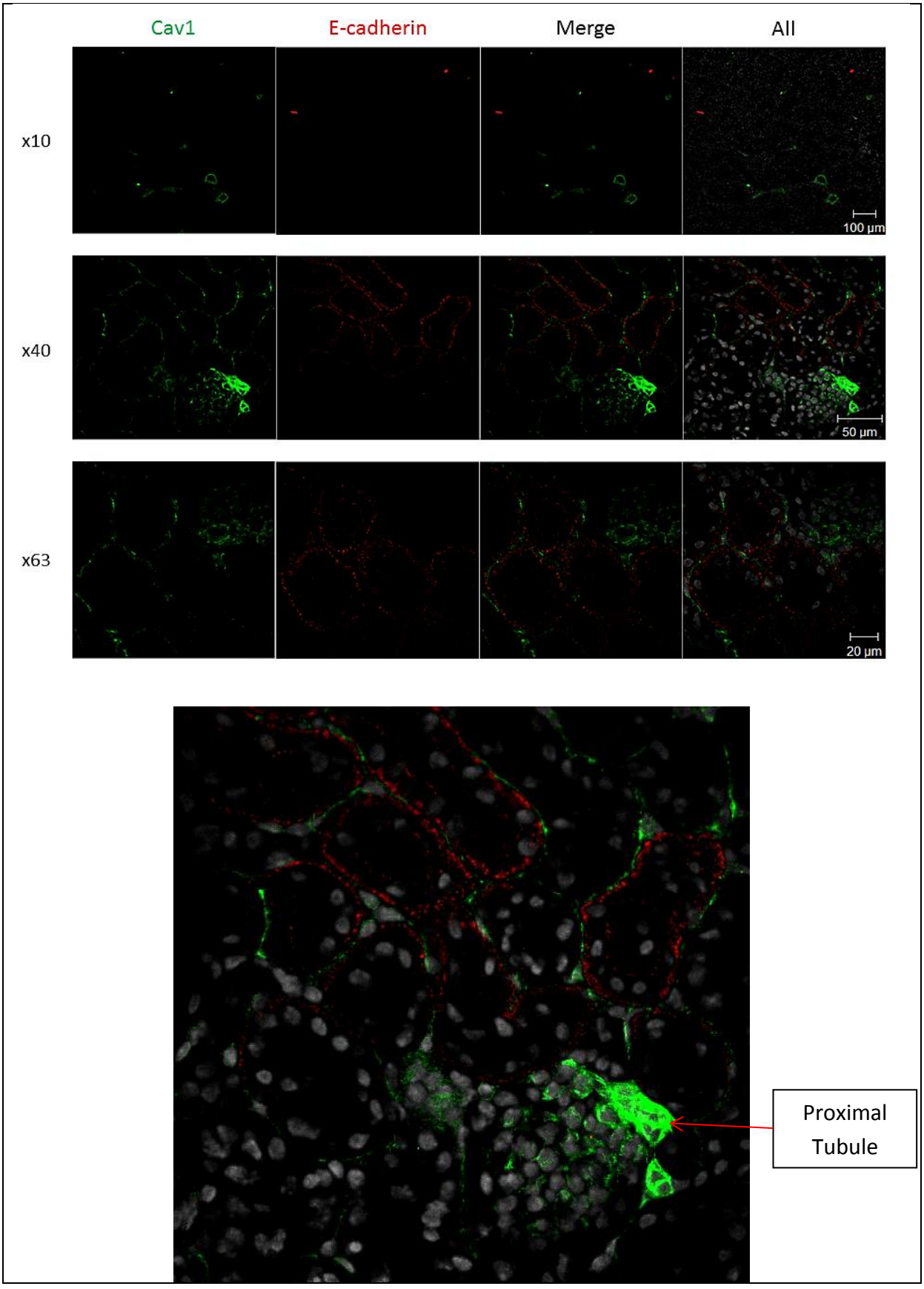

Podocytes reside within the glomerulus and are a common epithelial cell that becomes damaged in proteinuric diseases. The actin-based foot process of podocytes and interposed slit diaphragm are integral in preventing proteinuria. Synaptopodin is an actin-associated protein that is essential for the integrity of the podocyte cytoskeleton. In Figure 6-5, Cav1 is not associated with synaptopodin staining.

Figure 6-5 Synaptopodin (red) and caveolin-1 (green) confocal images

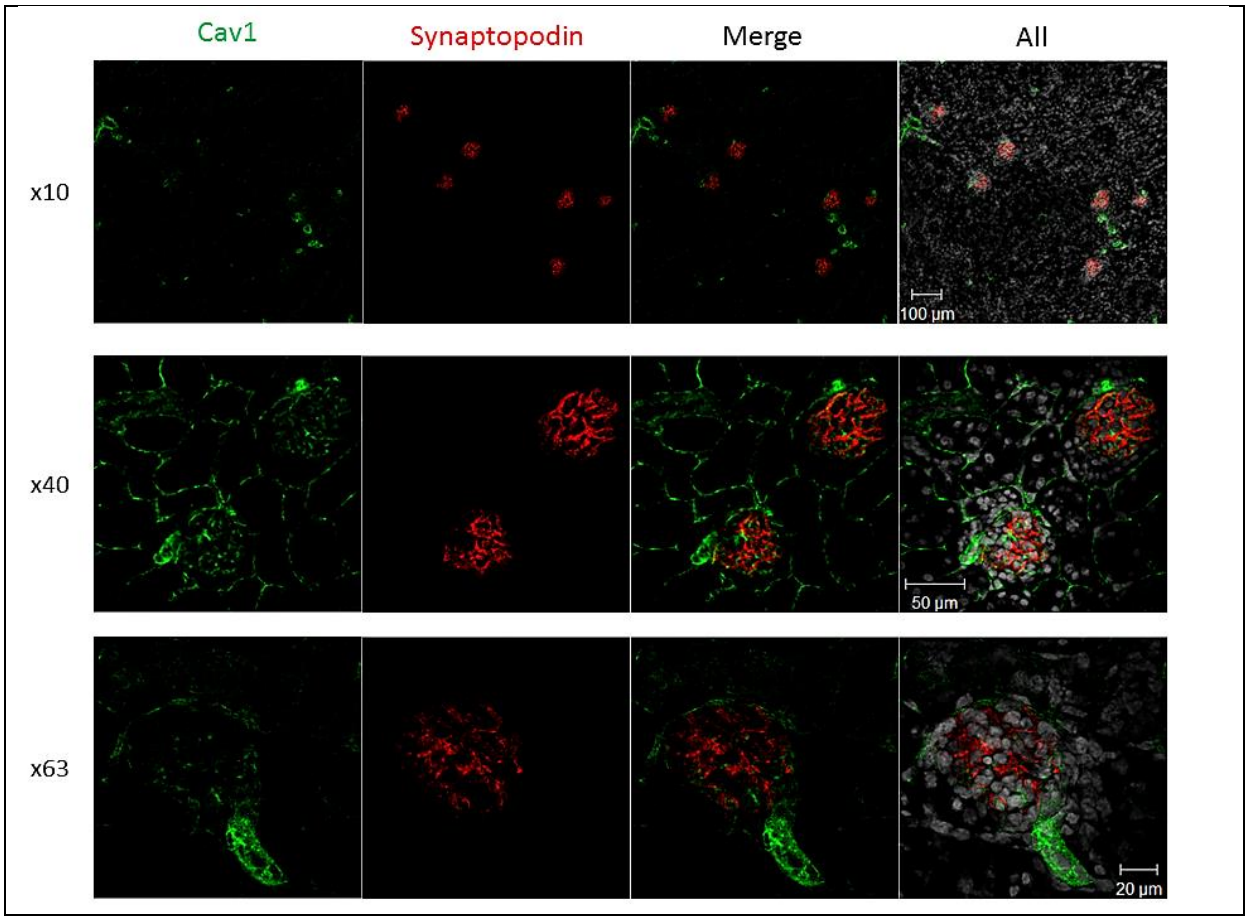

Wild-type mouse embryonic fibroblasts were isolated from day 13.5 embryos prior to the thesis by myself and stored in liquid nitrogen containers. These were thawed, and 2000 cells per well were cultured on a 6 well plate slide prior to being fixed in acetone and stained for caveolin-1 to confirm presence on this mouse strain fibroblasts (Figure 6-6).

Figure 6-6 Mouse embryonic fibroblasts stained with caveolin-1 (green) and DAPI for nuclei staining (grey)

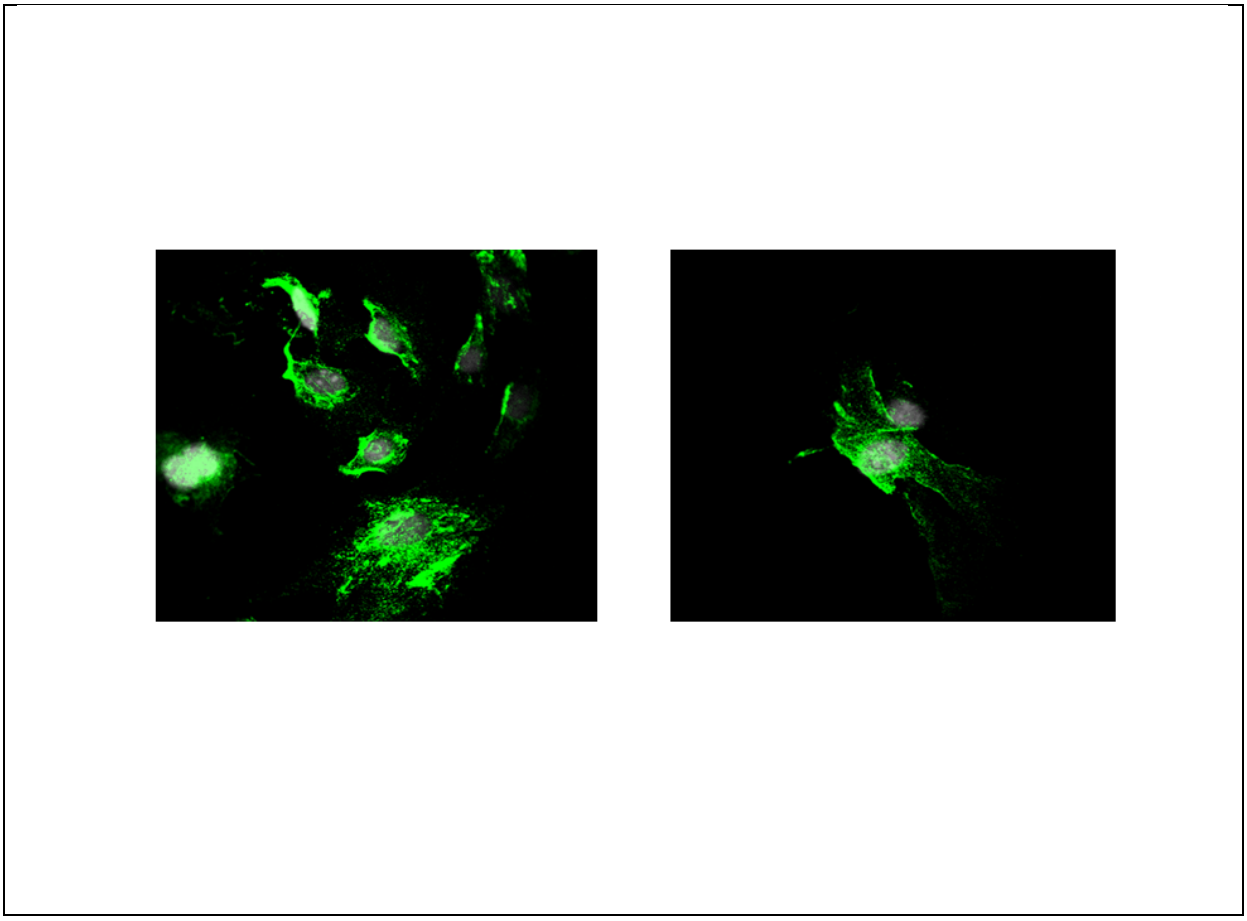

6.1.2 Immune cell and caveolin-1 staining

Three antibodies were chosen to screen for immune cells in the kidney: CD45 (leucocytes), CD3e (T cells) and F4/80 (macrophages). However, it should be noted that CD3e may also stain for other T cells such as the Treg and Th17 cells as well as natural killer cells. CD3e stains for the 20kDa protein in the T cell receptor complex. F4/80 may also stain renal dendritic cells but these tend to express lower levels of F4/80 than renal macrophages (259).

In Figure 6-7, CD45 staining revealed a small number of leucocytes are present in the non-injured wild-type kidney with only one cell with co-localisation (yellow) with Cav1.

Figure 6-7 CD45 (red) and caveolin-1 (green) confocal images

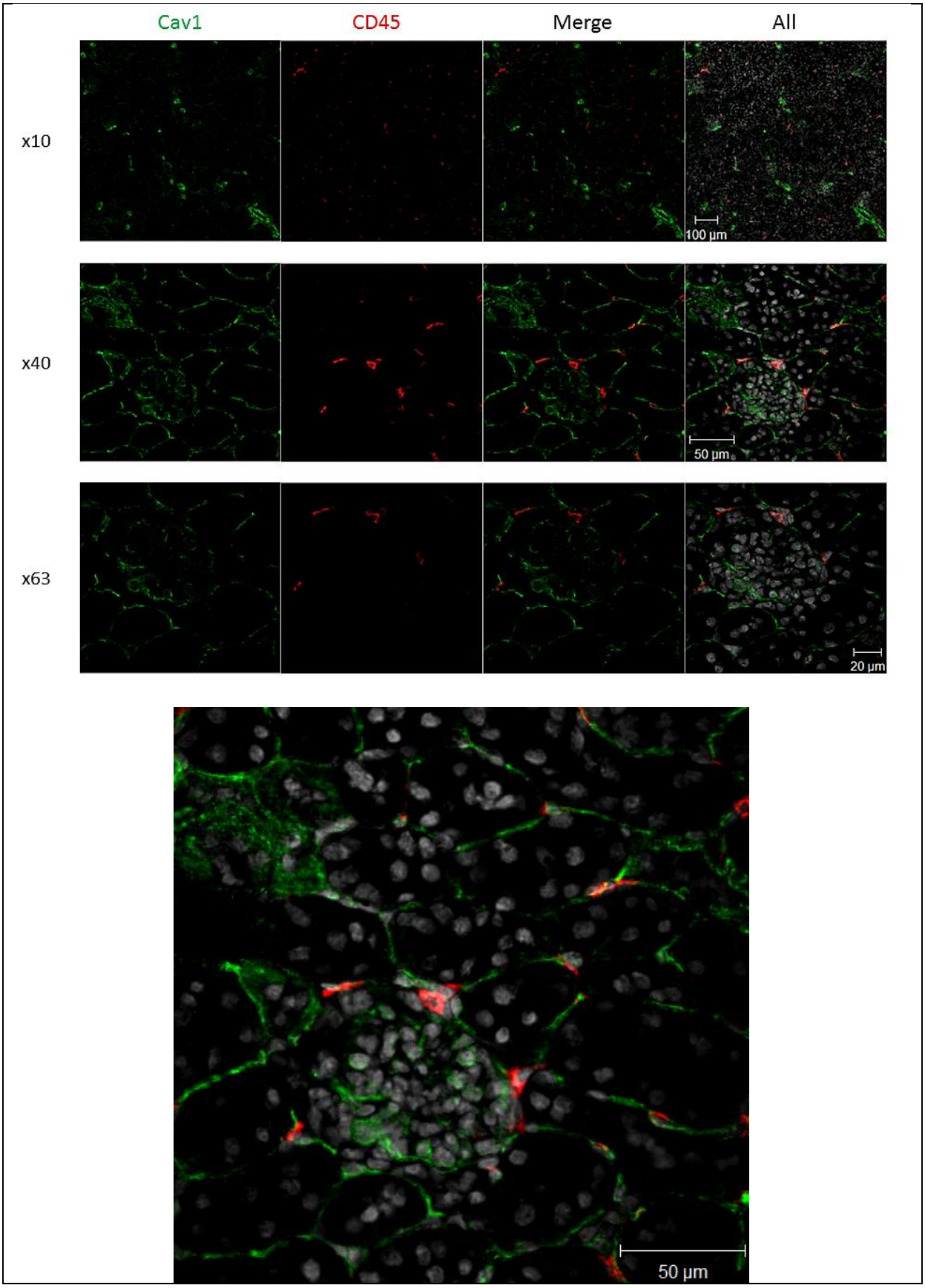

Figure 6-8 shows only isolated CD3e positive cells in the kidney with Cav1 surrounding the same nuclei.

Figure 6-8 CD3e (red) and caveolin-1 (green) confocal images

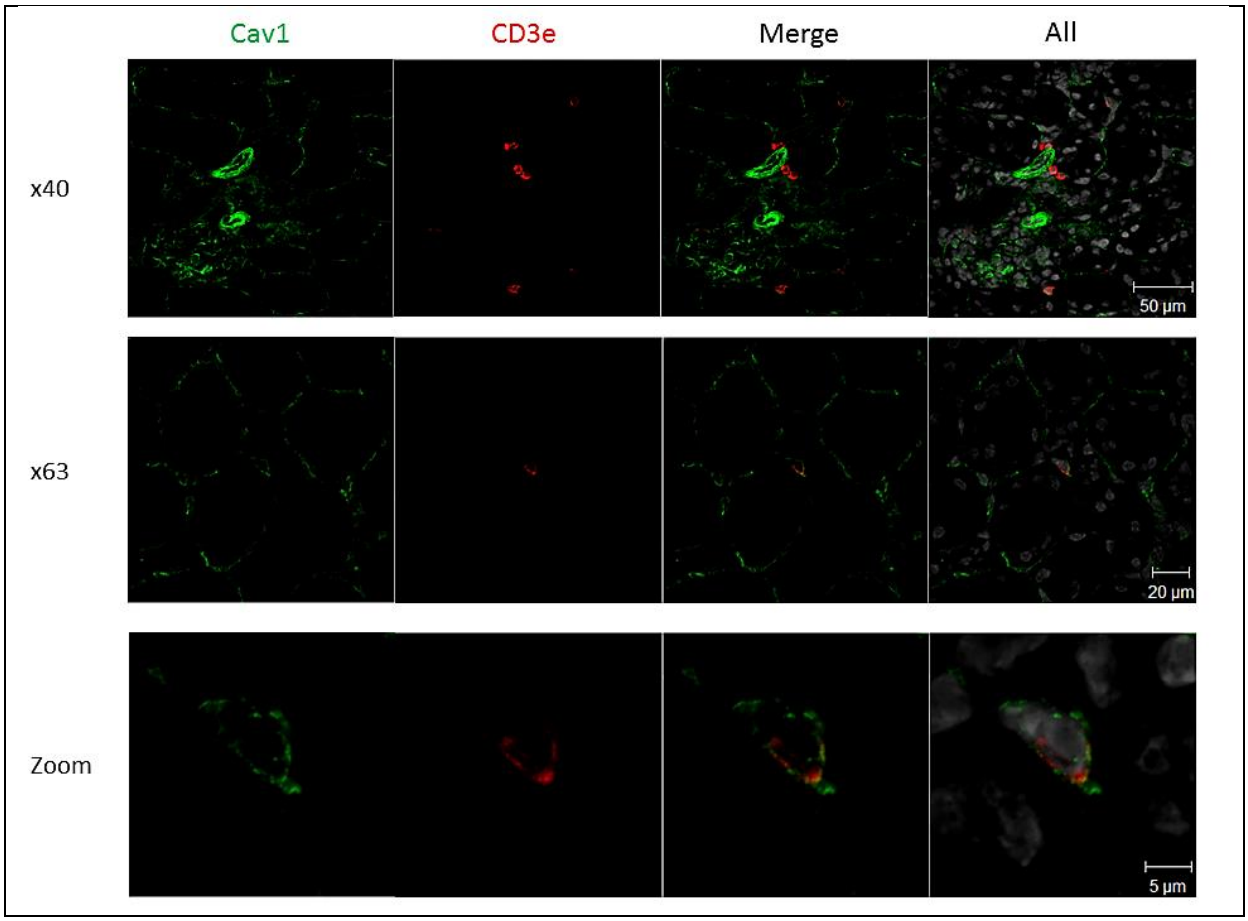

There are majority of leucocytes in the non-injured wild-type kidney were stained positively with F4/80 (Figure 6-9).

Figure 6-9 F4/80 (red) and caveolin-1 (green) confocal images

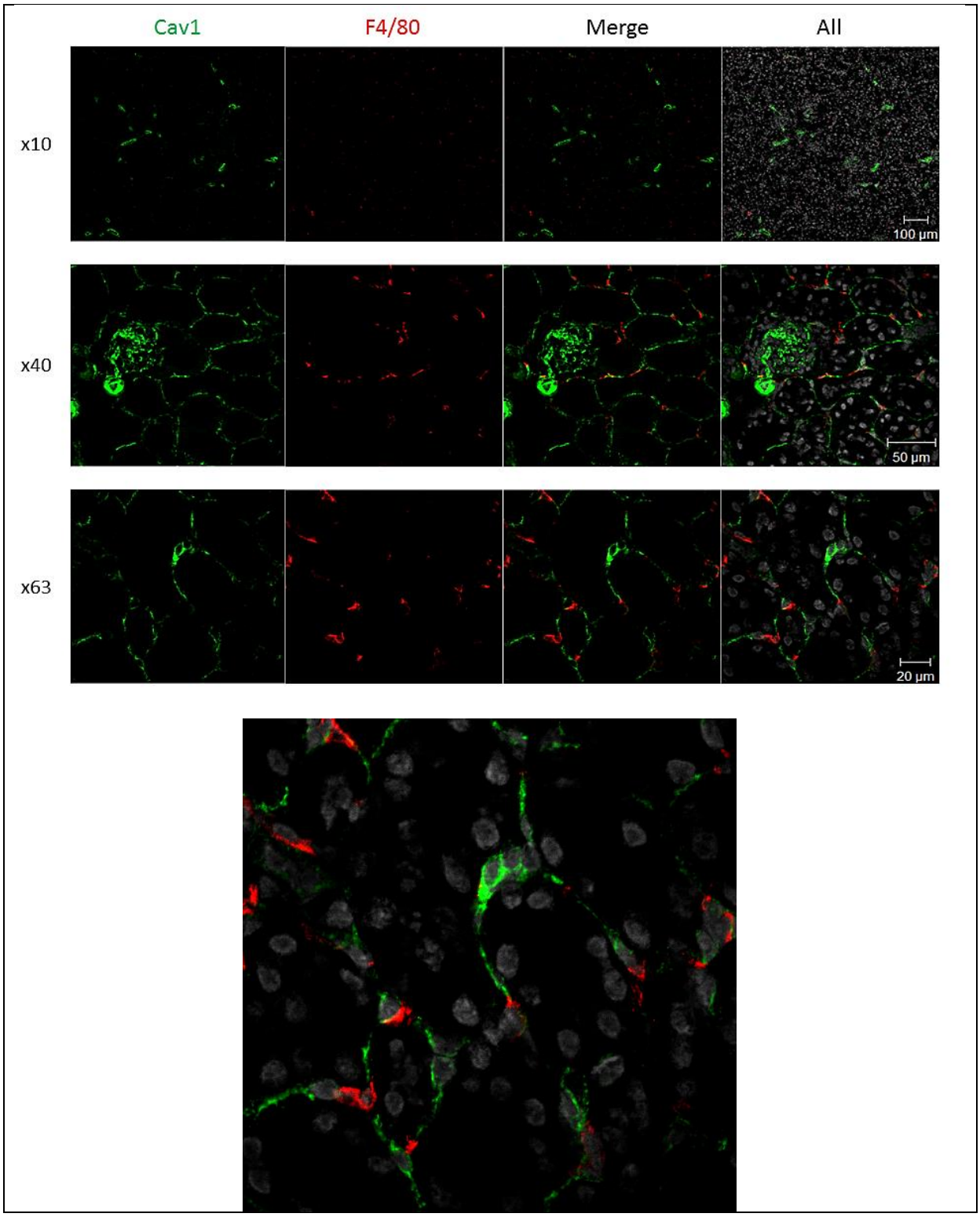

6.2 Small animal models of renal fibrosis in the caveolin-1 knockout mouse

In order to investigate the effects of caveolin-1 in renal fibrosis, two models of renal fibrosis were used in the wild-type and caveolin-1 knockout (CKO) mouse. The aim of these were to see what happens to caveolin-1 expression in renal fibrosis and if caveolin-1 knockout led to more renal fibrosis.

6.2.1 Ciclosporin model of renal fibrosis

As this model had not been trialled in Birmingham before, pilot studies were carried out using wild-type mice. For the first pilot, C57BL/6 mice were used as this was the major strain of the CKO mouse. Unfortunately, on the fourth day of the subcutaneous injections (and despite the mice from the vehicle group looking well) the CsA treated group displayed unhealthy toxic fur and facial features so the mice were culled. They were then investigated to see what had happened. It is likely the combination of CsA with Cremophor EL and ethanol induced an acutely toxic hepatic and acute kidney injury which was reflected in their weight ($p=0.01$ with reduction in weight in the CsA treated mice, Mann-Whitney U) and blood results with deteriorating kidney and liver function tests (Figure 6-10).

Hepatic histology also revealed similar changes with H&E staining showing acute liver injury with vacuolation and loss of architecture. Renal histology showed features consistent with acute kidney injury with marked vacuolation of tubules Figure 6-11.

Figure 6-10 First ciclosporin model pilot results (n=4). Control group received vehicle and treatment group received ciclosporin in the vehicle

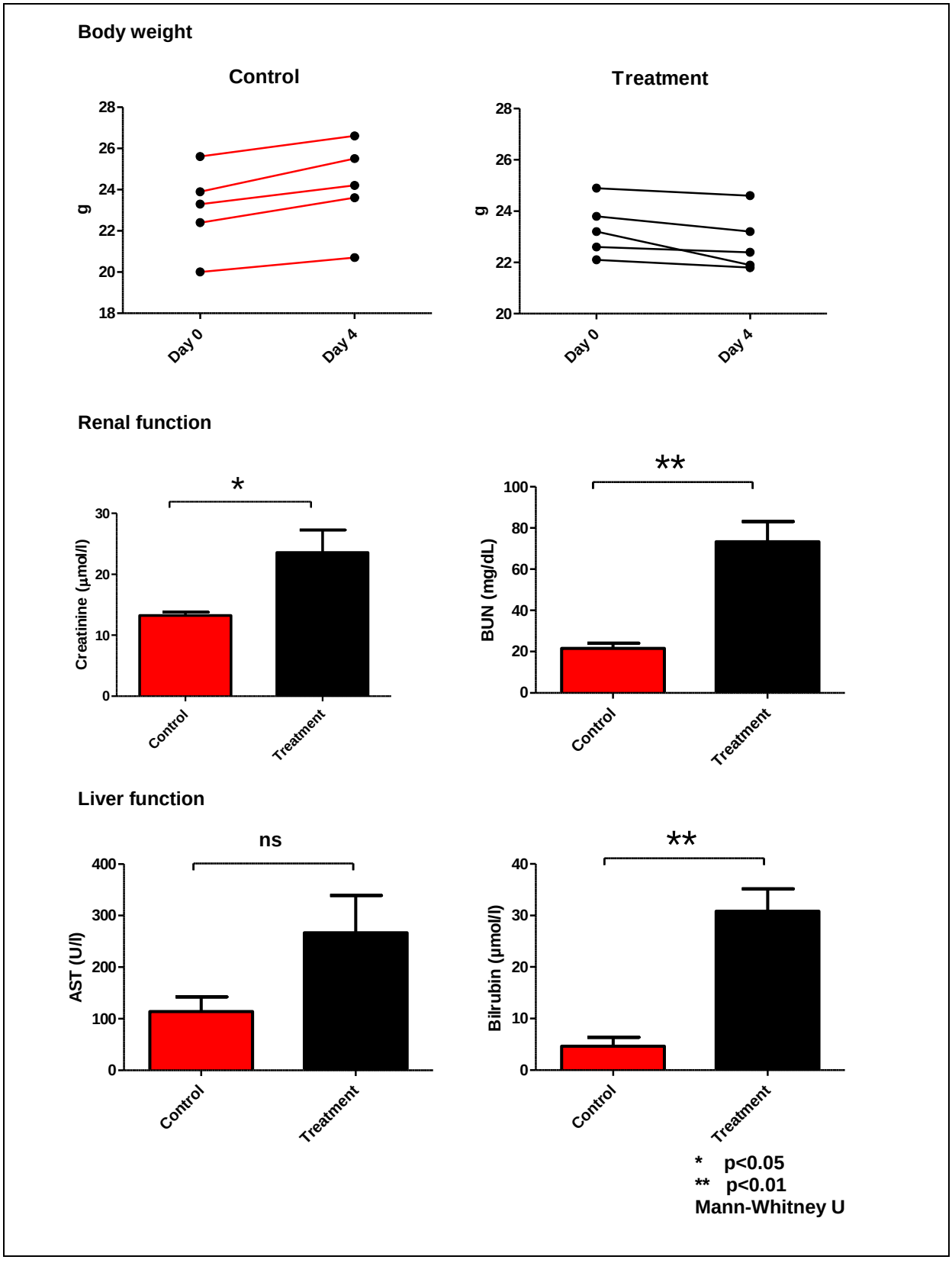

Figure 6-11 Representative H&E sections of liver and kidney tissue from the initial ciclosporin pilot

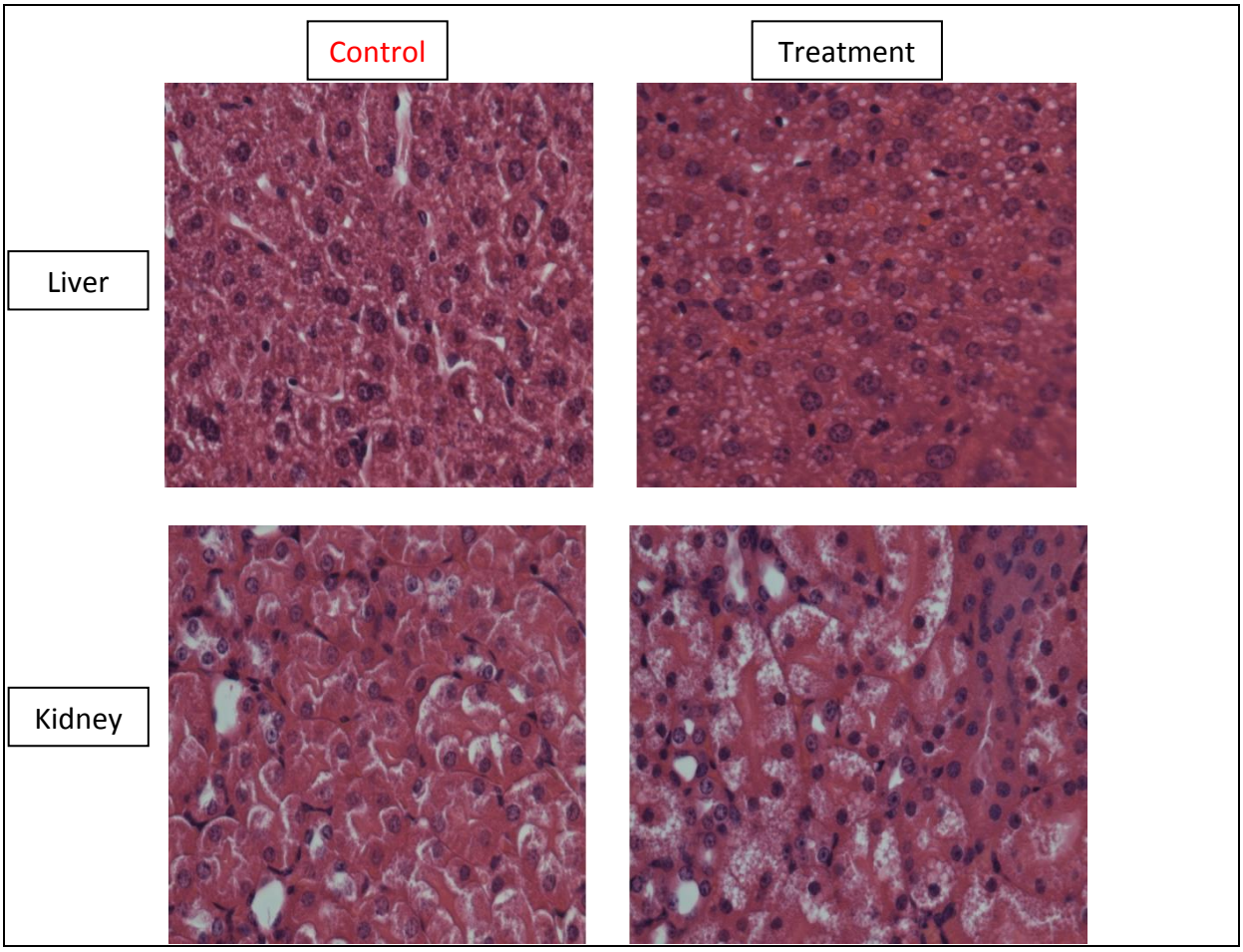

The vehicle was changed to olive oil instead of Cremophor that allowed a marked reduction of 94% ethanol to be used to dissolve the ciclosporin (50mg ciclosporin in 0.35mls 94% ethanol and 4.65mls of olive oil = [10mg/ml]). This emulsion could now be drawn up into a 1ml syringe easily. An initial 14 day toxicity trial (with preceding 7 day low salt diet) was conducted with one mouse in each 10mg/Kg, 15mg/Kg, 20mg/Kg and 30mg/Kg group and two mice receiving 3mls/Kg vehicle (to estimate similar volumes of the CsA receiving group). As there was no overt toxicity displayed, the 30mg/Kg and vehicle only mice continued to receive subcutaneous injections until day 28, with the addition of two 30mg/Kg CsA

receiving mice, and a further vehicle only receiving mouse. All mice successfully reached the end of the pilot.

Upon blood sampling, there was no significant difference in renal and liver function between the 30mg/Kg receiving CsA and the control vehicle receiving mice (n=3, Table 6-1). There was no increased fibrosis staining seen on renal histology.

Table 6-1 Blood sampling results from the second ciclosporin model pilot; treatment (Rx) group and vehicle (Control) group

Mouse	BUN (mg/dl)	Creatinine (µmol/l)	Total Billirubin (µmol/l)	Dosage of CsA (mg/Kg)
Rx1	17.60	14.4	4.6	10.0
Rx2	16.31	15.6	4.1	15.0
Rx3	28.05	13.2	3.7	20.0
Rx4	22.77	17.2	4.3	30.0
Rx5	38.57	20.0	3	30.0
Rx6	76.07	72.0	4	30.0
Control 1	21.40	11.4	2.5	0.0
Control 2	17.46	16.7	2.4	0.0
Control 3	21.43	15	2.0	0.0

A third pilot study was designed to use CD-1 mice instead of the C57BL/6 strain, as per Andoh et al in 1997 (189). Five CD-1 mice received the vehicle, whilst five mice received 30mg/Kg/day of subcutaneous CsA treatment. There were no significant differences between renal function and weight changes of the groups. The ciclosporin levels were undetectable in the control group (reported as <20µg/l) and average of 450 µg/l (standard deviation: 101µg/l) in the treatment group (Figure 6-12).

Figure 6-12 Results from the third ciclosporin pilot model of renal fibrosis (n=5)

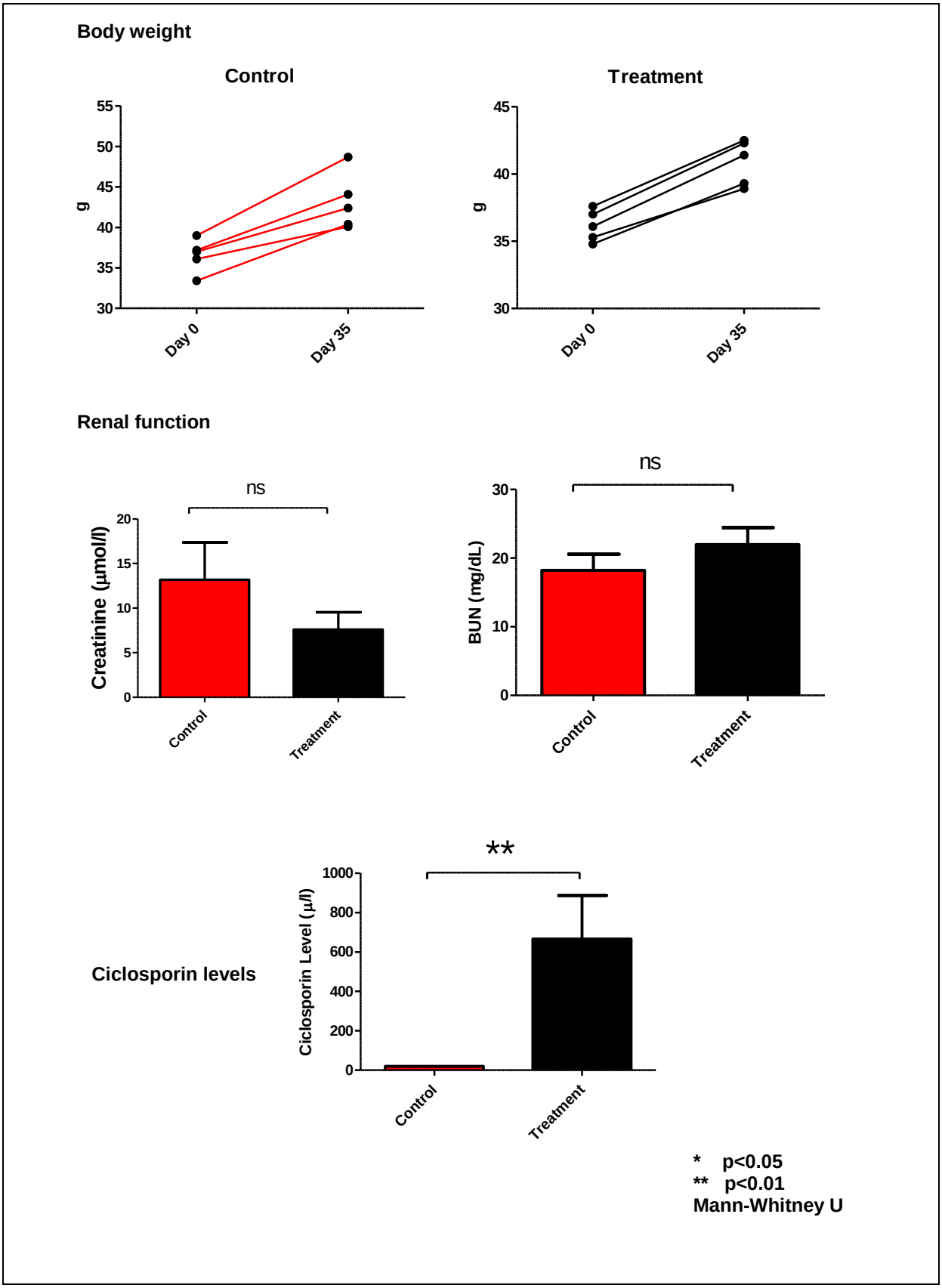

Upon blinded histopathologist review, the expected patchy fibrosis was quite minor for this model compared to control (Figure 6-13).

Figure 6-13 Representative Masson Trichrome stain for control and post CsA treatment mice. Note the subtle patchy blue fibrosis highlighted by the blue rectangle

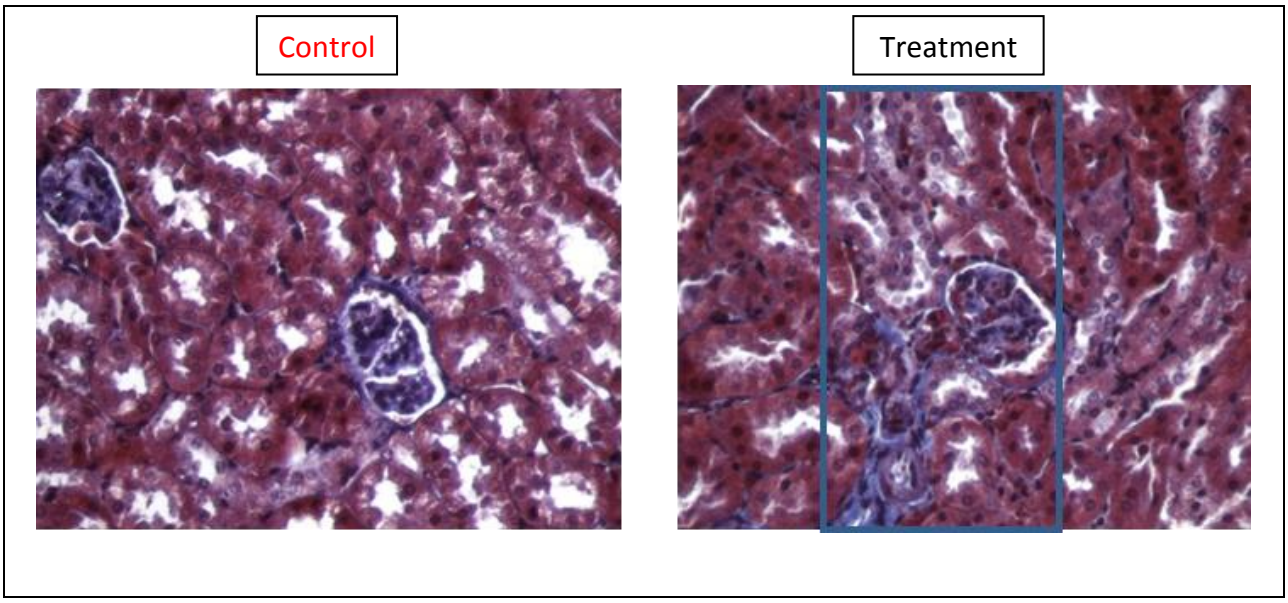

There was no significant difference seen on RT-qPCR mRNA fold induction (Figure 6-14) for Cav1, TGFβ-1, collagen 1α1 and collagen 3α1 between vehicle receiving mice (control) and CsA receiving mice (treatment).

Figure 6-14 RT-qPCR mRNA fold induction in control and treatment groups in the third ciclosporin model pilot of renal fibrosis (n=5)

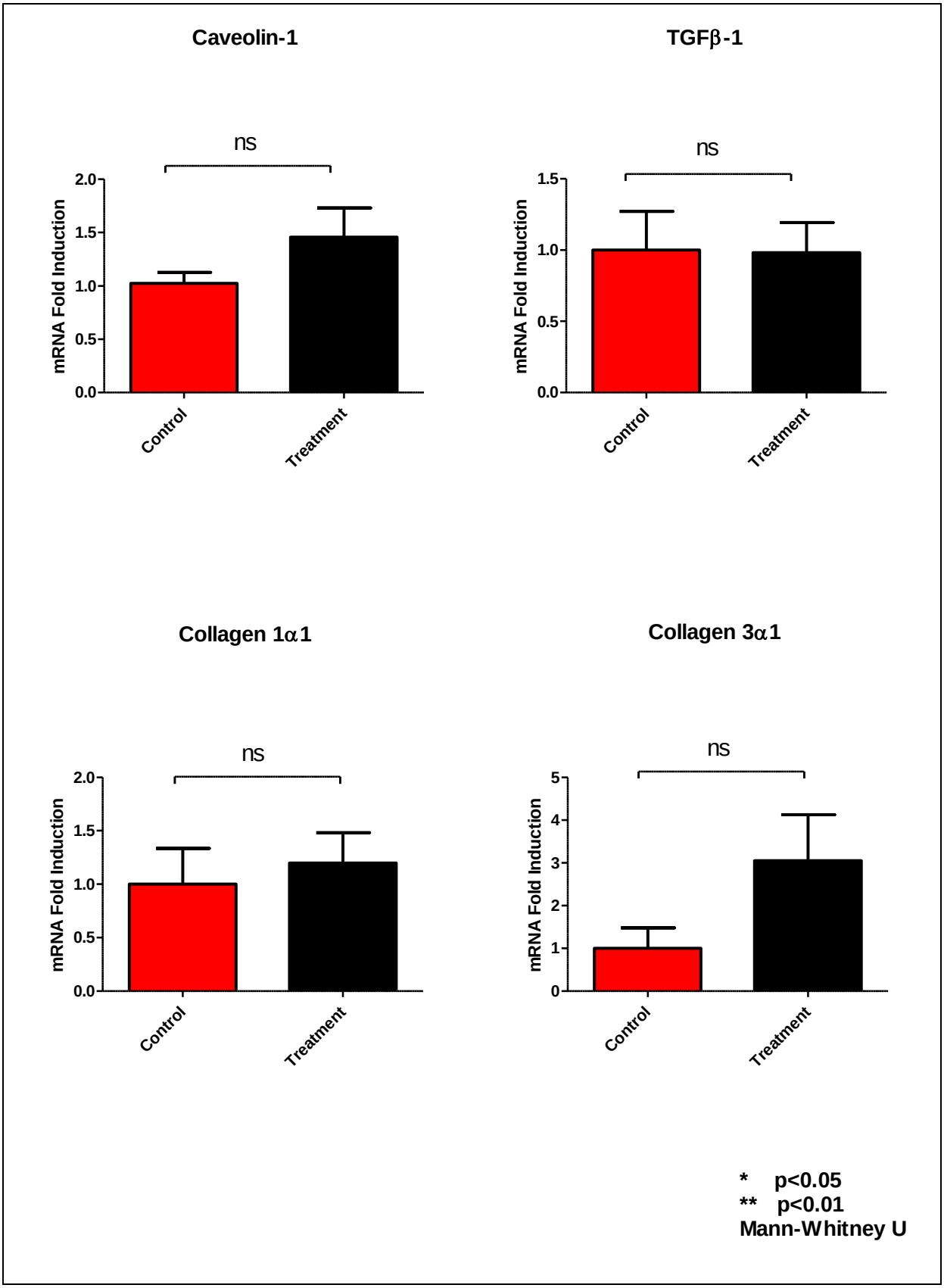

In light of these findings and in conjunction with the BMSU, it was decided not pursue this model. There have been a number of issues with the CsA model despite the success of the non-toxicity pilot. The strain switch from C57BL/6 to CD-1 was made as no overt fibrosis was seen and previous studies have shown a tubular necrotic rather than an interstitial fibrotic picture using this strain (260). However the third pilot using CD-1 mice was thought to be too much of a subtle fibrotic model and would require a large number of animals to continue the experiments themselves and the number/generations required to backcross the CKO mouse onto the pure CD-1 background, which as an outbred strain has inherent problems as well. Thus, this model was abandoned.

As a result, an additional time-point was added to the UUO model at day 3 so the early inflammatory/fibrotic stage effects of Cav1 in the wild-type and the KO could be examined. The confocal/histology frozen snapped tissue had evidence of freeze burn in the CsA models so tissue storage was changed so kidneys were fixed in PFA 4% immediately for 2 hours at room temperature and then placed in 18% sucrose overnight at 4°C. The tissue quarters were then embedded in OCT that is frozen using liquid nitrogen vapour.

6.2.2 Unilateral ureteric obstruction model of renal fibrosis

6.2.2.1 Introduction

Unilateral ureteric obstruction (UUO) causes a cascade of events that leads to marked interstitial fibrosis between day 7-14 after obstruction (261). The overall renal function is not affected due to the non-obstructed (contra-lateral) kidney undergoing hypertrophy to compensate for loss of renal filtration. Thus it is essential that separate sham operated mice

are used as control rather than using the contra-lateral kidney as control due to variations in compensation (262). The UUO animal model has been used to investigate renal fibrosis for over 50 years initially in rabbits (263), but lately in rats and mice due to their susceptibility to gene alterations allowing investigation of the respective gene deletion upon interstitial fibrosis. The development of interstitial fibrosis is the resultant effect from angiotensin type 1 receptor stimulation and TGFβ-1 induction, due to reduction of renal blood flow with the first 24 hours of UUO. After several days, hydronephrosis occurs on the side of the UUO with interstitial inflammatory macrophages influx and tubular cell death from apoptosis and necrosis (262). Myofibroblasts are abundant from epithelial and endothelial mesenchymal transition (EMT and endo-MT respectively) and vascular rarefaction from destabilisation after pericyte transformation to myofibroblasts (264). This leads to collagen 1 and III interstitial deposition as well as collagen IV mainly in the tubular basement membrane.

Initially a pilot model was performed to see if the model could be reproducible in my hands using C57BL/6 mice as wild-type controls and then in the CKO mouse. Vascular clips were used to obstruct the ureter initially but I noted that occasionally the clips could injure the ureter and if not closed sufficiently, urine would be allowed to pass through. To counter this, two sutures were placed around the ureter to cause obstruction and not allow urine to pass through. From the initial pilot, it was observed that the CKO group had a marked destruction of the renal architecture at day 14 of the UUO model as compared to its wild-type counterpart upon histological staining Figure 6-15. There was a non-significant reduction in the kidney:body weight Figure 6-16.

Figure 6-15 Haemtoxylin and eosin staining of day 14 UUO left kidneys in the wild-type and caveolin-1 knockout mouse. There is marked destruction of the renal architecture with volume loss and tubular atrophy.

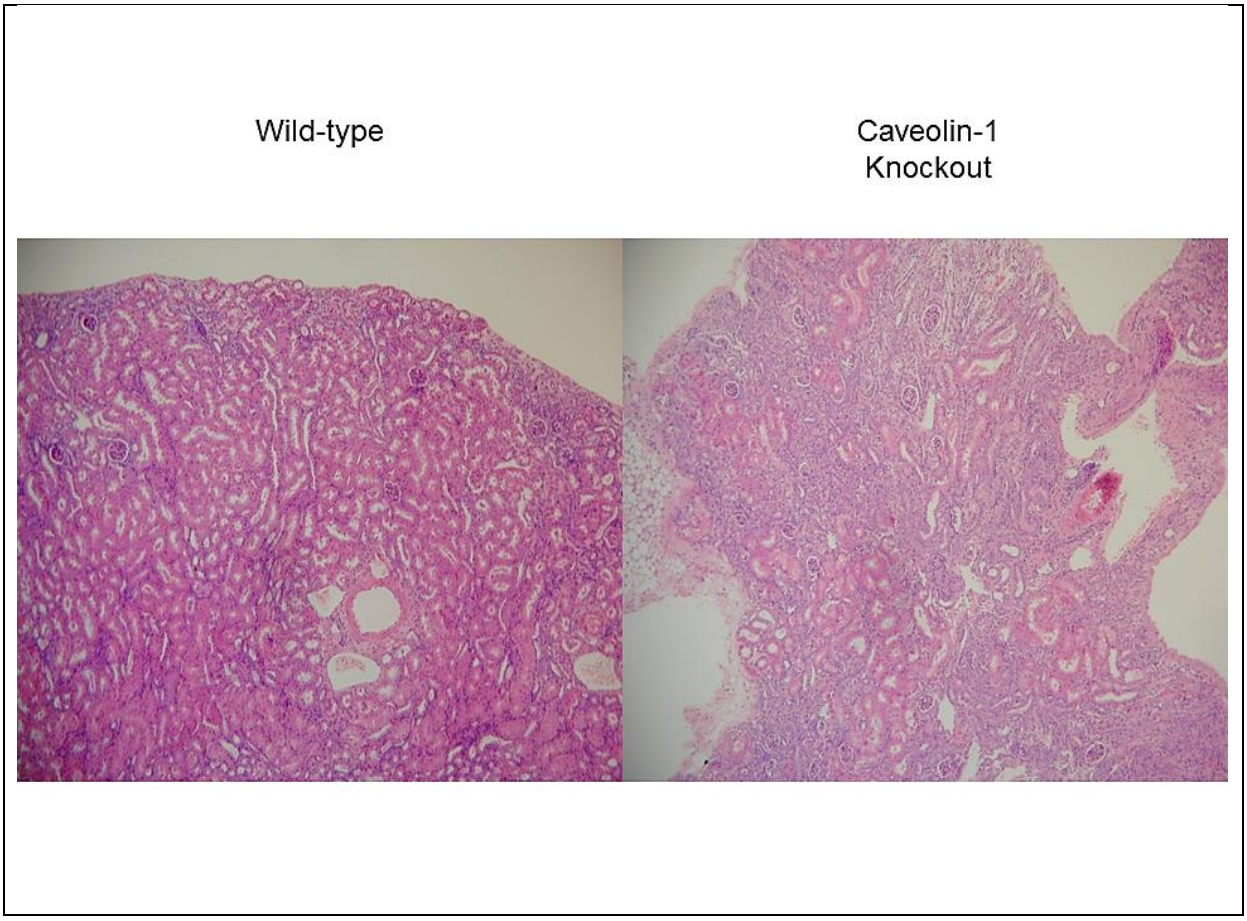

Figure 6-16 The kidney to body weight ratio of the left kidney was non-significantly reduced in knockout mouse (n=3, Mann-Whitney U)

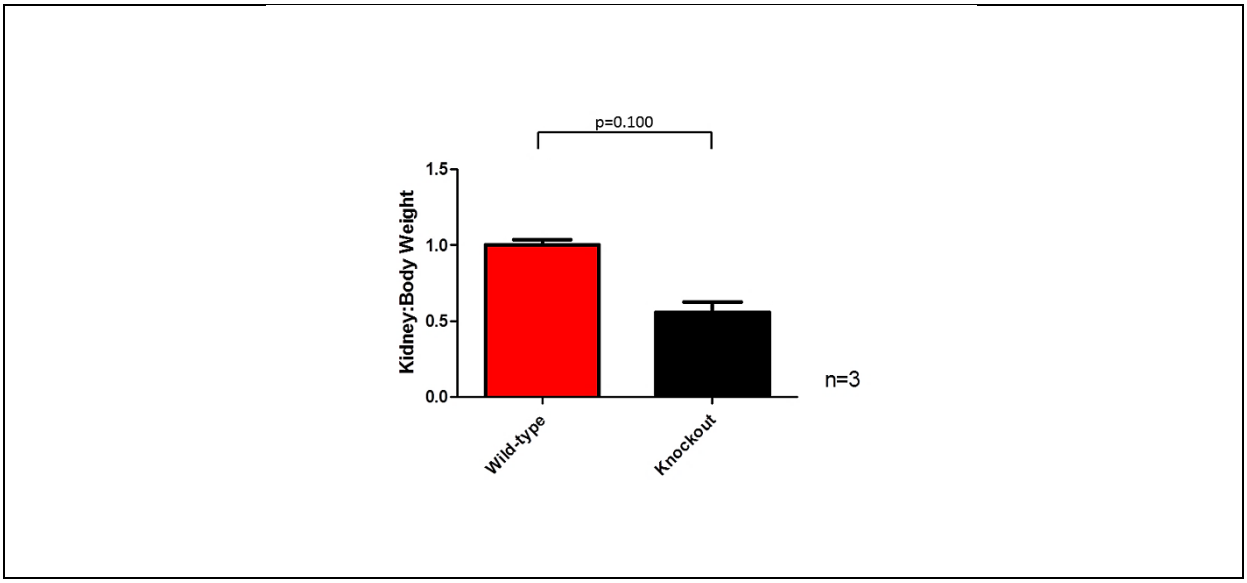

6.2.2.2 Caveolin-1 expression in the UUO model of renal fibrosis

Caveolin-1 expression is increased in the left obstructed kidney as compared to sham operated wild-type mice. RT-qPCR mRNA fold induction was increased significantly to sham in the day 14 model (p=0.022) and increased in the day 3 model, but this did not attain statistical significance (p=0.055). After calculating mRNA the fold induction using the sham operating mouse as control (see methods 2.1.2.6), there was a relative 6.9 (±2.5) fold increase in Cav1 mRNA in the day 14 as compared to the day 3 left obstructed kidney (p=0.033, Figure 6-17).

Figure 6-17 Relative fold induction ratio caveolin-1 increase in day 14 compared to day 3 model of the left obstructed kidney

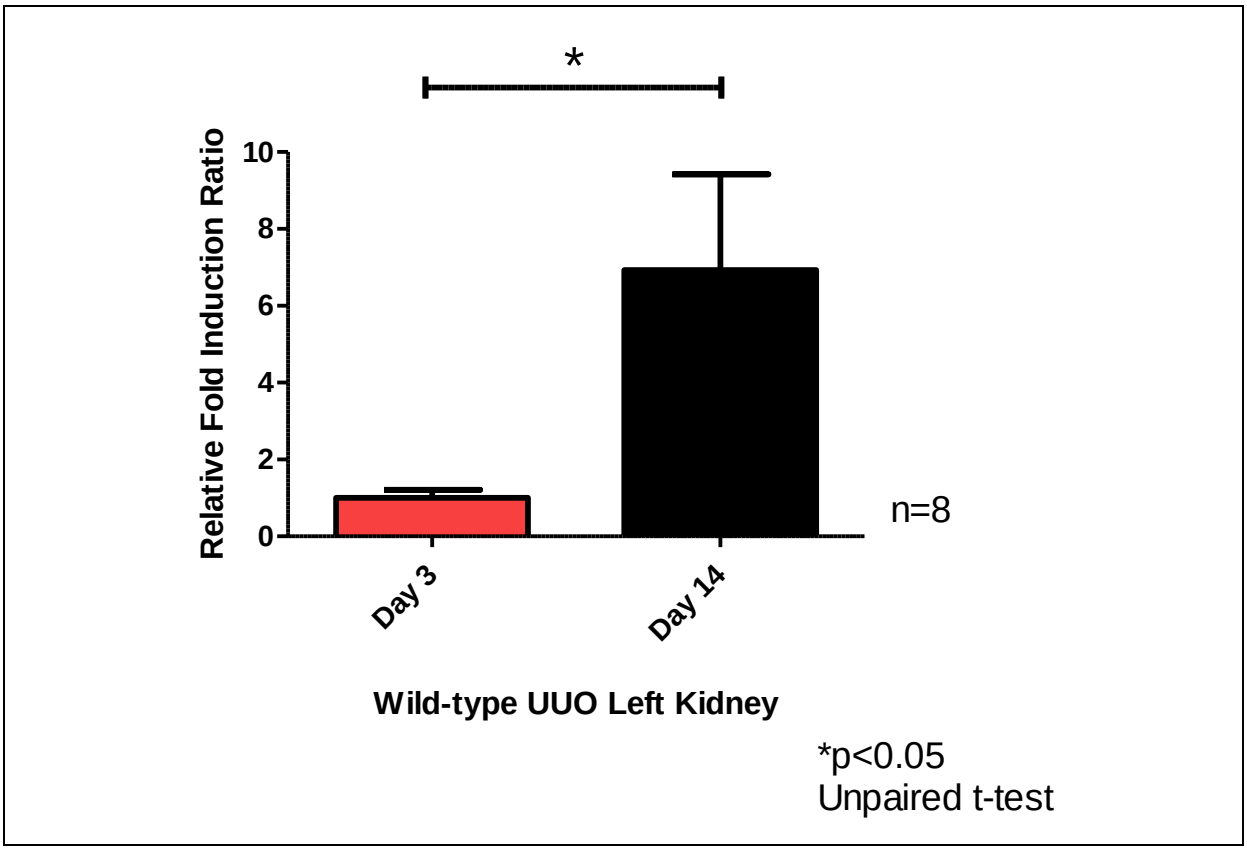

Cav1 protein expression was also increased as seen with Western blotting, the longer the model of fibrosis studied (Figure 6-18). Representative images using confocal microscopy also show an increase in Cav1 staining as the temporal length of fibrotic injury progresses compared to sham (Figure 6-19).

Figure 6-18 Representative Western blot showing the caveolin-1 protein expression in relation to β actin in the left kidney: day 14 versus day 3 models of renal fibrosis

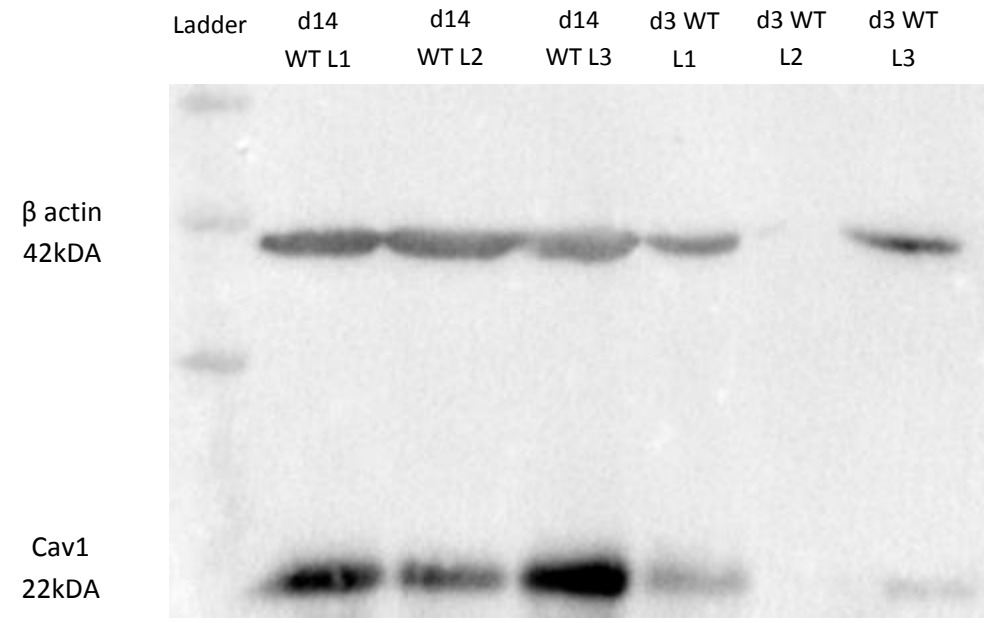

Key: Cav1: caveolin-1; d14: day 14; d3: day 3, WT: wild-type, L: left

Figure 6-19 Confocal microscopy (x10) of caveolin-1 staining in the left UUO kidney

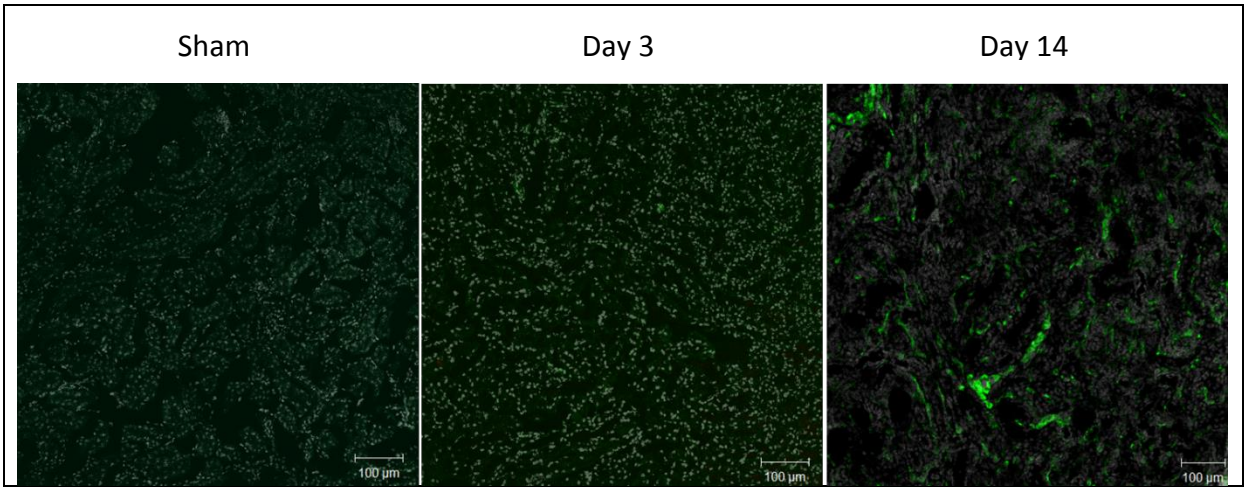

When comparing the contralateral kidneys, there was over 3 fold induction significant increase in Cav1 mRNA corresponding to the physiological compensation of the right kidney in UUO injury, as well as increased Cav1 protein expression (Figure 6-20 and Figure 6-21 respectively). This highlights that sham operated mice should be used as controls rather than the right kidney in the UUO model of injury. There was a non-significant rise in right kidney Cav1 mRNA between days 3 and 14 of the model (p=0.51, unpaired t-test).

Figure 6-20 Comparison of the caveolin-1 fold induction change of the right compensatory kidney in UUO wild-type mice to the left sham operated kidney. One-way ANOVA (top line) to compare difference between groups and post Dunnett's multiple comparison test for day 3 and day 14 to right sham operated kidney

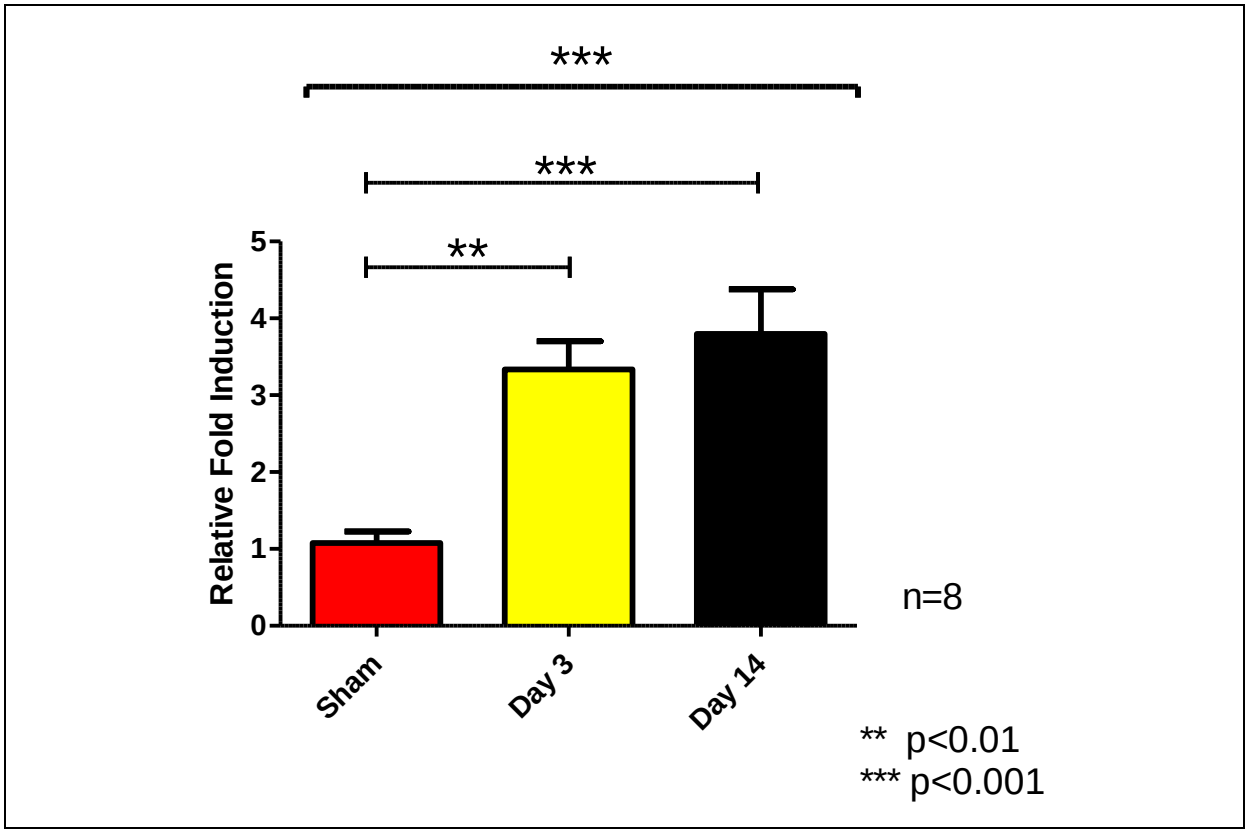

Figure 6-21 Western blot of the wild-type right kidney in UUO. Knockout left kidney included that shows no caveolin-1 protein expression present.

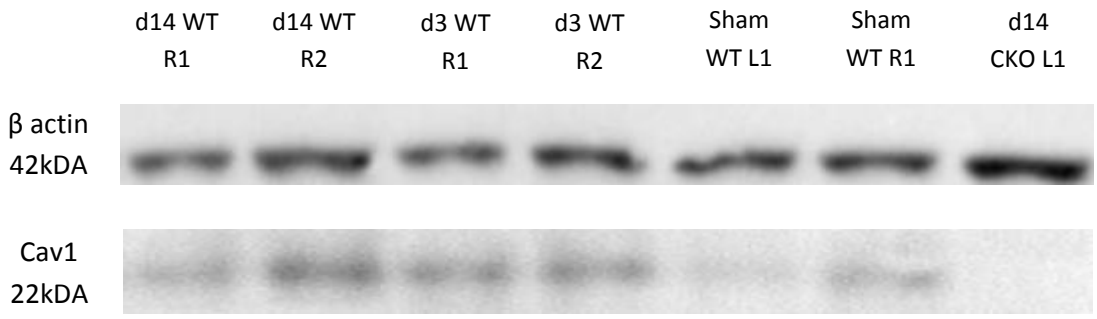

Key: Cav1: caveolin-1; d14: day 14; d3: day 3, WT: wild-type, R: right, L: left, CKO: caveolin-1 knockout

6.2.2.3 Other markers of fibrosis in UUO

As the model advances with time, there are significant increases in TGFβ-1, collagen 1α1 and collagen 3α1 fold induction as well as a non-significant increase in Gomori staining of fibrosis (Figure 6-22). Wild-type mice of the day 3 model of UUO lose weight as compared to day 14.

Figure 6-22 Relative fold induction ratio, weight change and Gomori staining of wild-type UUO

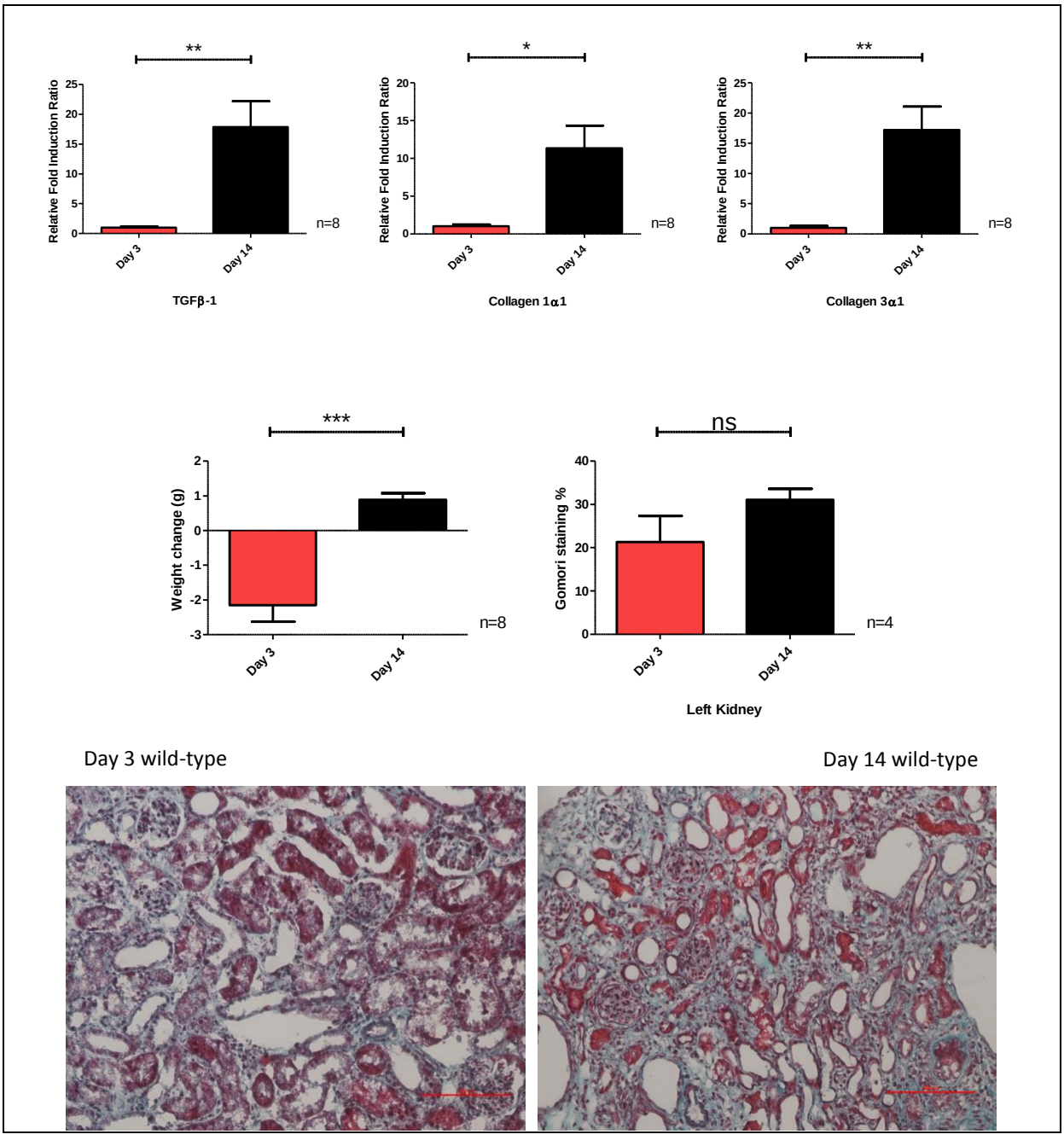

Confocal microscopy shows an increase in CD31, F4/80 and αSMA positive staining in day 3 and day 14 models as compared to sham operated mice (Figure 6-23).

Figure 6-23 CD31, F4/80 and αSMA confocal staining in wildtype mice in UUO models of fibrosis

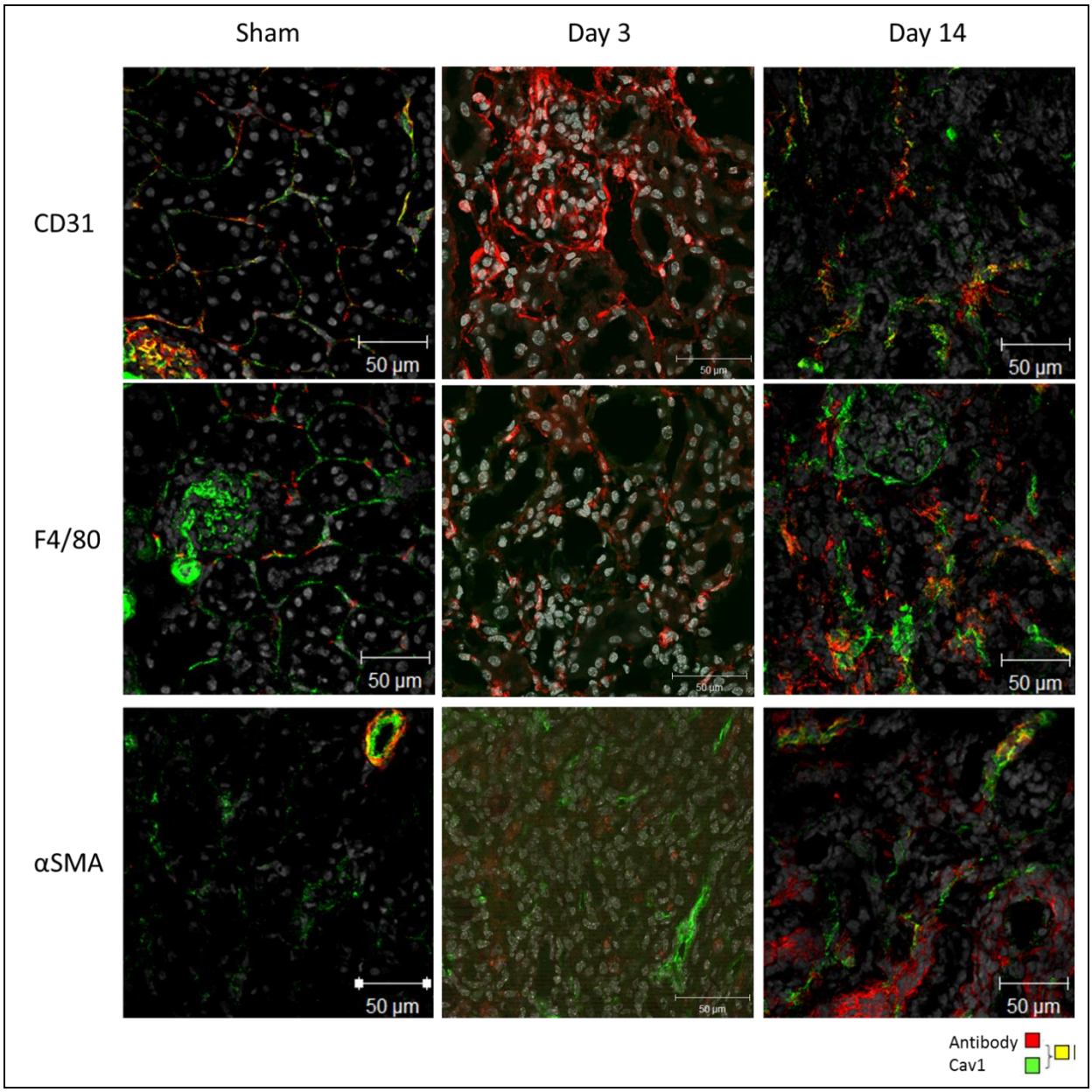

6.2.2.4 Unilateral ureteric obstruction in caveolin-1 knockout mice

Sham operated wild-type and CKO mice did not significantly differ in the fold induction of TGFβ-1, collagen 1α1 or collagen 3α1 (Figure 6-24).

Figure 6-24 Wild-type (WT) and caveolin-1 knockout (KO) mice sham operated mice show non-significant (ns) mRNA fold induction changes

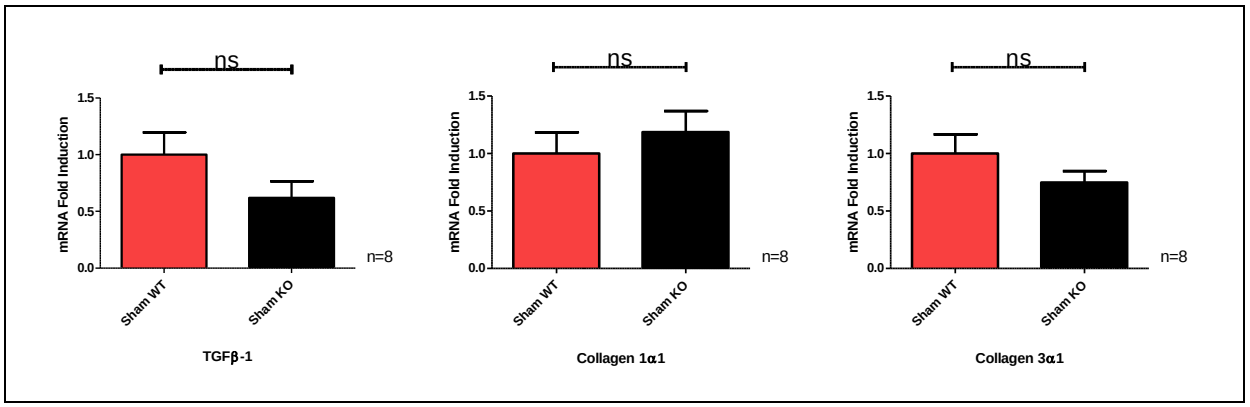

The CKO mice show a similar pattern of progressive fibrosis as the UUO model temporally progresses. As the model advances with time, there are significant increases in TGFβ-1, collagen 1α1 and collagen 3α1 fold induction as well as a significant increase in Gomori staining of fibrosis. The CKO mice lose more weight at day 3 than at day 14 time points of the UUO model (Figure 6-25).

Figure 6-25 Relative fold induction ratio, weight change and Gomori staining of knockout left obstructed kidney at day 3 and day 14 of the UUO model

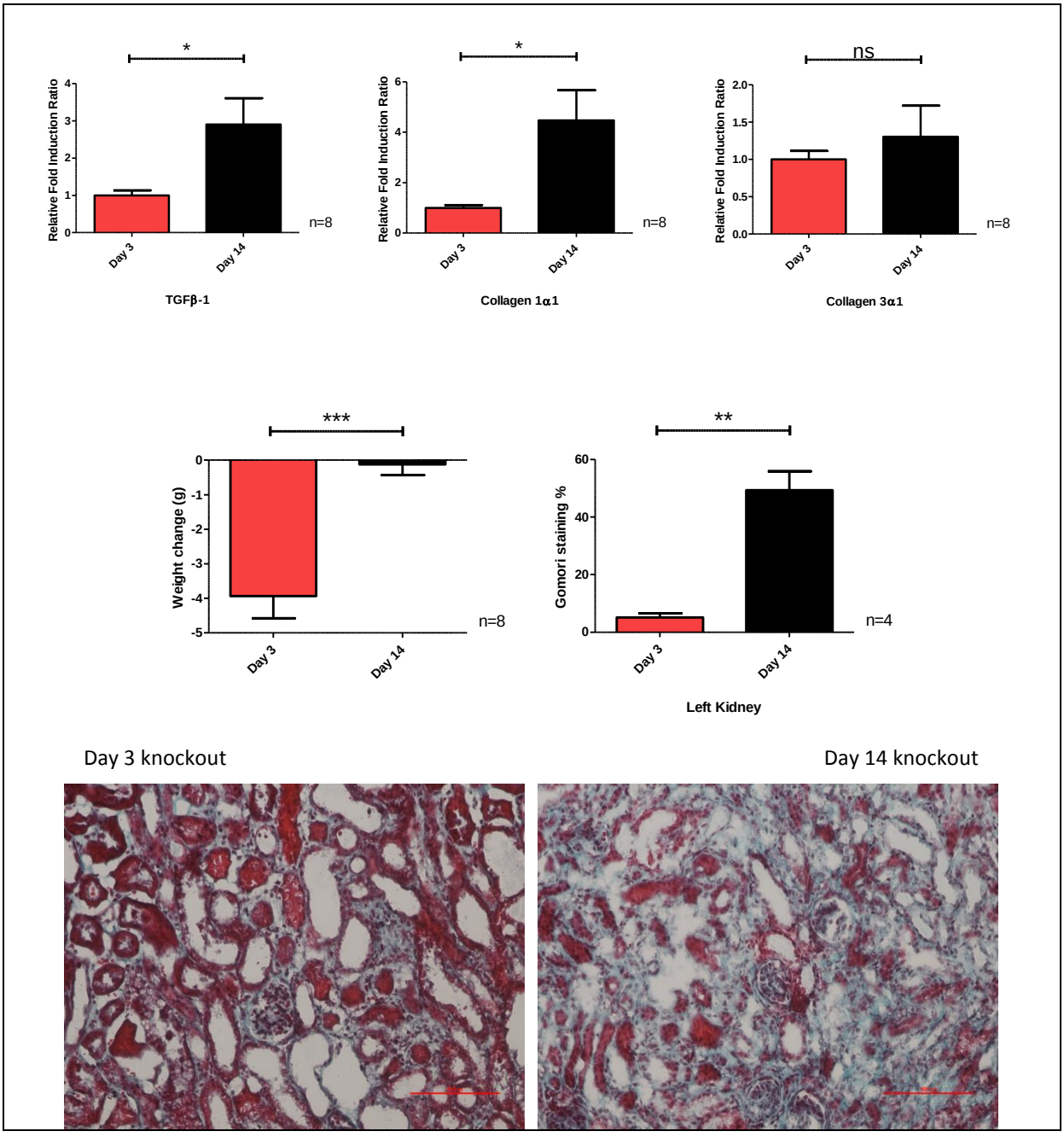

Whilst there are significant increases in the mRNA fold induction ratios of TGFβ-1, collagen 1α1 and collagen 3α1, and more weight reduction in the CKO mouse group at day 3, there is an increase in the Gomori fibrosis percentage seen in the wild-type group (Figure 6-26).

Figure 6-26 Relative fold induction ratio, weight change and Gomori staining of left obstructed kidney, comparing wild-type to caveolin-1 knockout at day 3

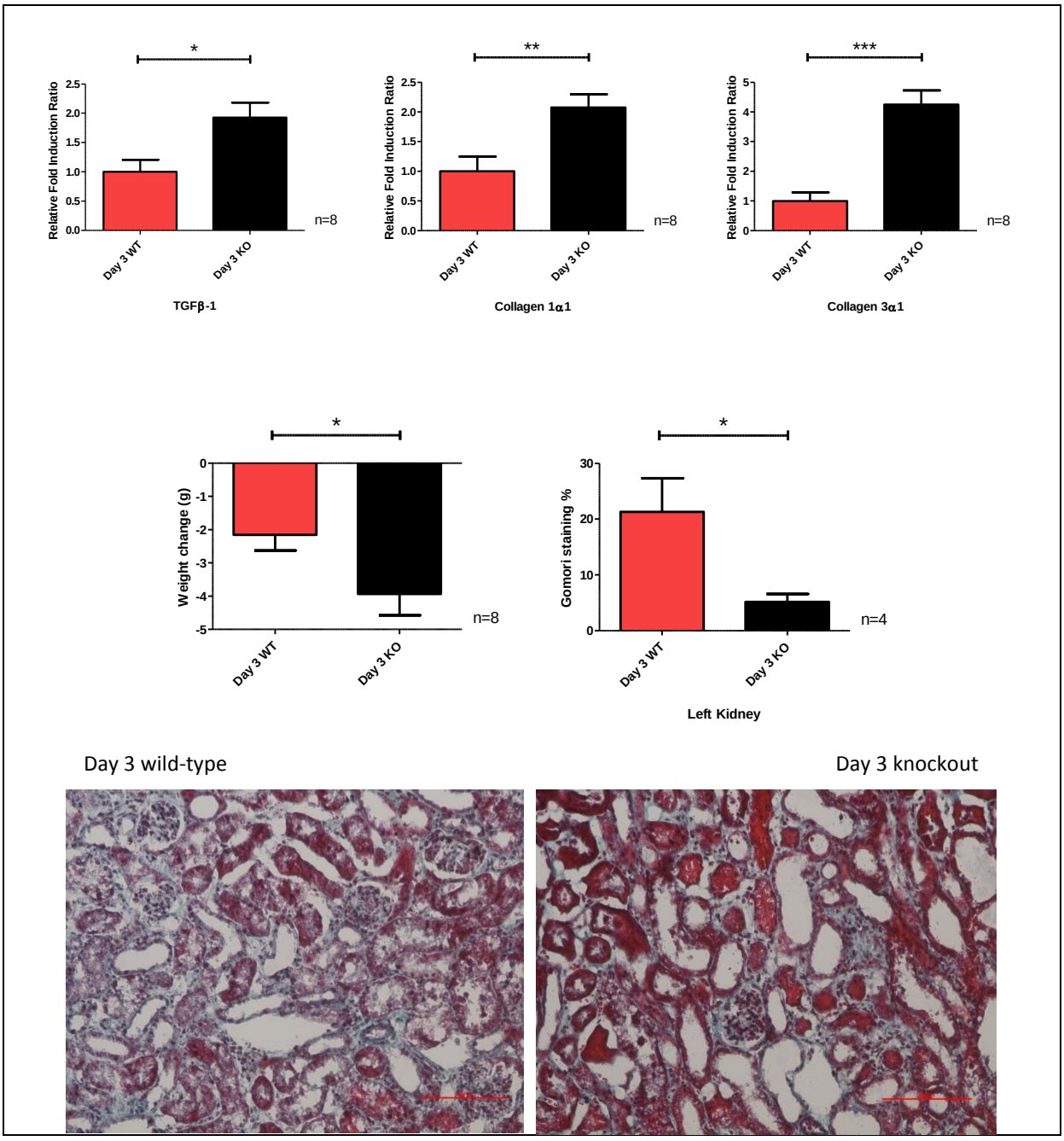

Whilst there are significant decreases in the mRNA fold induction ratios of TGFβ-1 and collagen 3α1, and weight reduction in the CKO mouse group at day 14, there is an increase in the Gomori fibrosis percentage seen in the CKO group, which is the opposite seen at day 3 (Figure 6-27).

Figure 6-27 Relative fold induction ratio, weight change and Gomori staining of left obstructed kidney, comparing wild-type to caveolin-1 knockout at day 14

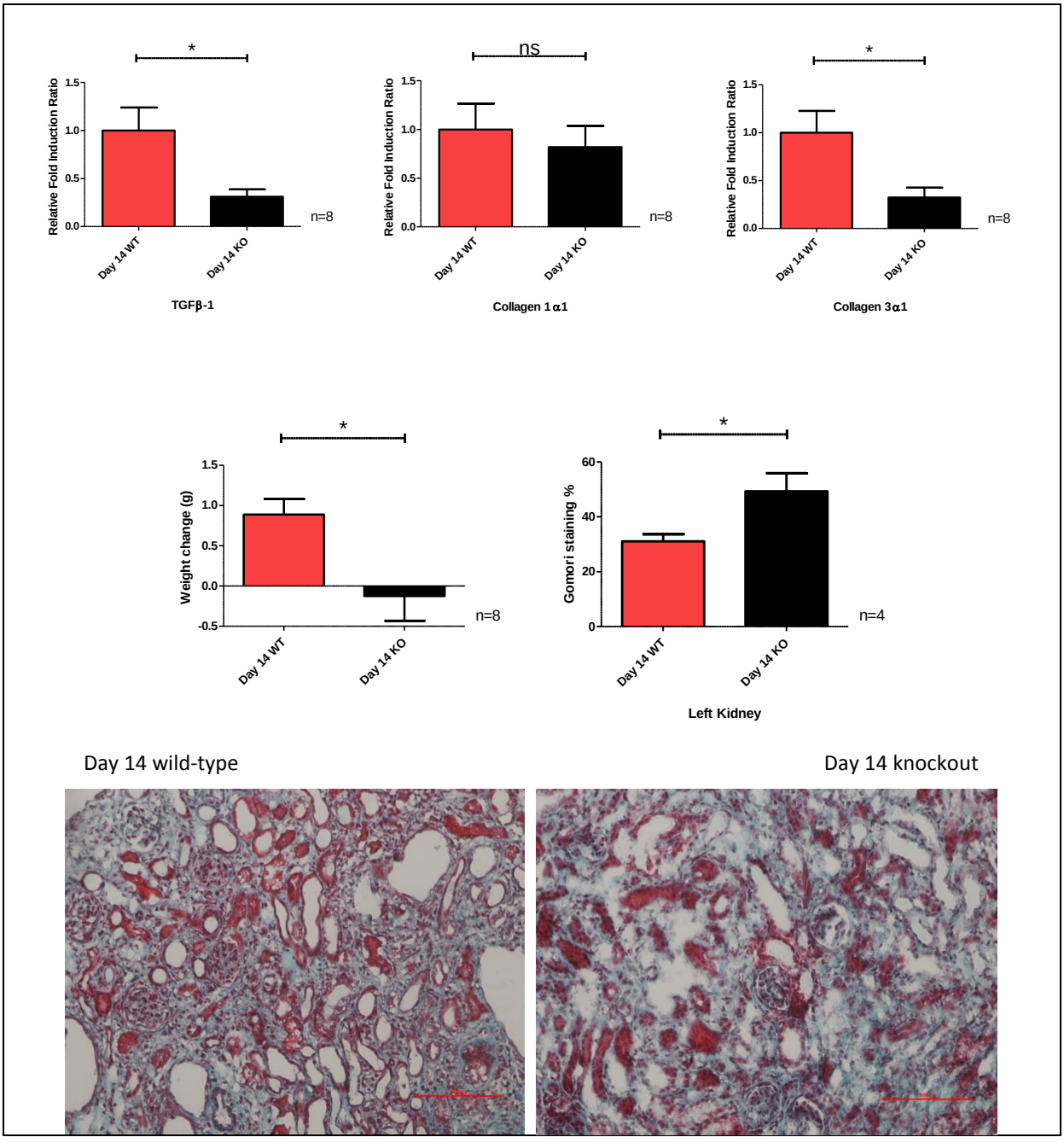

The most striking difference with confocal microscopy between wild-type and CKO groups is the amount of F4/80 staining seen as the model progresses with time. This staining is more visible in the wild-type than CKO group (Figure 6-28).

Figure 6-28 Confocal F4/80 staining in wild-type and caveolin-1 knockout mice

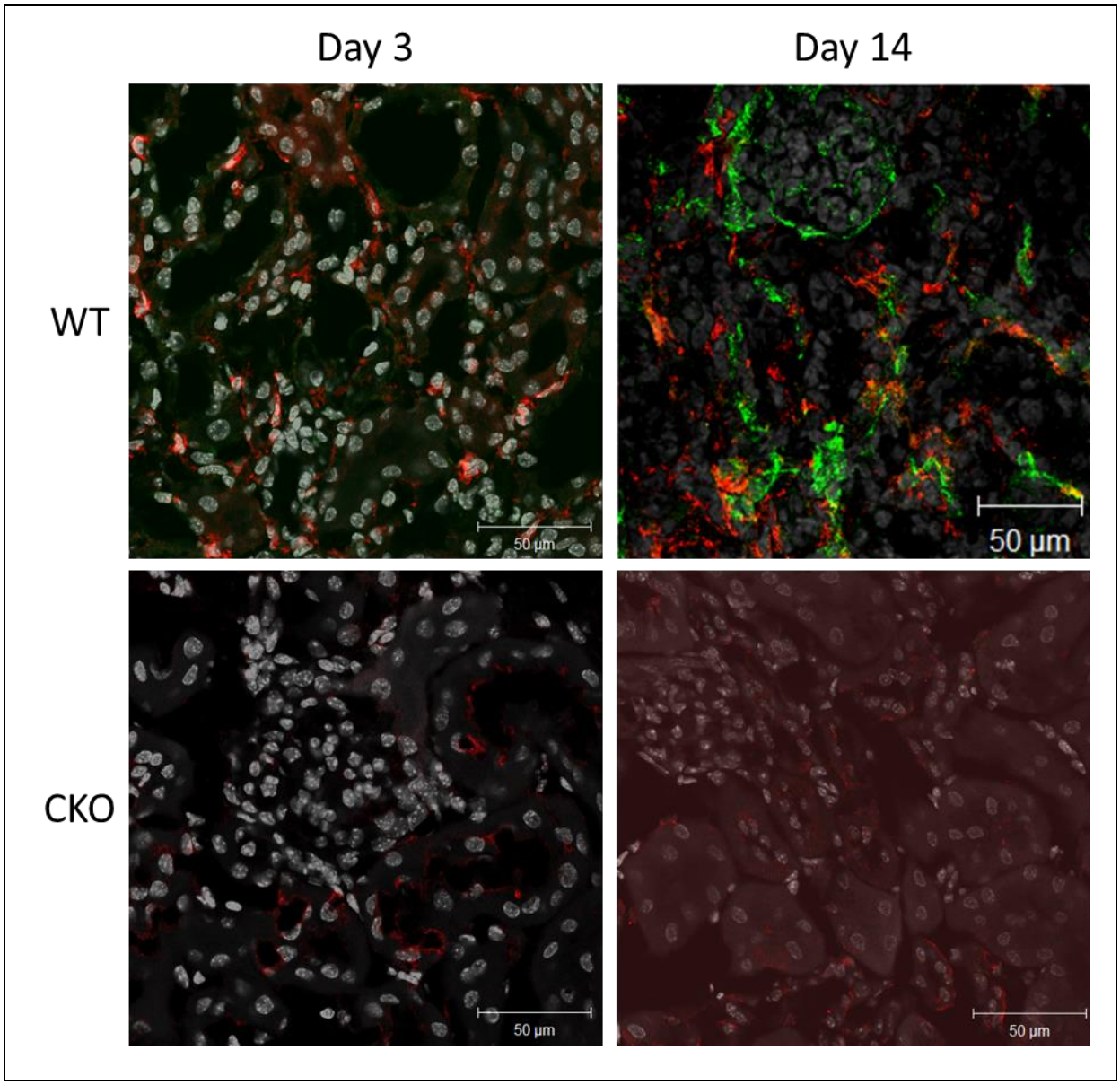

There were non-significant increases in the fold induction ratio changes in the right compensatory kidney between day 3 and day 14 models and wild-type and CKO groups. There were no changes in the Gomori staining of the right kidneys in UUO (Figure 6-29).

Figure 6-29 Right compensatory kidneys relative fold induction ratios and Gomori staining at day 3 and day 14 in wild-type and caveolin-1 knockout groups

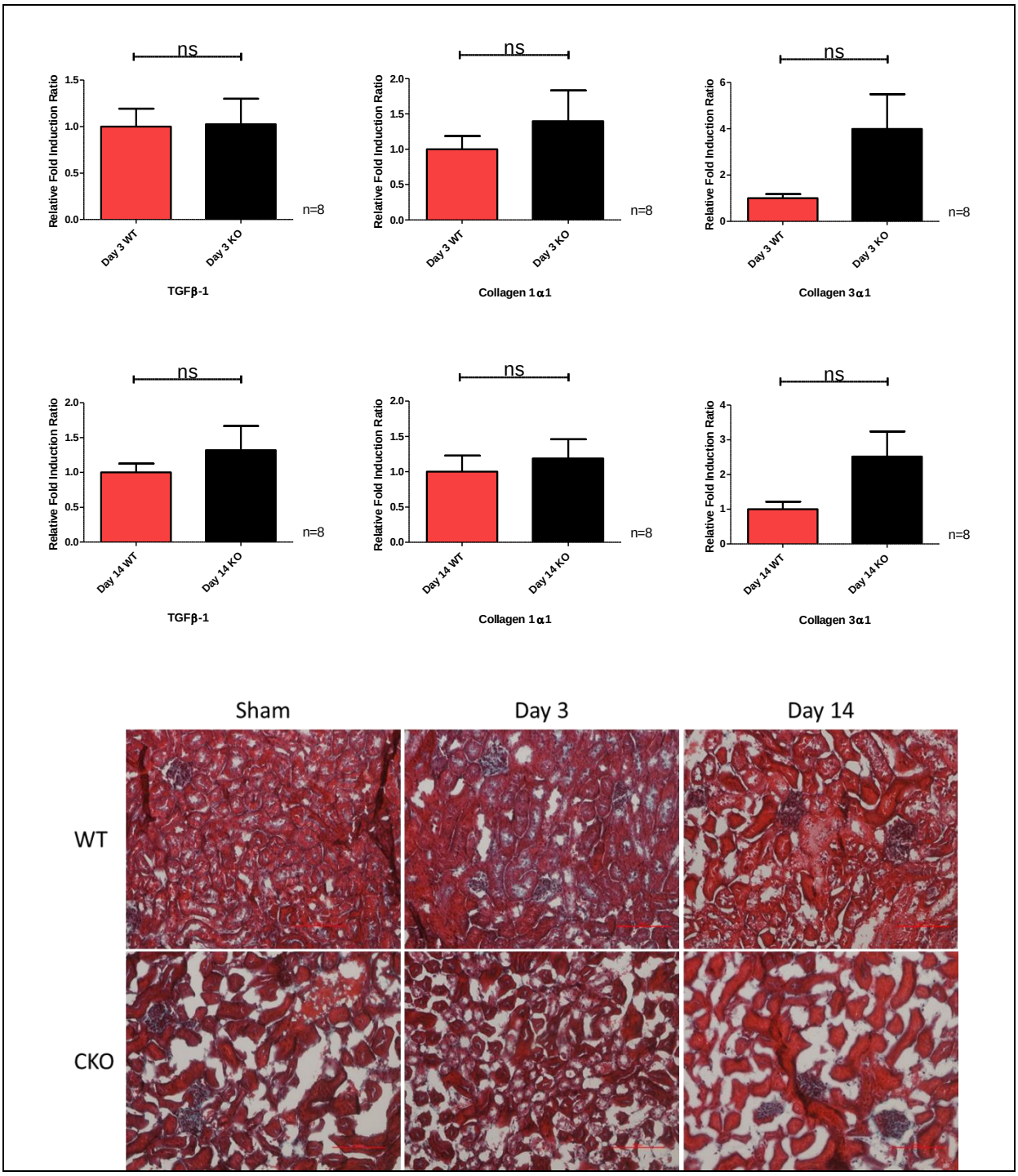

6.2.3 Discussion

From the staining seen on confocal microscopy, caveolin-1 is expressed in the renal endothelium including the glomerular endothelium, vasculature and basolateral aspects of tubules, F4/80 and CD3e staining positive cells. There was an increase in caveolin-1 expression, whether at a protein or mRNA level, seen in the UUO model of renal fibrosis in the injured kidney in the wild-type mouse as compared to sham. This is consistent with the literature described in section 1.2.5.1 where there is an observed increase in caveolin-1 expression upon injury to the human and murine kidney. Cav1 expression was more pronounced the later the UUO injury had occurred.

After an initial increase in CD31 confocal staining at day 3 of the UUO model (as compared to sham operated mice), there was decrease in CD31 staining by day 14, whilst αSMA staining was increased at day 14 as compared to day 3. This phenomenon has been noted previously in murine UUO and represents a likely endothelial to mesenchymal transition to myofibroblasts (265).

Align to this, at day 3 there was a decline in the murine weight. Although this could be due to the recent surgery, it could reflect an inflammatory systemic milieu that was more pronounced in the CKO group, hence less Gomori staining with increased TGFβ-1 and collagen I and III mRNA in the CKO group at day 3. There was also a failure of weight gain the CKO group at day 14 as compared to the day 14 wild-type mice, with a reduction in TGFβ-1 and collagen I and III mRNA and increased Gomori collagen staining. The fibrotic matrix is rich in fibrillar collagen I and III (266). This is likely to reflect the established accelerated

fibrosis in the CKO day 14 group compared to wild-type. Wild-type Cav1 expression was also increased in the compensatory right non-obstructed kidney as compared to sham at day 3 and day 14. This highlights that the contralateral kidney should not be used as control in the UUO model.

The most striking difference between the wild-type and knockout groups is the F4/80 positive staining cells, which was greater in the wild-type model. During the initial injury from UUO, tubular cell death and extracellular matrix remodelling lead to the release a hetergenous set of molecules called danger associated molecular pattern molecules (such as hylauronan, fibronectin and uromodulin) that trigger sterile inflammation via the innate immune system (267). They promote polarization of resident and infiltrating macrophages to either M1 (known as classical or pro-inflammatory) or M2 (alternative or regulatory/pro-fibrotic) phenotypes. M1b macrophages predominate during the onset of sterile inflammation (268) and injury with pericyte detachment and vascular rarefaction (269), releasing pro-inflammatory cytokines and reactive oxygen species, exacerbating the initial injury promoting epithelial and endothelial mesenchymal transition via metalloproteinases and degrading the extracellular matrix. M2 macrophages release TGFβ-1, IL-10, VEGF and phagocytose (270). With *Cav1* deletion, macrophages have been shown to have a reduced phagocytic ability after lipopolysaccharide challenge and thus a potential reduced ability to clear apoptotic cells, releasing more inflammatory cytokines (271). In cardiac models of fibrosis, *Cav1* deletion has led to a maladaptive repair process with increased inflammatory molecules as well as more M2 polarized macrophages at an earlier time-point as compared to wild-type (272). In the CKO UUO group at day 3, the mRNA of TGFβ-1, collagen I and III were all increased suggesting there is more M2 phenotype as well. However by day 14 in the

CKO versus wild-type group, the initial M2 'wound' healing macrophage phenotype is maladaptive with substantial remodelling of the interstitium with collagen-based scar tissue as shown by Gomori staining.

The worsening of fibrosis in the CKO day 14 group mirrors the findings of the only published literature of the UUO model of renal fibrosis in Cav1 knockout mice. Park et al showed that at day 10 of UUO, there was a reduced surge in mesenchymal stem cells with associated worse fibrosis in the CKO group (119). Cav1 is required for renal stem cell engraftment as CXCR4 dimerization induced by stromal cell-derived factor-1 occurs in caveolae. It should be noted however Park et al has used a different strain for the wild-type compared to the CKO group, thus with different mouse strains have varying susceptibility to fibrosis, this may have affected the changes seen.

In conclusion, *Cav1* mRNA and expression on Western blotting is increased at day 3 and further increased day 14 UUO, in line with published murine and human data in renal disease. However, upon its deletion, fibrosis worsens at day 14 of the UUO model compared to wild-type.

CHAPTER 7:

GENERAL DISCUSSION

7.1 General Discussion

Patients with CKD suffer adverse effects as a result of their disease or side-effects of the treatment required to treat their underlying illness. It is paramount to be able to risk stratify these patients' phenotype in regards to these adverse effects in order to introduce a personalised approach to future therapy. Patients with CKD suffer from increased morbidity and mortality related to cardiovascular disease, infection and malignancy as compared to the general population. This thesis has highlighted the use of *CAV1* SNP rs4730751 in identifying those patients with increased morbidity and mortality, not only within a systemic disease such as AAV that encompasses cardiovascular, infection and malignancy related death but also progression of renal disease to ESRD. Arterial stiffness has also been associated with an increased risk of cardiovascular disease as CKD progresses, and as shown in chapter 3.1.1, the expressed SNP is associated with differing arterial stiffness. The common finding in the thesis is that the CC genotype is associated with a protective phenotype in the adverse effects of CKD. However, the question remains as to whether this SNP's association relates to direct mechanistic causality, as the SNP is found on the non-coding intron of the *CAV1* gene (Figure 7-1). In general, intronic SNP could be in linkage disequilibrium with another gene, however, rs4730751 is not in linkage disequilibrium with genetic variants in exons that may truncate or alter CAV1 protein (158). Thus its effect may be by influencing resulting transcripts or splicing (273). In mice, intronic variance in the *Cav1* gene has shown changes in the predominance of the isoform of caveolin-1 expressed (274).

Figure 7-1 Caveolin-1 single nucleotide polymorphism rs4730751 location on chromosome 7

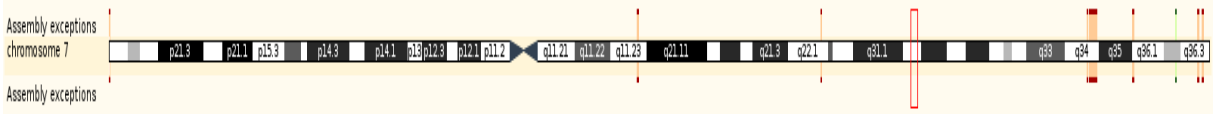

Key: Red rectangle showing location of CAV1 SNP rs4730751

As eNOS is bound to CAV1, *eNOS* SNP rs1799983 was also found to risk stratify patients with evidence of left ventricular wall remodelling in early stage CKD. Although *CAV1* rs4730751 SNP was not shown to be associated with NODAT, the use of SNP variants in common genes which are associated with the development of NODAT following kidney transplantation, offered a hypothesis generating method to our understanding of mechanisms involved in NODAT development and the potential for risk-stratifying patients pre-transplantation. As shown in this thesis, patients' phenotype could be differentiated in kidney disease by *CAV1* and related candidate gene SNPs.

The murine models of renal fibrosis did show that lack of Cav1 led to an increased fibrotic phenotype. Although this has been shown in non-renal organ fibrotic diseases, it was important to show this in the kidney, as the fibrotic response is dependent on the local tissue microenvironment of specialised structures, resident organ cells and response to infiltrating cells in the target organ. The majority of the existing renal in vivo CAV1 research has shown an increased expression with a worse renal phenotype in children with congenital ureteric obstruction (131) and in adult based glomerular disease (132), with authors indicating that CAV1 expression was detrimental. Use of the CKO mouse has shown a protective phenotype in a largely glomerular disease model of diabetic nephropathy using steptozotocin (133), and similar protection in mesangial matrix expansion using pathological

light chains (134). These latter studies serve to highlight that glomerulus is a specialised microenvironment within the kidney where CAV1 expression leads to a worse phenotype, whilst in models of interstitial fibrosis, this thesis and Park et al (119) have shown that CAV1 expression is protective. The exact mechanism is likely multifactorial with Park et al showing the surge of mesenchymal stem cell is curtailed with no CXCR4 dimerization without caveolae as well as observed differences in F4/80 positive staining cells in this thesis. Park et al did show that overexpression of caveolin-1 was associated with an increased neointimal formation suggesting the interplay between inflammation, matrix turnover, wound fibrogenesis/healing and scar formation is key in forming an adaptive or maladaptive repair process, with CAV1 expression central to this process. Luminex could be used to examine the cytokine profile in the differing time-points of the UUO model in the CKO and wild-type groups. Flow cytometry could also be used to identify the types of macrophages seen in the UUO model between the groups.

The exact timing of increased CAV1 protein or gene expression in a renal disease process either acutely, glomerular based or in reversing a scarring process remains to be elucidated as does its role in influencing improved renal outcome. Future studies would look to use a conditional knockout to investigate models of renal fibrosis at different time-points to find the optimal timing of any negative effects of Cav1 expression. It would also be preferable to use a more chronic model of renal fibrosis such as the folic acid model of nephropathy with resulting reduced eGFR and use other models that mimic immune mediated and heavily proteinuric diseases to reflect the diversity seen in human disease. To answer the question of the effects of infiltrating leucocytes into the kidney, bone marrow chimeras of the wild-type and knockout animal can be used in the renal models of fibrosis. It is also exciting to see

that the non-phosphorylatable CAV1 Y14 prevented VEGF-induced RhoA activation and fibronectin upregulation in mesangial cells (127) and future studies should consider the use of this non-phosphorylatable CAV1 Y14 in potentially reducing renal interstitial fibrosis.

By using a patient's *CAV1* rs4730751 genotype, future studies could look to tailor treatment balancing the risk and intensity of therapy such as immunosuppression in cardiovascular, infective and malignant associated related mortality to likely progression of the renal disease itself. Renal biopsies could be used from these patients to examine the degree of interstitial fibrosis and caveolin-1 expression including the dominant isoform expressed to see if there is an overt functional difference between the genotypes. From the Lancet in July 2016, thirteen fibrotic genes predicting future fibrosis in renal allografts was found from examining the renal transplant biopsy transcriptome (275). A similar approach could be extended to see if any genetic differences can be found in biopsy tissue depending on patient's genotype in renal allografts as previously donor *CAV1* SNP rs4730751 genotype predicted renal allograft survival and fibrosis (82, 158). This could assist understanding of how variation with this SNP could lead to fibrotic change. Future potential therapy could include delivering CAV1 to donor kidneys whilst being machine perfused prior to transplantation.

In conclusion, the *CAV1* rs4730751 SNP could be used as a marker of disease risk either in isolation or as part of a clinical risk score to counsel patients on the likely prognosis of their condition. The pleiotropic effects of CAV1 can differentiate patients' phenotype in CKD. Manipulation of CAV1 expression has the potential in manipulating the renal fibrotic process by altering macrophage number and potentially phenotype, and altering TGFβ-1 expression and the endothelial to mesenchymal transitional process.

CHAPTER 8:

REFERENCES

8.1 References

1. Coresh J, Selvin E, Stevens LA, Manzi J, Kusek JW, Eggers P, et al. Prevalence of chronic kidney disease in the United States. Jama. 2007;298(17):2038-47.
2. Kerr M, Bray B, Medcalf J, O'Donoghue DJ, Matthews B. Estimating the financial cost of chronic kidney disease to the NHS in England. Nephrol Dial Transplant. 2012;27 Suppl 3:iii73-80.
3. Levey AS, Bosch JP, Lewis JB, Greene T, Rogers N, Roth D. A more accurate method to estimate glomerular filtration rate from serum creatinine: a new prediction equation. Modification of Diet in Renal Disease Study Group. Ann Intern Med. 1999;130(6):461-70.
4. Levey AS, Coresh J, Greene T, Marsh J, Stevens LA, Kusek JW, et al. Expressing the Modification of Diet in Renal Disease Study equation for estimating glomerular filtration rate with standardized serum creatinine values. Clin Chem. 2007;53(4):766-72.
5. Klag MJ, Whelton PK, Randall BL, Neaton JD, Brancati FL, Ford CE, et al. Blood pressure and end-stage renal disease in men. N Engl J Med. 1996;334(1):13-8.
6. Ruilope LM, Campo C, Rodriguez-Artalejo F, Lahera V, Garcia-Robles R, Rodicio JL. Blood pressure and renal function: therapeutic implications. J Hypertens. 1996;14(11):1259-63.
7. Fraser SD, Roderick PJ, Aitken G, Roth M, Mindell JS, Moon G, et al. Chronic kidney disease, albuminuria and socioeconomic status in the Health Surveys for England 2009 and 2010. J Public Health (Oxf). 2014;36(4):577-86.
8. Aitken GR, Roderick PJ, Fraser S, Mindell JS, O'Donoghue D, Day J, et al. Change in prevalence of chronic kidney disease in England over time: comparison of nationally representative cross-sectional surveys from 2003 to 2010. BMJ Open. 2014;4(9):e005480.
9. Weiner DE, Tighiouart H, Amin MG, Stark PC, MacLeod B, Griffith JL, et al. Chronic kidney disease as a risk factor for cardiovascular disease and all-cause mortality: a pooled analysis of community-based studies. J Am Soc Nephrol. 2004;15(5):1307-15.
10. Chapter 1: Definition and classification of CKD. Kidney Int Suppl (2011). 2013;3(1):19-62.
11. Scott RP, Quaggin SE. Review series: The cell biology of renal filtration. J Cell Biol. 2015;209(2):199-210.
12. Tampe B, Zeisberg M. Contribution of genetics and epigenetics to progression of kidney fibrosis. Nephrol Dial Transplant. 2014;29 Suppl 4:iv72-9.
13. Reese PP, Cappola AR, Shults J, Townsend RR, Gadegbeku CA, Anderson C, et al. Physical performance and frailty in chronic kidney disease. Am J Nephrol. 2013;38(4):307-15.
14. Tonelli M, Wiebe N, Guthrie B, James MT, Quan H, Fortin M, et al. Comorbidity as a driver of adverse outcomes in people with chronic kidney disease. Kidney Int. 2015;88(4):859-66.
15. Smyth LJ, Duffy S, Maxwell AP, McKnight AJ. Genetic and epigenetic factors influencing chronic kidney disease. Am J Physiol Renal Physiol. 2014;307(7):F757-76.
16. Igarashi P, Somlo S. Genetics and pathogenesis of polycystic kidney disease. J Am Soc Nephrol. 2002;13(9):2384-98.
17. Genomes Project C, Auton A, Brooks LD, Durbin RM, Garrison EP, Kang HM, et al. A global reference for human genetic variation. Nature. 2015;526(7571):68-74.
18. Thomas PD. Single Nucleotide Polymorphisms in Human Disease and Evolution: Phylogenies and Genealogies. eLS: John Wiley & Sons, Ltd; 2001.
19. Keller BJ, Martini S, Sedor JR, Kretzler M. A systems view of genetics in chronic kidney disease. Kidney Int. 2012;81(1):14-21.
20. Renkema KY, Stokman MF, Giles RH, Knoers NV. Next-generation sequencing for research and diagnostics in kidney disease. Nat Rev Nephrol. 2014;10(8):433-44.
21. Kottgen A, Pattaro C, Boger CA, Fuchsberger C, Olden M, Glazer NL, et al. New loci associated with kidney function and chronic kidney disease. Nat Genet. 2010;42(5):376-84.

22. Stanescu HC, Arcos-Burgos M, Medlar A, Bockenhauer D, Kottgen A, Dragomirescu L, et al. Risk HLA-DQA1 and PLA(2)R1 alleles in idiopathic membranous nephropathy. N Engl J Med. 2011;364(7):616-26.
23. Beck LH, Jr., Bonegio RG, Lambeau G, Beck DM, Powell DW, Cummins TD, et al. M-type phospholipase A2 receptor as target antigen in idiopathic membranous nephropathy. N Engl J Med. 2009;361(1):11-21.
24. Bullich G, Ballarin J, Oliver A, Ayasreh N, Silva I, Santin S, et al. HLA-DQA1 and PLA2R1 polymorphisms and risk of idiopathic membranous nephropathy. Clin J Am Soc Nephrol. 2014;9(2):335-43.
25. Lyons PA, Rayner TF, Trivedi S, Holle JU, Watts RA, Jayne DR, et al. Genetically distinct subsets within ANCA-Associated Vasculitis. N Engl J Med. 2012;367(3):214-23.
26. Fraga MF, Ballestar E, Paz MF, Ropero S, Setien F, Ballestar ML, et al. Epigenetic differences arise during the lifetime of monozygotic twins. Proc Natl Acad Sci U S A. 2005;102(30):10604-9.
27. Simmonds MJ, Benavente D, Brand OJ, Moore J, Ball S, Ferro CJ, et al. Skewing of female X-chromosome inactivation: an epigenetic risk factor for kidney transplantation outcome. Transplantation. 2013;95(5):e25-8.
28. Chand S, McKnight AJ, Borrows R. Genetic polymorphisms and kidney transplant outcomes. Curr Opin Nephrol Hypertens. 2014;23(6):605-10.
29. Israni A, Leduc R, Holmes J, Jacobson PA, Lamba V, Guan W, et al. Single-nucleotide polymorphisms, acute rejection, and severity of tubulitis in kidney transplantation, accounting for center-to-center variation. Transplantation. 2010;90(12):1401-8.
30. O'Brien RP, Phelan PJ, Conroy J, O'Kelly P, Green A, Keogan M, et al. A genome-wide association study of recipient genotype and medium-term kidney allograft function. Clin Transplant. 2013;27(3):379-87.
31. Hou W, Huang Z, Ji Z, Zhou J. Human leukocyte antigen-G-14-base-pair-insertion/deletion polymorphism and graft survival in kidney transplant recipients. Exp Clin Transplant. 2014;12(2):89-94.
32. Littera R, Piredda G, Pani A, Frongia M, Onano B, Michittu MB, et al. Role of human leukocyte antigen-G 14-base pair polymorphism in kidney transplantation outcomes. J Nephrol. 2013;26(6):1170-8.
33. Israni AK, Leduc R, Jacobson PA, Wildebush W, Guan W, Schladt D, et al. Inflammation in the setting of chronic allograft dysfunction post-kidney transplant: phenotype and genotype. Clin Transplant. 2013;27(3):348-58.
34. Bay JT, Schejbel L, Madsen HO, Sorensen SS, Hansen JM, Garred P. Low C4 gene copy numbers are associated with superior graft survival in patients transplanted with a deceased donor kidney. Kidney Int. 2013;84(3):562-9.
35. Engela AU, Boer K, Roodnat JI, Peeters AM, Eilers PH, Kal-van Gestel JA, et al. Genetic variants of FOXP3 influence graft survival in kidney transplant patients. Hum Immunol. 2013;74(6):751-7.
36. Karimi MH, Hejr S, Geramizadeh B, Yaghobi R, Sagheb MM, Kamali-Sarvestani E. Combined analysis of cytokine gene polymorphism and the level of expression with allograft function in kidney transplant recipients. Transpl Immunol. 2014;30(1):46-51.
37. Hejr S, Karimi MH, Yaghobi R, Kamali-Sarvestani E, Geramizadeh B, Roozbeh J. Association of IL-17, IL-21, and IL-23R gene polymorphisms with HBV infection in kidney transplant patients. Viral Immunol. 2013;26(3):201-6.
38. El-Gezawy EM, Eldin EN, Mohamed WS, Mahmoud MS, Saied SA, Abd El-Latif HH, et al. Tumor necrosis factor-alfa and monocyte chemoattractant protein-1 gene polymorphisms in kidney transplant recipients. Saudi J Kidney Dis Transpl. 2013;24(4):688-95.

39. Lee JP, Kim do H, Yang SH, Hwang JH, An JN, Min SI, et al. Serum bilirubin affects graft outcomes through UDP-glucuronosyltransferase sequence variation in kidney transplantation. PLoS One. 2014;9(4):e93633.
40. Kim TH, Jeong KH, Kim SK, Lee SH, Ihm CG, Lee TW, et al. TLR9 gene polymorphism (rs187084, rs352140): association with acute rejection and estimated glomerular filtration rate in renal transplant recipients. Int J Immunogenet. 2013;40(6):502-8.
41. Vu D, Tellez-Corrales E, Shah T, Hutchinson I, Min DI. Influence of Cyclooxygenase-2 (COX-2) gene promoter-1195 and allograft inflammatory factor-1 (AIF-1) polymorphisms on allograft outcome in Hispanic kidney transplant recipients. Hum Immunol. 2013;74(10):1386-91.
42. Wu X, Wan Q, Ye Q, Zhou J. Mannose-binding lectin-2 and ficolin-2 gene polymorphisms and clinical risk factors for acute rejection in kidney transplantation. Transpl Immunol. 2014;30(2-3):71-5.
43. Ge YZ, Wu R, Jia RP, Liu H, Yu P, Zhao Y, et al. Association between interferon gamma +874 T>A polymorphism and acute renal allograft rejection: evidence from published studies. Mol Biol Rep. 2013;40(10):6043-51.
44. Gaafar A, Iqniebi A, Sheereen A, Eldali A, Turpeinen H, Adra C, et al. Study of the cytokine polymorphisms in correlation to rejection and graft survival in renal allograft donors and recipients from a homogenous Saudi population. Transpl Immunol. 2014;30(1):34-9.
45. Dhaouadi T, Sfar I, Bardi R, Jendoubi-Ayed S, Abdallah TB, Ayed K, et al. Cytokine gene polymorphisms in kidney transplantation. Transplant Proc. 2013;45(6):2152-7.
46. Kloda K, Domanski L, Pawlik A, Safranow K, Ciechanowski K. The impact of ICAM1 and VCAM1 gene polymorphisms on long-term renal transplant function and recipient outcomes. Ann Transplant. 2013;18:231-7.
47. Pawlik A, Dabrowska-Zamojcin E, Dziedziejko V, Safranow K, Domanski L. Association between IVS3 +17T/C CD28 gene polymorphism and the acute kidney allograft rejection. Transpl Immunol. 2014;30(2-3):84-7.
48. La Manna G, Cappuccilli ML, Capelli I, Baraldi O, Cuna V, Battaglino G, et al. The impact of apoptosis and inflammation gene polymorphisms on transplanted kidney function. Ann Transplant. 2013;18:256-64.
49. Wan QQ, Li JL, Ye QF, Zhou JD. Genetic association of tumor necrosis factor-beta, interleukin-10, and interleukin-1 gene cluster polymorphism with susceptibility to pneumonia in kidney transplant recipients. Transplant Proc. 2013;45(6):2211-4.
50. Chen Z, Bouamar R, Van Schaik RH, De Fijter JW, Hartmann A, Zeier M, et al. Genetic polymorphisms in IL-2, IL-10, TGF-beta1, and IL-2RB and acute rejection in renal transplant patients. Clin Transplant. 2014.
51. Krichen H, Gorgi Y, Dhaouadi T, Mecheri Y, Sfar I, Bardi R, et al. Toll-like receptor 4 and CD14 gene polymorphisms in Tunisian kidney transplantation. Transplant Proc. 2013;45(10):3472-7.
52. Kloda K, Domanski L, Bobrek-Lesiakowska K, Pawlik A, Safranow K, Kwiatkowska E, et al. The impact of CTLA4 and PTPN22 genes polymorphisms on long-term renal allograft function and transplant outcomes. Ren Fail. 2013;35(9):1223-7.
53. Suzuki Y, Itoh H, Fujioka T, Sato F, Kawasaki K, Sato Y, et al. Association of plasma concentration of 4beta-hydroxycholesterol with CYP3A5 polymorphism and plasma concentration of indoxyl sulfate in stable kidney transplant recipients. Drug Metab Dispos. 2014;42(1):105-10.
54. Stifft F, Stolk LM, Undre N, van Hooff JP, Christiaans MH. Lower variability in 24-hour exposure during once-daily compared to twice-daily tacrolimus formulation in kidney transplantation. Transplantation. 2014;97(7):775-80.
55. Wu MJ, Chang CH, Cheng CY, Shu KH, Chen CH, Cheng CH, et al. Reduced variability of tacrolimus trough level in once-daily tacrolimus-based Taiwanese kidney transplant recipients with high-expressive genotype of cytochrome P450 3A5. Transplant Proc. 2014;46(2):403-5.

56. Vannaprasaht S, Reungjui S, Supanya D, Sirivongs D, Pongskul C, Avihingsanon Y, et al. Personalized tacrolimus doses determined by CYP3A5 genotype for induction and maintenance phases of kidney transplantation. Clin Ther. 2013;35(11):1762-9.
57. Niioka T, Kagaya H, Miura M, Numakura K, Saito M, Inoue T, et al. Pharmaceutical and genetic determinants for interindividual differences of tacrolimus bioavailability in renal transplant recipients. Eur J Clin Pharmacol. 2013;69(9):1659-65.
58. Passey C, Birnbaum AK, Brundage RC, Oetting WS, Israni AK, Jacobson PA. Dosing equation for tacrolimus using genetic variants and clinical factors. Br J Clin Pharmacol. 2011;72(6):948-57.
59. Boughton O, Borgulya G, Cecconi M, Fredericks S, Moreton-Clack M, MacPhee IA. A published pharmacogenetic algorithm was poorly predictive of tacrolimus clearance in an independent cohort of renal transplant recipients. Br J Clin Pharmacol. 2013;76(3):425-31.
60. Shuker N, Bouamar R, van Schaik RH, Clahsen-van Groningen MC, Damman J, Baan CC, et al. A Randomized Controlled Trial Comparing the Efficacy of Cyp3a5 Genotype-Based With Body-Weight-Based Tacrolimus Dosing After Living Donor Kidney Transplantation. Am J Transplant. 2016;16(7):2085-96.
61. Spierings N, Holt DW, MacPhee IA. CYP3A5 genotype had no impact on intrapatient variability of tacrolimus clearance in renal transplant recipients. Ther Drug Monit. 2013;35(3):328-31.
62. Li DY, Teng RC, Zhu HJ, Fang Y. CYP3A4/5 polymorphisms affect the blood level of cyclosporine and tacrolimus in Chinese renal transplant recipients. Int J Clin Pharmacol Ther. 2013;51(6):466-74.
63. Tavira B, Coto E, Diaz-Corte C, Alvarez V, Lopez-Larrea C, Ortega F. A search for new CYP3A4 variants as determinants of tacrolimus dose requirements in renal-transplanted patients. Pharmacogenet Genomics. 2013;23(8):445-8.
64. Chitnis SD, Ogasawara K, Schniedewind B, Gohh RY, Christians U, Akhlaghi F. Concentration of tacrolimus and major metabolites in kidney transplant recipients as a function of diabetes mellitus and cytochrome P450 3A gene polymorphism. Xenobiotica. 2013;43(7):641-9.
65. Elens L, Capron A, van Schaik RH, De Meyer M, De Pauw L, Eddour DC, et al. Impact of CYP3A4*22 allele on tacrolimus pharmacokinetics in early period after renal transplantation: toward updated genotype-based dosage guidelines. Ther Drug Monit. 2013;35(5):608-16.
66. Shilbayeh S. The impact of genetic polymorphisms on time required to attain the target tacrolimus levels and subsequent pharmacodynamic outcomes in pediatric kidney transplant patients. Saudi J Kidney Dis Transpl. 2014;25(2):266-77.
67. Mostafa-Hedeab G, Saber-Ayad MM, Latif IA, Elkashab SO, Elshaboney TH, Mostafa MI, et al. Functional G1199A ABCB1 polymorphism may have an effect on cyclosporine blood concentration in renal transplanted patients. J Clin Pharmacol. 2013;53(8):827-33.
68. Ogasawara K, Chitnis SD, Gohh RY, Christians U, Akhlaghi F. Multidrug resistance-associated protein 2 (MRP2/ABCC2) haplotypes significantly affect the pharmacokinetics of tacrolimus in kidney transplant recipients. Clin Pharmacokinet. 2013;52(9):751-62.
69. Vafadari R, Bouamar R, Hesselink DA, Kraaijeveld R, van Schaik RH, Weimar W, et al. Genetic polymorphisms in ABCB1 influence the pharmacodynamics of tacrolimus. Ther Drug Monit. 2013;35(4):459-65.
70. Kazancioglu HO, Ak G, Turkmen A, Ozbek U, Tuncer FN, Karabulut A. The role of MDR1 C3435T gene polymorphism on gingival hyperplasia in Turkish renal transplant patients treated with cyclosporine in the absence of calcium channel blockers. Transplant Proc. 2013;45(6):2233-7.
71. Quaglia M, Terrazzino S, Boldorini R, Stratta P, Genazzani AA. Severe acute nephrotoxicity in a kidney transplant patient despite low tacrolimus levels: a possible interaction between donor and recipient genetic polymorphisms. J Clin Pharm Ther. 2013;38(4):333-6.
72. Valderhaug TG, Hjelmesaeth J, Hartmann A, Roislien J, Bergrem HA, Leivestad T, et al. The association of early post-transplant glucose levels with long-term mortality. Diabetologia. 2011;54(6):1341-9.

73. McCaughan JA, McKnight AJ, Maxwell AP. Genetics of new-onset diabetes after transplantation. J Am Soc Nephrol. 2014;25(5):1037-49.
74. Tavira B, Gomez J, Diaz-Corte C, Llobet L, Ruiz-Pesini E, Ortega F, et al. Mitochondrial DNA haplogroups and risk of new-onset diabetes among tacrolimus-treated renal transplanted patients. Gene. 2014;538(1):195-8.
75. Nicoletto BB, Souza GC, Fonseca NK, Centenaro A, Manfro RC, Canani LH, et al. Association between 276G/T adiponectin gene polymorphism and new-onset diabetes after kidney transplantation. Transplantation. 2013;96(12):1059-64.
76. Chudek J, Szotowska M, Karkoszka H, Verbeke F, Trautsolt W, Gumprecht J, et al. Genotypes of renin-angiotensin system and plasma adiponectin concentration in kidney transplant patients. Ann Transplant. 2013;18:593-603.
77. Reeves-Daniel AM, DePalma JA, Bleyer AJ, Rocco MV, Murea M, Adams PL, et al. The APOL1 gene and allograft survival after kidney transplantation. Am J Transplant. 2011;11(5):1025-30.
78. Kofman T, Audard V, Narjoz C, Gribouval O, Matignon M, Leibler C, et al. APOL1 polymorphisms and development of CKD in an identical twin donor and recipient pair. Am J Kidney Dis. 2014;63(5):816-9.
79. Han SS, Lee H, Oh YJ, Lee JP, Kim S, Ha J, et al. Identification of the effects of aging-related gene-matrix metalloproteinase on allograft outcomes in kidney transplantation. Transplant Proc. 2013;45(6):2158-64.
80. Moore J, McKnight AJ, Dohler B, Simmonds MJ, Courtney AE, Brand OJ, et al. Donor ABCB1 variant associates with increased risk for kidney allograft failure. J Am Soc Nephrol. 2012;23(11):1891-9.
81. Naesens M, Lerut E, de Jonge H, Van Damme B, Vanrenterghem Y, Kuypers DR. Donor age and renal P-glycoprotein expression associate with chronic histological damage in renal allografts. J Am Soc Nephrol. 2009;20(11):2468-80.
82. Moore J, McKnight AJ, Simmonds MJ, Courtney AE, Hanvesakul R, Brand OJ, et al. Association of caveolin-1 gene polymorphism with kidney transplant fibrosis and allograft failure. Jama. 2010;303(13):1282-7.
83. Palade GE. Fine Structure of Blood Capillaries. J Appl Phys. 1953;24(11):1424-.
84. Yamada E. The fine structure of the renal glomerulus of the mouse. J Biophys Biochem Cytol. 1955;1(6):551-66.
85. Cohen AW, Hnasko R, Schubert W, Lisanti MP. Role of caveolae and caveolins in health and disease. Physiol Rev. 2004;84(4):1341-79.
86. Fan JY, Carpentier JL, van Obberghen E, Grunfeld C, Gorden P, Orci L. Morphological changes of the 3T3-L1 fibroblast plasma membrane upon differentiation to the adipocyte form. J Cell Sci. 1983;61:219-30.
87. Glenney JR, Jr., Zokas L. Novel tyrosine kinase substrates from Rous sarcoma virus-transformed cells are present in the membrane skeleton. J Cell Biol. 1989;108(6):2401-8.
88. Glenney JR, Jr. Tyrosine phosphorylation of a 22-kDa protein is correlated with transformation by Rous sarcoma virus. J Biol Chem. 1989;264(34):20163-6.
89. Rothberg KG, Heuser JE, Donzell WC, Ying YS, Glenney JR, Anderson RG. Caveolin, a protein component of caveolae membrane coats. Cell. 1992;68(4):673-82.
90. Scherer PE, Lewis RY, Volonte D, Engelman JA, Galbiati F, Couet J, et al. Cell-type and tissue-specific expression of caveolin-2. Caveolins 1 and 2 co-localize and form a stable hetero-oligomeric complex in vivo. J Biol Chem. 1997;272(46):29337-46.
91. Scheiffele P, Verkade P, Fra AM, Virta H, Simons K, Ikonen E. Caveolin-1 and -2 in the exocytic pathway of MDCK cells. J Cell Biol. 1998;140(4):795-806.
92. Tang Z, Scherer PE, Okamoto T, Song K, Chu C, Kohtz DS, et al. Molecular cloning of caveolin-3, a novel member of the caveolin gene family expressed predominantly in muscle. J Biol Chem. 1996;271(4):2255-61.

93. Chidlow JH, Jr., Sessa WC. Caveolae, caveolins, and cavins: complex control of cellular signalling and inflammation. Cardiovasc Res. 2010;86(2):219-25.
94. Parton RG, Simons K. The multiple faces of caveolae. Nat Rev Mol Cell Biol. 2007;8(3):185-94.
95. Tanase C. CAV1 (caveolin 1, caveolae protein, 22kDA). Atlas Genet Cytogenet Oncol Haematol. 2009;13(11):788-92.
96. Engelman JA, Zhang XL, Lisanti MP. Sequence and detailed organization of the human caveolin-1 and -2 genes located near the D7S522 locus (7q31.1). Methylation of a CpG island in the 5' promoter region of the caveolin-1 gene in human breast cancer cell lines. FEBS Lett. 1999;448(2-3):221-30.
97. Engelman JA, Zhang X, Galbiati F, Volonte D, Sotgia F, Pestell RG, et al. Molecular genetics of the caveolin gene family: implications for human cancers, diabetes, Alzheimer disease, and muscular dystrophy. Am J Hum Genet. 1998;63(6):1578-87.
98. Schubert W, Frank PG, Razani B, Park DS, Chow CW, Lisanti MP. Caveolae-deficient endothelial cells show defects in the uptake and transport of albumin in vivo. J Biol Chem. 2001;276(52):48619-22.
99. Norkin LC, Anderson HA, Wolfrom SA, Oppenheim A. Caveolar endocytosis of simian virus 40 is followed by brefeldin A-sensitive transport to the endoplasmic reticulum, where the virus disassembles. J Virol. 2002;76(10):5156-66.
100. del Pozo MA, Balasubramanian N, Alderson NB, Kiosses WB, Grande-Garcia A, Anderson RG, et al. Phospho-caveolin-1 mediates integrin-regulated membrane domain internalization. Nat Cell Biol. 2005;7(9):901-8.
101. Sharma DK, Brown JC, Choudhury A, Peterson TE, Holicky E, Marks DL, et al. Selective stimulation of caveolar endocytosis by glycosphingolipids and cholesterol. Mol Biol Cell. 2004;15(7):3114-22.
102. Goligorsky MS, Li H, Brodsky S, Chen J. Relationships between caveolae and eNOS: everything in proximity and the proximity of everything. Am J Physiol Renal Physiol. 2002;283(1):F1-10.
103. Meng XM, Tang PM, Li J, Lan HY. TGF-beta/Smad signaling in renal fibrosis. Front Physiol. 2015;6:82.
104. Razani B, Zhang XL, Bitzer M, von Gersdorff G, Bottinger EP, Lisanti MP. Caveolin-1 regulates transforming growth factor (TGF)-beta/SMAD signaling through an interaction with the TGF-beta type I receptor. J Biol Chem. 2001;276(9):6727-38.
105. Sigismund S, Argenzio E, Tosoni D, Cavallaro E, Polo S, Di Fiore PP. Clathrin-mediated internalization is essential for sustained EGFR signaling but dispensable for degradation. Dev Cell. 2008;15(2):209-19.
106. Shi F, Sottile J. Caveolin-1-dependent beta1 integrin endocytosis is a critical regulator of fibronectin turnover. J Cell Sci. 2008;121(Pt 14):2360-71.
107. Rizzo V, Morton C, DePaola N, Schnitzer JE, Davies PF. Recruitment of endothelial caveolae into mechanotransduction pathways by flow conditioning in vitro. Am J Physiol Heart Circ Physiol. 2003;285(4):H1720-9.
108. Yu J, Bergaya S, Murata T, Alp IF, Bauer MP, Lin MI, et al. Direct evidence for the role of caveolin-1 and caveolae in mechanotransduction and remodeling of blood vessels. J Clin Invest. 2006;116(5):1284-91.
109. Sedding DG, Hermsen J, Seay U, Eickelberg O, Kummer W, Schwencke C, et al. Caveolin-1 facilitates mechanosensitive protein kinase B (Akt) signaling in vitro and in vivo. Circ Res. 2005;96(6):635-42.
110. Di Guglielmo GM, Le Roy C, Goodfellow AF, Wrana JL. Distinct endocytic pathways regulate TGF-beta receptor signalling and turnover. Nat Cell Biol. 2003;5(5):410-21.
111. Li Z, Wermuth PJ, Benn BS, Lisanti MP, Jimenez SA. Caveolin-1 deficiency induces spontaneous endothelial-to-mesenchymal transition in murine pulmonary endothelial cells in vitro. Am J Pathol. 2013;182(2):325-31.

112. Ito T, Williams JD, Fraser DJ, Phillips AO. Hyaluronan regulates transforming growth factor-beta1 receptor compartmentalization. J Biol Chem. 2004;279(24):25326-32.
113. Zhang XL, Topley N, Ito T, Phillips A. Interleukin-6 regulation of transforming growth factor (TGF)-beta receptor compartmentalization and turnover enhances TGF-beta1 signaling. J Biol Chem. 2005;280(13):12239-45.
114. Peng F, Wu D, Ingram AJ, Zhang B, Gao B, Krepinsky JC. RhoA activation in mesangial cells by mechanical strain depends on caveolae and caveolin-1 interaction. J Am Soc Nephrol. 2007;18(1):189-98.
115. Zhang Y, Peng F, Gao B, Ingram AJ, Krepinsky JC. Mechanical strain-induced RhoA activation requires NADPH oxidase-mediated ROS generation in caveolae. Antioxid Redox Signal. 2010;13(7):959-73.
116. Bocanegra V, Manucha W, Pena MR, Cacciamani V, Valles PG. Caveolin-1 and Hsp70 interaction in microdissected proximal tubules from spontaneously hypertensive rats as an effect of Losartan. J Hypertens. 2010;28(1):143-55.
117. Wei Y, Yang X, Liu Q, Wilkins JA, Chapman HA. A role for caveolin and the urokinase receptor in integrin-mediated adhesion and signaling. J Cell Biol. 1999;144(6):1285-94.
118. Pontrelli P, Ursi M, Ranieri E, Capobianco C, Schena FP, Gesualdo L, et al. CD40L proinflammatory and profibrotic effects on proximal tubular epithelial cells: role of NF-kappaB and lyn. J Am Soc Nephrol. 2006;17(3):627-36.
119. Park HC, Yasuda K, Ratliff B, Stoessel A, Sharkovska Y, Yamamoto I, et al. Postobstructive regeneration of kidney is derailed when surge in renal stem cells during course of unilateral ureteral obstruction is halted. Am J Physiol Renal Physiol. 2010;298(2):F357-64.
120. Yamaguchi T, Murata Y, Fujiyoshi Y, Doi T. Regulated interaction of endothelin B receptor with caveolin-1. Eur J Biochem. 2003;270(8):1816-27.
121. Percy C, Waters MJ, Gobe G. Caveolins in the repair phase of acute renal failure after oxidative stress. Nephrology (Carlton). 2004;9(6):374-80.
122. Ren Z, Liang W, Chen C, Yang H, Singhal PC, Ding G. Angiotensin II induces nephrin dephosphorylation and podocyte injury: role of caveolin-1. Cell Signal. 2012;24(2):443-50.
123. Couet J, Li S, Okamoto T, Ikezu T, Lisanti MP. Identification of peptide and protein ligands for the caveolin-scaffolding domain. Implications for the interaction of caveolin with caveolae-associated proteins. J Biol Chem. 1997;272(10):6525-33.
124. Liu P, Ying Y, Ko YG, Anderson RG. Localization of platelet-derived growth factor-stimulated phosphorylation cascade to caveolae. J Biol Chem. 1996;271(17):10299-303.
125. Torres VA, Tapia JC, Rodriguez DA, Lladser A, Arredondo C, Leyton L, et al. E-cadherin is required for caveolin-1-mediated down-regulation of the inhibitor of apoptosis protein survivin via reduced beta-catenin-Tcf/Lef-dependent transcription. Mol Cell Biol. 2007;27(21):7703-17.
126. Ko YG, Lee JS, Kang YS, Ahn JH, Seo JS. TNF-alpha-mediated apoptosis is initiated in caveolae-like domains. J Immunol. 1999;162(12):7217-23.
127. Wu T, Zhang B, Ye F, Xiao Z. A potential role for caveolin-1 in VEGF-induced fibronectin upregulation in mesangial cells: involvement of VEGFR2 and Src. Am J Physiol Renal Physiol. 2013;304(6):F820-30.
128. Lin MI, Yu J, Murata T, Sessa WC. Caveolin-1-deficient mice have increased tumor microvascular permeability, angiogenesis, and growth. Cancer Res. 2007;67(6):2849-56.
129. Nishiyama A, Hitomi H. Role of caveolin and heat shock protein 70 interaction in the antioxidative effects of an angiotensin II type 1 receptor blocker in spontaneously hypertensive rats proximal tubules. J Hypertens. 2010;28(1):9-12.
130. Trujillo J, Ramirez V, Perez J, Torre-Villalvazo I, Torres N, Tovar AR, et al. Renal protection by a soy diet in obese Zucker rats is associated with restoration of nitric oxide generation. Am J Physiol Renal Physiol. 2005;288(1):F108-16.

131. Valles PG, Manucha W, Carrizo L, Vega Perugorria J, Seltzer A, Ruete C. Renal caveolin-1 expression in children with unilateral ureteropelvic junction obstruction. Pediatr Nephrol. 2007;22(2):237-48.
132. Moriyama T, Tsuruta Y, Shimizu A, Itabashi M, Takei T, Horita S, et al. The significance of caveolae in the glomeruli in glomerular disease. J Clin Pathol. 2011;64(6):504-9.
133. Guan TH, Chen G, Gao B, Janssen MR, Uttarwar L, Ingram AJ, et al. Caveolin-1 deficiency protects against mesangial matrix expansion in a mouse model of type 1 diabetic nephropathy. Diabetologia. 2013;56(9):2068-77.
134. Herrera GA, Turbat-Herrera EA, Teng J. Animal Models of Light Chain Deposition Disease Provide a Better Understanding of Nodular Glomerulosclerosis. Nephron. 2016.
135. Yamamoto I, Horita S, Takahashi T, Kobayashi A, Toki D, Tanabe K, et al. Caveolin-1 expression is a distinct feature of chronic rejection-induced transplant capillaropathy. Am J Transplant. 2008;8(12):2627-35.
136. Tourkina E, Richard M, Oates J, Hofbauer A, Bonner M, Gooz P, et al. Caveolin-1 regulates leucocyte behaviour in fibrotic lung disease. Ann Rheum Dis. 2010;69(6):1220-6.
137. Wang XM, Zhang Y, Kim HP, Zhou Z, Feghali-Bostwick CA, Liu F, et al. Caveolin-1: a critical regulator of lung fibrosis in idiopathic pulmonary fibrosis. J Exp Med. 2006;203(13):2895-906.
138. Del Galdo F, Sotgia F, de Almeida CJ, Jasmin JF, Musick M, Lisanti MP, et al. Decreased expression of caveolin 1 in patients with systemic sclerosis: crucial role in the pathogenesis of tissue fibrosis. Arthritis Rheum. 2008;58(9):2854-65.
139. Miyasato SK, Loeffler J, Shohet R, Zhang J, Lindsey M, Le Saux CJ. Caveolin-1 modulates TGF-beta1 signaling in cardiac remodeling. Matrix Biol. 2011;30(5-6):318-29.
140. Zhang GY, Yu Q, Cheng T, Liao T, Nie CL, Wang AY, et al. Role of caveolin-1 in the pathogenesis of tissue fibrosis by keloid-derived fibroblasts in vitro. Br J Dermatol. 2011;164(3):623-7.
141. Tsai TH, Chen SF, Huang TY, Tzeng CF, Chiang AS, Kou YR, et al. Impaired Cd14 and Cd36 expression, bacterial clearance, and Toll-like receptor 4-Myd88 signaling in caveolin-1-deleted macrophages and mice. Shock. 2011;35(1):92-9.
142. Gadjeva M, Paradis-Bleau C, Priebe GP, Fichorova R, Pier GB. Caveolin-1 modifies the immunity to Pseudomonas aeruginosa. J Immunol. 2010;184(1):296-302.
143. Guo Q, Shen N, Yuan K, Li J, Wu H, Zeng Y, et al. Caveolin-1 plays a critical role in host immunity against Klebsiella pneumoniae by regulating STAT5 and Akt activity. Eur J Immunol. 2012;42(6):1500-11.
144. Zeitlin PL. Pseudomonas aeruginosa: can studies in engineered cells tell us why is it such a problem in people with cystic fibrosis? Focus on "Cystic fibrosis transmembrane conductance regulator and caveolin-1 regulate epithelial cell internalization of Pseudomonas aeruginosa". Am J Physiol Cell Physiol. 2009;297(2):C235-7.
145. Sharon-Friling R, Shenk T. Human cytomegalovirus pUL37x1-induced calcium flux activates PKCalpha, inducing altered cell shape and accumulation of cytoplasmic vesicles. Proc Natl Acad Sci U S A. 2014;111(12):E1140-8.
146. Moriyama T, Marquez JP, Wakatsuki T, Sorokin A. Caveolar endocytosis is critical for BK virus infection of human renal proximal tubular epithelial cells. J Virol. 2007;81(16):8552-62.
147. Fu Y, Moore XL, Lee MK, Fernandez-Rojo MA, Parat MO, Parton RG, et al. Caveolin-1 Plays a Critical Role in the Differentiation of Monocytes into Macrophages. Arterioscler Thromb Vasc Biol. 2012.
148. Schwencke C, Schmeisser A, Walter C, Wachter R, Pannach S, Weck B, et al. Decreased caveolin-1 in atheroma: loss of antiproliferative control of vascular smooth muscle cells in atherosclerosis. Cardiovasc Res. 2005;68(1):128-35.
149. Zhou X, He P. Endothelial [Ca2+]i and caveolin-1 antagonistically regulate eNOS activity and microvessel permeability in rat venules. Cardiovasc Res. 2010;87(2):340-7.

150. Schwencke C, Braun-Dullaeus RC, Wunderlich C, Strasser RH. Caveolae and caveolin in transmembrane signaling: Implications for human disease. Cardiovasc Res. 2006;70(1):42-9.
151. Williams TM, Lisanti MP. Caveolin-1 in oncogenic transformation, cancer, and metastasis. Am J Physiol Cell Physiol. 2005;288(3):C494-506.
152. Sotgia F, Martinez-Outschoorn UE, Howell A, Pestell RG, Pavlides S, Lisanti MP. Caveolin-1 and cancer metabolism in the tumor microenvironment: markers, models, and mechanisms. Annu Rev Pathol. 2012;7:423-67.
153. Mathieu R, Klatte T, Lucca I, Mbeutcha A, Seitz C, Karakiewicz PI, et al. Prognostic value of Caveolin-1 in patients treated with radical prostatectomy: a multicentric validation study. BJU Int. 2015.
154. Karlsson M, Thorn H, Parpal S, Stralfors P, Gustavsson J. Insulin induces translocation of glucose transporter GLUT4 to plasma membrane caveolae in adipocytes. FASEB journal : official publication of the Federation of American Societies for Experimental Biology. 2002;16(2):249-51.
155. Pojoga LH, Yao TM, Opsasnick LA, Garza AE, Reslan OM, Adler GK, et al. Dissociation of hyperglycemia from altered vascular contraction and relaxation mechanisms in caveolin-1 null mice. J Pharmacol Exp Ther. 2014;348(2):260-70.
156. Asterholm IW, Mundy DI, Weng J, Anderson RG, Scherer PE. Altered mitochondrial function and metabolic inflexibility associated with loss of caveolin-1. Cell Metab. 2012;15(2):171-85.
157. Yang Y, Tong Y, Gong M, Lu Y, Wang C, Zhou M, et al. Activation of PPARbeta/delta protects pancreatic beta cells from palmitate-induced apoptosis by upregulating the expression of GLP-1 receptor. Cell Signal. 2014;26(2):268-78.
158. Van der Hauwaert C, Savary G, Pincon C, Gnemmi V, Noel C, Broly F, et al. Donor caveolin 1 (CAV1) genetic polymorphism influences graft function after renal transplantation. Fibrogenesis Tissue Repair. 2015;8:8.
159. Testa A, Spoto B, Sanguedolce MC, Parlongo RM, Pisano A, Tripepi G, et al. eNOS and caveolin-1 gene polymorphisms interaction and intima media thickness: a proof of concept study in ESRD patients. Am J Hypertens. 2012;25(1):103-8.
160. Tampe B, Zeisberg M. Contribution of genetics and epigenetics to progression of kidney fibrosis. Nephrology, dialysis, transplantation : official publication of the European Dialysis and Transplant Association - European Renal Association. 2013.
161. Chue CD, Townend JN, Steeds RP, Ferro CJ. Arterial stiffness in chronic kidney disease: causes and consequences. Heart. 2010;96(11):817-23.
162. Go AS, Chertow GM, Fan D, McCulloch CE, Hsu CY. Chronic kidney disease and the risks of death, cardiovascular events, and hospitalization. N Engl J Med. 2004;351(13):1296-305.
163. Odudu A, Eldehni MT, Fakis A, McIntyre CW. Rationale and design of a multi-centre randomised controlled trial of individualised cooled dialysate to prevent left ventricular systolic dysfunction in haemodialysis patients. BMC Nephrol. 2012;13:45.
164. Breidthardt T, McIntyre CW. Dialysis-induced myocardial stunning: the other side of the cardiorenal syndrome. Rev Cardiovasc Med. 2011;12(1):13-20.
165. Ferguson JF, Matthews GJ, Townsend RR, Raj DS, Kanetsky PA, Budoff M, et al. Candidate gene association study of coronary artery calcification in chronic kidney disease: findings from the CRIC study (Chronic Renal Insufficiency Cohort). Journal of the American College of Cardiology. 2013;62(9):789-98.
166. McNamara DM, Holubkov R, Postava L, Ramani R, Janosko K, Mathier M, et al. Effect of the Asp298 variant of endothelial nitric oxide synthase on survival for patients with congestive heart failure. Circulation. 2003;107(12):1598-602.
167. Velloso MW, Pereira SB, Gouveia L, Chermont S, Tardin OM, Goncalves R, et al. Endothelial nitric oxide synthase Glu298Asp gene polymorphism in a multi-ethnical population with heart failure and controls. Nitric Oxide. 2010;22(3):220-5.

168. Page A, Reich H, Zhou J, Lai V, Cattran DC, Scholey JW, et al. Endothelial nitric oxide synthase gene/gender interactions and the renal hemodynamic response to angiotensin II. J Am Soc Nephrol. 2005;16(10):3053-60.
169. Vlachopoulos C, Aznaouridis K, Stefanadis C. Prediction of cardiovascular events and all-cause mortality with arterial stiffness: a systematic review and meta-analysis. Journal of the American College of Cardiology. 2010;55(13):1318-27.
170. Flossmann O, Berden A, de Groot K, Hagen C, Harper L, Heijl C, et al. Long-term patient survival in ANCA-associated vasculitis. Ann Rheum Dis. 2011;70(3):488-94.
171. Sharif A, Baboolal K. Risk factors for new-onset diabetes after kidney transplantation. Nat Rev Nephrol. 2010;6(7):415-23.
172. Kim YG, Ihm CG, Lee TW, Lee SH, Jeong KH, Moon JY, et al. Association of genetic polymorphisms of interleukins with new-onset diabetes after transplantation in renal transplantation. Transplantation. 2012;93(9):900-7.
173. Tavira B, Coto E, Torres A, Diaz-Corte C, Diaz-Molina B, Ortega F, et al. Association between a common KCNJ11 polymorphism (rs5219) and new-onset posttransplant diabetes in patients treated with Tacrolimus. Mol Genet Metab. 2012;105(3):525-7.
174. Anders HJ, Schlondorff DO. Innate immune receptors and autophagy: implications for autoimmune kidney injury. Kidney Int. 2010;78(1):29-37.
175. Eddy AA. Progression in chronic kidney disease. Adv Chronic Kidney Dis. 2005;12(4):353-65.
176. Fujita Y, Maruyama S, Kogo H, Matsuo S, Fujimoto T. Caveolin-1 in mesangial cells suppresses MAP kinase activation and cell proliferation induced by bFGF and PDGF. Kidney Int. 2004;66(5):1794-804.
177. Park DS, Cohen AW, Frank PG, Razani B, Lee H, Williams TM, et al. Caveolin-1 null (-/-) mice show dramatic reductions in life span. Biochemistry. 2003;42(51):15124-31.
178. Insel PA, Patel HH. Do studies in caveolin-knockouts teach us about physiology and pharmacology or instead, the ways mice compensate for 'lost proteins'? Br J Pharmacol. 2007;150(3):251-4.
179. Gabriel S, Ziaugra L, Tabbaa D. SNP genotyping using the Sequenom MassARRAY iPLEX platform. Curr Protoc Hum Genet. 2009;Chapter 2:Unit 2 12.
180. Edwards NC, Ferro CJ, Kirkwood H, Chue CD, Young AA, Stewart PM, et al. Effect of spironolactone on left ventricular systolic and diastolic function in patients with early stage chronic kidney disease. Am J Cardiol. 2010;106(10):1505-11.
181. Chue CD, Townend JN, Moody WE, Zehnder D, Wall NA, Harper L, et al. Cardiovascular effects of sevelamer in stage 3 CKD. J Am Soc Nephrol. 2013;24(5):842-52.
182. Stringer S, Sharma P, Dutton M, Jesky M, Ng K, Kaur O, et al. The natural history of, and risk factors for, progressive chronic kidney disease (CKD): the Renal Impairment in Secondary care (RIISC) study; rationale and protocol. BMC Nephrol. 2013;14:95.
183. Graffelman J, Weir BS. Testing for Hardy-Weinberg equilibrium at biallelic genetic markers on the X chromosome. Heredity (Edinb). 2016;116(6):558-68.
184. Maceira AM, Prasad SK, Khan M, Pennell DJ. Normalized left ventricular systolic and diastolic function by steady state free precession cardiovascular magnetic resonance. J Cardiovasc Magn Reson. 2006;8(3):417-26.
185. Lang RM, Bierig M, Devereux RB, Flachskampf FA, Foster E, Pellikka PA, et al. Recommendations for chamber quantification: a report from the American Society of Echocardiography's Guidelines and Standards Committee and the Chamber Quantification Writing Group, developed in conjunction with the European Association of Echocardiography, a branch of the European Society of Cardiology. J Am Soc Echocardiogr. 2005;18(12):1440-63.
186. Nagueh SF, Appleton CP, Gillebert TC, Marino PN, Oh JK, Smiseth OA, et al. Recommendations for the evaluation of left ventricular diastolic function by echocardiography. J Am Soc Echocardiogr. 2009;22(2):107-33.

187. Chapman CB, Ewer SM, Kelly AF, Jacobson KM, Leal MA, Rahko PS. Classification of left ventricular diastolic function using American Society of Echocardiography Guidelines: agreement among echocardiographers. Echocardiography. 2013;30(9):1022-31.
188. Purcell S, Neale B, Todd-Brown K, Thomas L, Ferreira MA, Bender D, et al. PLINK: a tool set for whole-genome association and population-based linkage analyses. Am J Hum Genet. 2007;81(3):559-75.
189. Andoh TF, Lam TT, Lindsley J, Alpers CE, Bennett WM. Enhancement of chronic cyclosporine nephrotoxicity by sodium depletion in an experimental mouse model. Nephrology. 1997;3(5):471-8.
190. Eddy AA, Lopez-Guisa JM, Okamura DM, Yamaguchi I. Investigating mechanisms of chronic kidney disease in mouse models. Pediatr Nephrol. 2012;27(8):1233-47.
191. Chand S, Edwards NC, Chue CD, Jesky M, Stringer S, Simmonds MJ, et al. Caveolin-1 single-nucleotide polymorphism and arterial stiffness in non-dialysis chronic kidney disease. Nephrol Dial Transplant. 2015.
192. Sarnak MJ, Levey AS. Cardiovascular disease and chronic renal disease: a new paradigm. Am J Kidney Dis. 2000;35(4 Suppl 1):S117-31.
193. Kranzhofer R, Schmidt J, Pfeiffer CA, Hagl S, Libby P, Kubler W. Angiotensin induces inflammatory activation of human vascular smooth muscle cells. Arterioscler Thromb Vasc Biol. 1999;19(7):1623-9.
194. Takagishi T, Murahashi N, Azagami S, Morimatsu M, Sasaguri Y. Effect of angiotensin II and thromboxane A2 on the production of matrix metalloproteinase by human aortic smooth muscle cells. Biochem Mol Biol Int. 1995;35(2):265-73.
195. Moody WE, Edwards NC, Chue CD, Ferro CJ, Townend JN. Arterial disease in chronic kidney disease. Heart. 2013;99(6):365-72.
196. Baumann M, Wassertheurer S, Suttmann Y, Burkhardt K, Heemann U. Aortic pulse wave velocity predicts mortality in chronic kidney disease stages 2-4. J Hypertens. 2014;32(4):899-903.
197. Hickson SS, Butlin M, Broad J, Avolio AP, Wilkinson IB, McEniery CM. Validity and repeatability of the Vicorder apparatus: a comparison with the SphygmoCor device. Hypertens Res. 2009;32(12):1079-85.
198. Tang L, Wang H, Ziolo MT. Targeting NOS as a therapeutic approach for heart failure. Pharmacol Ther. 2013.
199. Massy ZA, Stenvinkel P, Drueke TB. The role of oxidative stress in chronic kidney disease. Semin Dial. 2009;22(4):405-8.
200. Hassan GS, Williams TM, Frank PG, Lisanti MP. Caveolin-1-deficient aortic smooth muscle cells show cell autonomous abnormalities in proliferation, migration, and endothelin-based signal transduction. Am J Physiol Heart Circ Physiol. 2006;290(6):H2393-401.
201. Matsushita K, Sang Y, Ballew SH, Shlipak M, Katz R, Rosas SE, et al. Subclinical atherosclerosis measures for cardiovascular prediction in CKD. J Am Soc Nephrol. 2015;26(2):439-47.
202. Ortiz A, Covic A, Fliser D, Fouque D, Goldsmith D, Kanbay M, et al. Epidemiology, contributors to, and clinical trials of mortality risk in chronic kidney failure. Lancet. 2014;383(9931):1831-43.
203. Baigent C, Landray M. Which cardiovascular risk factors matter in chronic kidney disease? Nephrol Dial Transplant. 2007;22(1):9-11.
204. Zoccali C, Benedetto FA, Maas R, Mallamaci F, Tripepi G, Malatino LS, et al. Asymmetric dimethylarginine, C-reactive protein, and carotid intima-media thickness in end-stage renal disease. J Am Soc Nephrol. 2002;13(2):490-6.
205. Chand S, Chue CD, Edwards NC, Hodson J, Simmonds MJ, Hamilton A, et al. Endothelial nitric oxide synthase single nucleotide polymorphism and left ventricular function in early chronic kidney disease. PLoS One. 2015;10(1):e0116160.
206. Tesauro M, Thompson WC, Rogliani P, Qi L, Chaudhary PP, Moss J. Intracellular processing of endothelial nitric oxide synthase isoforms associated with differences in severity of cardiopulmonary

diseases: cleavage of proteins with aspartate vs. glutamate at position 298. Proc Natl Acad Sci U S A. 2000;97(6):2832-5.
207. Veldman BA, Spiering W, Doevendans PA, Vervoort G, Kroon AA, de Leeuw PW, et al. The Glu298Asp polymorphism of the NOS 3 gene as a determinant of the baseline production of nitric oxide. J Hypertens. 2002;20(10):2023-7.
208. Joshi MS, Mineo C, Shaul PW, Bauer JA. Biochemical consequences of the NOS3 Glu298Asp variation in human endothelium: altered caveolar localization and impaired response to shear. FASEB J. 2007;21(11):2655-63.
209. Joshi MS, Bauer JA. Preliminary computational modeling of nitric oxide synthase 3 interactions with caveolin-1: influence of exon 7 Glu298Asp polymorphism. Acta Biochim Biophys Sin (Shanghai). 2008;40(1):47-54.
210. Tardin OM, Pereira SB, Velloso MW, Balieiro HM, Costa B, Alves TO, et al. Genetic polymorphism G894T and the prognosis of heart failure outpatients. Arq Bras Cardiol. 2013;101(4):352-8.
211. Zhang X, Lynch AI, Davis BR, Ford CE, Boerwinkle E, Eckfeldt JH, et al. Pharmacogenetic association of NOS3 variants with cardiovascular disease in patients with hypertension: the GenHAT study. PLoS One. 2012;7(3):e34217.
212. Massion PB, Dessy C, Desjardins F, Pelat M, Havaux X, Belge C, et al. Cardiomyocyte-restricted overexpression of endothelial nitric oxide synthase (NOS3) attenuates beta-adrenergic stimulation and reinforces vagal inhibition of cardiac contraction. Circulation. 2004;110(17):2666-72.
213. Philip I, Plantefeve G, Vuillaumier-Barrot S, Vicaut E, LeMarie C, Henrion D, et al. G894T polymorphism in the endothelial nitric oxide synthase gene is associated with an enhanced vascular responsiveness to phenylephrine. Circulation. 1999;99(24):3096-8.
214. Brunner F, Andrew P, Wolkart G, Zechner R, Mayer B. Myocardial contractile function and heart rate in mice with myocyte-specific overexpression of endothelial nitric oxide synthase. Circulation. 2001;104(25):3097-102.
215. Chand S, Holle JU, Hilhorst M, Simmonds MJ, Smith S, Kamesh L, et al. Caveolin-1 single nucleotide polymorphism in antineutrophil cytoplasmic antibody associated vasculitis. PLoS One. 2013;8(7):e69022.
216. Ntatsaki E, Watts RA, Scott DG. Epidemiology of ANCA-associated vasculitis. Rheum Dis Clin North Am. 2010;36(3):447-61.
217. Rahmattulla C, Mooyaart AL, van Hooven D, Schoones JW, Bruijn JA, Dekkers OM, et al. Genetic variants in ANCA-associated vasculitis: a meta-analysis. Ann Rheum Dis. 2015.
218. McGeoch L, Twilt M, Famorca L, Bakowsky V, Barra L, Benseler SM, et al. CanVasc Recommendations for the Management of Antineutrophil Cytoplasm Antibody-associated Vasculitides. J Rheumatol. 2016;43(1):97-120.
219. Hoffman GS, Kerr GS, Leavitt RY, Hallahan CW, Lebovics RS, Travis WD, et al. Wegener granulomatosis: an analysis of 158 patients. Ann Intern Med. 1992;116(6):488-98.
220. Fauci AS, Haynes BF, Katz P, Wolff SM. Wegener's granulomatosis: prospective clinical and therapeutic experience with 85 patients for 21 years. Ann Intern Med. 1983;98(1):76-85.
221. Willcocks LC, Lyons PA, Rees AJ, Smith KG. The contribution of genetic variation and infection to the pathogenesis of ANCA-associated systemic vasculitis. Arthritis Res Ther. 2010;12(1):202.
222. Morris H, Morgan MD, Wood AM, Smith SW, Ekeowa UI, Herrmann K, et al. ANCA-associated vasculitis is linked to carriage of the Z allele of alpha(1) antitrypsin and its polymers. Ann Rheum Dis. 2011;70(10):1851-6.
223. Chand S, McKnight AJ, Shabir S, Chan W, McCaughan JA, Maxwell AP, et al. Analysis of single nucleotide polymorphisms implicate mTOR signalling in the development of new-onset diabetes after transplantation. BBA Clin. 2016;5:41-5.

224. Sharif A, Moore RH, Baboolal K. The use of oral glucose tolerance tests to risk stratify for new-onset diabetes after transplantation: An underdiagnosed phenomenon. Transplantation. 2006;82(12):1667-72.
225. Bergrem HA, Valderhaug TG, Hartmann A, Hjelmesaeth J, Leivestad T, Bergrem H, et al. Undiagnosed diabetes in kidney transplant candidates: a case-finding strategy. Clin J Am Soc Nephrol. 2010;5(4):616-22.
226. Kurzawski M, Dziewanowski K, Lapczuk J, Wajda A, Drozdzik M. Analysis of common type 2 diabetes mellitus genetic risk factors in new-onset diabetes after transplantation in kidney transplant patients medicated with tacrolimus. Eur J Clin Pharmacol. 2012;68(12):1587-94.
227. Donath MY, Ehses JA, Maedler K, Schumann DM, Ellingsgaard H, Eppler E, et al. Mechanisms of beta-cell death in type 2 diabetes. Diabetes. 2005;54 Suppl 2:S108-13.
228. Favaro E, Miceli I, Bussolati B, Schmitt-Ney M, Cavallo Perin P, Camussi G, et al. Hyperglycemia induces apoptosis of human pancreatic islet endothelial cells: effects of pravastatin on the Akt survival pathway. Am J Pathol. 2008;173(2):442-50.
229. Hara K, Tobe K, Okada T, Kadowaki H, Akanuma Y, Ito C, et al. A genetic variation in the PGC-1 gene could confer insulin resistance and susceptibility to Type II diabetes. Diabetologia. 2002;45(5):740-3.
230. Moon MK, Cho YM, Jung HS, Park YJ, Yoon KH, Sung YA, et al. Genetic polymorphisms in peroxisome proliferator-activated receptor gamma are associated with Type 2 diabetes mellitus and obesity in the Korean population. Diabet Med. 2005;22(9):1161-6.
231. Blattler SM, Cunningham JT, Verdeguer F, Chim H, Haas W, Liu H, et al. Yin Yang 1 deficiency in skeletal muscle protects against rapamycin-induced diabetic-like symptoms through activation of insulin/IGF signaling. Cell Metab. 2012;15(4):505-17.
232. Laplante M, Sabatini DM. mTOR signaling at a glance. J Cell Sci. 2009;122(Pt 20):3589-94.
233. Chan YS, Goke J, Lu X, Venkatesan N, Feng B, Su IH, et al. A PRC2-dependent repressive role of PRDM14 in human embryonic stem cells and induced pluripotent stem cell reprogramming. Stem Cells. 2013;31(4):682-92.
234. Chen H, Gu X, Su IH, Bottino R, Contreras JL, Tarakhovsky A, et al. Polycomb protein Ezh2 regulates pancreatic beta-cell Ink4a/Arf expression and regeneration in diabetes mellitus. Genes & Development. 2009;23(8):975-85.
235. Zhou JX, Dhawan S, Fu H, Snyder E, Bottino R, Kundu S, et al. Combined modulation of polycomb and trithorax genes rejuvenates beta cell replication. The Journal of clinical investigation. 2013;123(11):4849-58.
236. Fougeray S, Loriot MA, Nicaud V, Legendre C, Thervet E, Pallet N. Increased body mass index after kidney transplantation in activating transcription factor 6 single polymorphism gene carriers. Transplant Proc. 2011;43(9):3418-22.
237. Odisho T, Zhang L, Volchuk A. ATF6beta regulates the Wfs1 gene and has a cell survival role in the ER stress response in pancreatic beta-cells. Experimental cell research. 2015;330(1):111-22.
238. Gu N, Ma X, Zhang J, Dong A, Jin M, Feng N, et al. Obesity has an interactive effect with genetic variation in the activating transcription factor 6 gene on the risk of pre-diabetes in individuals of Chinese Han descent. PLoS One. 2014;9(10):e109805.
239. Thameem F, Farook VS, Bogardus C, Prochazka M. Association of amino acid variants in the activating transcription factor 6 gene (ATF6) on 1q21-q23 with type 2 diabetes in Pima Indians. Diabetes. 2006;55(3):839-42.
240. Yang J, Hutchinson, II, Shah T, Min DI. Genetic and clinical risk factors of new-onset diabetes after transplantation in Hispanic kidney transplant recipients. Transplantation. 2011;91(10):1114-9.
241. Byrne MM, Sturis J, Menzel S, Yamagata K, Fajans SS, Dronsfield MJ, et al. Altered insulin secretory responses to glucose in diabetic and nondiabetic subjects with mutations in the diabetes susceptibility gene MODY3 on chromosome 12. Diabetes. 1996;45(11):1503-10.

242. Mohlke KL, Boehnke M. The role of HNF4A variants in the risk of type 2 diabetes. Curr Diab Rep. 2005;5(2):149-56.
243. Wang H, Maechler P, Antinozzi PA, Hagenfeldt KA, Wollheim CB. Hepatocyte nuclear factor 4alpha regulates the expression of pancreatic beta -cell genes implicated in glucose metabolism and nutrient-induced insulin secretion. J Biol Chem. 2000;275(46):35953-9.
244. Charos AE, Reed BD, Raha D, Szekely AM, Weissman SM, Snyder M. A highly integrated and complex PPARGC1A transcription factor binding network in HepG2 cells. Genome Res. 2012;22(9):1668-79.
245. Schmidt SF, Mandrup S. Gene program-specific regulation of PGC-1{alpha} activity. Genes & Development. 2011;25(14):1453-8.
246. Lopes PC, Fuhrmann A, Carvalho F, Sereno J, Santos MR, Pereira MJ, et al. Cyclosporine A enhances gluconeogenesis while sirolimus impairs insulin signaling in peripheral tissues after 3 weeks of treatment. Biochem Pharmacol. 2014;91(1):61-73.
247. Barlow AD, Nicholson ML, Herbert TP. Evidence for rapamycin toxicity in pancreatic beta-cells and a review of the underlying molecular mechanisms. Diabetes. 2013;62(8):2674-82.
248. Gyurus E, Kaposztas Z, Kahan BD. Sirolimus therapy predisposes to new-onset diabetes mellitus after renal transplantation: a long-term analysis of various treatment regimens. Transplant Proc. 2011;43(5):1583-92.
249. Veroux M, Tallarita T, Corona D, Sinagra N, Giaquinta A, Zerbo D, et al. Conversion to sirolimus therapy in kidney transplant recipients with new onset diabetes mellitus after transplantation. Clin Dev Immunol. 2013;2013:496974.
250. Guerra G, Ciancio G, Gaynor JJ, Zarak A, Brown R, Hanson L, et al. Randomized trial of immunosuppressive regimens in renal transplantation. J Am Soc Nephrol. 2011;22(9):1758-68.
251. Claes K, Meier-Kriesche HU, Schold JD, Vanrenterghem Y, Halloran PF, Ekberg H. Effect of different immunosuppressive regimens on the evolution of distinct metabolic parameters: evidence from the Symphony study. Nephrol Dial Transplant. 2012;27(2):850-7.
252. Knoll GA, Kokolo MB, Mallick R, Beck A, Buenaventura CD, Ducharme R, et al. Effect of sirolimus on malignancy and survival after kidney transplantation: systematic review and meta-analysis of individual patient data. BMJ. 2014;349:g6679.
253. Lieberman MD, Cunningham WA. Type I and Type II error concerns in fMRI research: re-balancing the scale. Soc Cogn Affect Neurosci. 2009;4(4):423-8.
254. Meigs JB, Shrader P, Sullivan LM, McAteer JB, Fox CS, Dupuis J, et al. Genotype score in addition to common risk factors for prediction of type 2 diabetes. N Engl J Med. 2008;359(21):2208-19.
255. Talmud PJ, Hingorani AD, Cooper JA, Marmot MG, Brunner EJ, Kumari M, et al. Utility of genetic and non-genetic risk factors in prediction of type 2 diabetes: Whitehall II prospective cohort study. BMJ. 2010;340:b4838.
256. Piepenhagen PA, Peters LL, Lux SE, Nelson WJ. Differential expression of Na(+)-K(+)-ATPase, ankyrin, fodrin, and E-cadherin along the kidney nephron. Am J Physiol. 1995;269(6 Pt 1):C1417-32.
257. Lee SY, Han SM, Kim JE, Chung KY, Han KH. Expression of E-cadherin in pig kidney. J Vet Sci. 2013;14(4):381-6.
258. Prozialeck WC, Lamar PC, Appelt DM. Differential expression of E-cadherin, N-cadherin and beta-catenin in proximal and distal segments of the rat nephron. BMC Physiol. 2004;4:10.
259. Kruger T, Benke D, Eitner F, Lang A, Wirtz M, Hamilton-Williams EE, et al. Identification and functional characterization of dendritic cells in the healthy murine kidney and in experimental glomerulonephritis. J Am Soc Nephrol. 2004;15(3):613-21.
260. LaSpina M, Tripathi S, Gatto LA, Bruch D, Maier KG, Kittur DS. An interleukin-6-neutralizing antibody prevents cyclosporine-induced nephrotoxicity in mice. J Surg Res. 2008;148(2):121-5.
261. Nagle RB, Bulger RE. Unilateral obstructive nephropathy in the rabbit. II. Late morphologic changes. Lab Invest. 1978;38(3):270-8.

262. Chevalier RL, Forbes MS, Thornhill BA. Ureteral obstruction as a model of renal interstitial fibrosis and obstructive nephropathy. Kidney Int. 2009;75(11):1145-52.
263. Nagle RB, Bulger RE, Cutler RE, Jervis HR, Benditt EP. Unilateral obstructive nephropathy in the rabbit. I. Early morphologic, physiologic, and histochemical changes. Lab Invest. 1973;28(4):456-67.
264. Smith SW, Chand S, Savage CO. Biology of the renal pericyte. Nephrol Dial Transplant. 2012;27(6):2149-55.
265. Maciel TT, Coutinho EL, Soares D, Achar E, Schor N, Bellini MH. Endostatin, an antiangiogenic protein, is expressed in the unilateral ureteral obstruction mice model. J Nephrol. 2008;21(5):753-60.
266. Duffield JS. Cellular and molecular mechanisms in kidney fibrosis. J Clin Invest. 2014;124(6):2299-306.
267. Anders HJ, Schaefer L. Beyond tissue injury-damage-associated molecular patterns, toll-like receptors, and inflammasomes also drive regeneration and fibrosis. J Am Soc Nephrol. 2014;25(7):1387-400.
268. Lech M, Anders HJ. Macrophages and fibrosis: How resident and infiltrating mononuclear phagocytes orchestrate all phases of tissue injury and repair. Biochim Biophys Acta. 2013;1832(7):989-97.
269. Fligny C, Duffield JS. Activation of pericytes: recent insights into kidney fibrosis and microvascular rarefaction. Curr Opin Rheumatol. 2013;25(1):78-86.
270. Braga TT, Agudelo JS, Camara NO. Macrophages During the Fibrotic Process: M2 as Friend and Foe. Front Immunol. 2015;6:602.
271. Li J, Scherl A, Medina F, Frank PG, Kitsis RN, Tanowitz HB, et al. Impaired phagocytosis in caveolin-1 deficient macrophages. Cell Cycle. 2005;4(11):1599-607.
272. Shivshankar P, Halade GV, Calhoun C, Escobar GP, Mehr AJ, Jimenez F, et al. Caveolin-1 deletion exacerbates cardiac interstitial fibrosis by promoting M2 macrophage activation in mice after myocardial infarction. J Mol Cell Cardiol. 2014;76:84-93.
273. Freedman ML, Monteiro AN, Gayther SA, Coetzee GA, Risch A, Plass C, et al. Principles for the post-GWAS functional characterization of cancer risk loci. Nat Genet. 2011;43(6):513-8.
274. Kogo H, Fujimoto T. Caveolin-1 isoforms are encoded by distinct mRNAs. Identification Of mouse caveolin-1 mRNA variants caused by alternative transcription initiation and splicing. FEBS Lett. 2000;465(2-3):119-23.
275. O'Connell PJ, Zhang W, Menon MC, Yi Z, Schroppel B, Gallon L, et al. Biopsy transcriptome expression profiling to identify kidney transplants at risk of chronic injury: a multicentre, prospective study. Lancet. 2016.

APPENDIX I: Primary papers published from the completion of this MD

Analysis of single nucleotide polymorphisms implicate mTOR signalling in the development of new-onset diabetes after transplantation. **Chand S**, McKnight AJ, Shabir S, Chan W, McCaughan J, Maxwell AP, Borrows R. BBA Clinical. 2016 Jun; 5(2):41-45

Caveolin-1 single nucleotide polymorphism and arterial stiffness in non-dialysis chronic kidney disease. **Chand S**, Edwards N, Chue C, Jesky M, Stringer S, Simmonds MJ, Duffy CE, Cockwell P, Harper L, Steeds RP, Townend JN, Ferro CJ, Borrows R. Nephrol Dial Transplant. 2015 Oct 3

eNOS Glu298Asp gene variation and left ventricular function in early chronic kidney disease. **Chand S**, Chue CD, Edwards NC, Simmonds MJ, Hamilton A, Gough SCL, Steeds RP, Townend JN, Ferro CJ, Borrows R. PLoS One. 2015 Jan 22;10(1):e0116160

Genetic polymorphisms and kidney transplant outcomes. **Chand S**, McKnight AJ, Borrows R. Curr Opin Nephrol Hypertens. 2014 Nov;23(6):605-10

Caveolin-1 single nucleotide polymorphism in antineutrophil cytoplasmic antibody associated vasculitis. **Chand S**, Holle J, Hilhorst M, Simmonds M, Smith S, Kamesh L, Hewins P, McKnight AJ, Maxwell AP, Cohen Tervaert JW, Wieczorek S, Harper L, Borrows R. PLoS One. 2013 Jul;8(7):e69022